ANALYSIS AND DEVELOPMENT OF OBJECT DETECTION TRACK ALGORITHM AND ITS APPLICATIONS

THESIS

submitted in fulfillment of the requirements of the award of degree of

DOCTOR OF PHILOSOPHY

to

J.C. BOSE UNIVERSITY OF SCIENCE & TECHNOLOGY, YMCA

by

RUCHIKA RANI

Registration No. YMCAUST/Ph19/2012

Under the supervision of

Dr. Munish Vashishath

Supervisor, Professor,
Deptt. of Electronics Engg.
J.C. Bose University of Sc. & Tech.
YMCA Faridabad

Dr. Shamimul Qamar

Co-Supervisor, Professor
Deptt. of Computer Network & Comm. Engg.
King Khalid University, Abha ,
Saudi Arabia

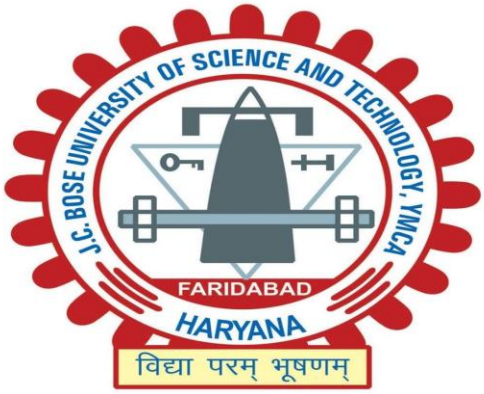

Department of Electronics Engineering

Faculty of Engineering and Technology

J.C. Bose University of Science & Technology,

YMCA Faridabad, Haryana, India

July, 2018

CANDIDATE'S DECLARATION

I hereby declare that this thesis entitled **ANALYSIS AND DEVELOPMENT OF OBJECT DETECTION TRACK ALGORITHM AND ITS APPLICATIONS** by **RUCHIKA RANI**, being submitted in fulfilment of the requirements for the Degree of Doctor of Philosophy in ELECTRONICS ENGINEERING under Faculty of Engineering & Technology of J.C. Bose University of Science & Technology, YMCA Faridabad, during the academic year 2017-2018, is a bonafide record of my original work carried out under guidance and supervision of **Dr. MUNISH VASHISHATH,** Professor, Electronics Engineering, J.C. Bose University of Science & Technology, YMCA Faridabad and **Dr. SHAMIMUL QAMAR,** Professor, Deptt. of Computer Network & Communication Engineering, King Khalid University, Abha, Saudi Arabia has not been presented elsewhere.

I further declare that the thesis does not contain any part of any work which has been submitted for the award of any degree either in this university or in any other university.

Ruchika Rani

Registration No.: YMCAUST/Ph19/2012

CERTIFICATE OF THE SUPERVISOR

This is to certify that this Thesis entitled **ANALYSIS AND DEVELOPMENT OF OBJECT DETECTION TRACK ALGORITHM AND ITS APPLICATIONS** by **RUCHIKA RANI (Registration No.: YMCAUST/Ph19/2012**), submitted in fulfillment of the requirement for the Degree of Doctor of Philosophy in **ELECTRONICS ENGINEERING** under Faculty of Engineering & Technology of J.C. Bose University of Science & Technology, YMCA Faridabad, during the academic year 2017-2018, is a bonafide record of work carried out under our guidance and supervision.

We further declare that to the best of our knowledge, the thesis does not contain any part of any work which has been submitted for the award of any degree either in this university or in any other university.

Dr. Munish Vashishath (Supervisor)
Professor
Department of Electronics Engineering
J.C. Bose University of Science & Tech.
YMCA Faridabad

Dr. Shamimul Qamar (Co-Supervisor)
Professor
Deptt.of Computer Network & Comm. Engg.
King Khalid University,
Abha, Saudi Arabia

Dated:

ACKNOWLEDGEMENT

I express my deep sense of gratitude and indebtedness to my supervisors **Dr. Munish Vashishath,** Professor, Electronics Engineering, J.C. Bose University of Science and Technology, YMCA Faridabad and **Dr. Shamimul Qamar,** Professor, Deptt. of Computer Network & Communication Engineering, King Khalid University, Abha, Saudi Arabia, for providing unreserved guidance, inspiring discussions and constant supervision throughout this research work. Their timely help, constructive criticism, and conscientious efforts made it possible to improve the quality of my research work. I will carry out their guidance throughout my life.

This thesis would not have been possible without the continuous and unconditional support of my family members and friends who gave me strength and will to succeed.

I want to express my sincere thanks to all those who directly or indirectly helped me at various stages of this work.

Above all, I express my indebtedness to the "**ALMIGHTY**" for all His blessings and kindness.

Ruchika Rani

Registration No.: YMCAUST/Ph19/2012

ABSTRACT

Digital Image processing is one of the viable areas of research. As technologies are advancing and becoming much cheaper than earlier, in last one decade digital image processing converting into integrated part of daily life, area of interest of researcher and scientist.

Computer vision, digital image processing and image analysis are areas which are complementary to each other. Due to efficiency in human eye, a man can see only things that falls under a limited portion of electromagnetic spectrum (EM). Machine vision is the area that provides visibility in other part of EM.

Image analysis analysed whole image or any part or object of image to achieve any specific objective. Digital Image processing consists of various techniques (viz. Image acquisition, enhancement, restoration, compression, segmentation and recognition) that can be applied for solving any particular problem related to images. These techniques of digital image processing can be either combined together or applied autonomously to solve any problem. Among the digital image processing techniques image enhancement and image segmentation are very common and interesting methods.

Image enhancement method improves the quality of image by diminishing the unwanted elements of image and enhanced the presentation image's objet that are of our interest. Segmentation subdivides an image into its constituent parts or objects. The level to which this subdivision is carried depends on the problem being viewed.

The proposed work analysed image detection techniques for infrared image of small boats in sea water to detect presence of boat.

Moreover, black and white spots are introduced into images during acquisition, transmission, and flooding waves. Therefore, aggregation operator based filter introduced to remove noise in sea water image.

Synthetic aperture radar or SAR images are used by Sub-aperture Cross-Correlation Magnitude (SCM) method as input to produces clear image of ships.

Edge detection is in particular one of the staple and popular segmentation techniques. This work analysed ant colony optimization (ACO) based technique of edge detection. To detect edges of ship fuzzy triangular membership function based ACO technique is introduced. Further, performance of proposed method is compared with fuzzy C- means ACO algorithm. The outcome of proposed work shows clear edges of small and partial objects in less time.

Proposed ACO based technique is followed by comparison of Gradient based edge detectors (viz. Perwitt, Sobel Operator) and Laplacian filter like LoG, Cannys and Roberts Edge Detection Method. Major findings of proposed research can be divided in to two parts. Firstly, findings based on enhancement techniques and secondly image segmentation techniques.

In first category, fuzzy linguistic quantifier based filter is introduced to remove salt pepper noise. As discussed earlier this noise introduces due to flooding waves of sea water. Fuzzy linguistic quantifier namely 'at least half', 'most', and 'as many as possible' were introduced by Yager in 1988. To remove impulse noise 'most' quantifier is used. The performance of this naïve filter is compared with median filter in terms of signal to noise ratio. Even though median filter is better known for removing impulse noise, but proposed filter shows better performance.

Second category, is segmentation based methodologies. That are further divided into dissimilarity and similarity based techniques. In first type to detect edges of a small boat triangular membership function based Ant Colony Optimization methodology. A final pheromone matrix constructed to reflect the edge information or degree of edginess. Heuristic information (η) is based on degree of edginess because movement of ant is trigger by greater degree of edginess at its neighborhood. 8-pixel neighborhood considered η is given by triangular fuzzy membership function.

Besides this, in discontinuity based image segmentation, pros and cons of gradient based edge detectors and Laplacian based methods are compared. The findings are, gradient based edge detectors are easy to implement, but time consuming and more sensitive towards noise. Laplacian based edge detection gives better detection especially in presence of noise, but malfunctions at corners and curves.

The key objective of using thresholding is to produce a clean segmented image of targeted ship by eliminating the noise and flood waves. Hence there is a requirement of a method that can be specifying threshold ‘T’.

Global thresholding is one of the successful similarity based technique in highly controlled environment, whereas sea water is much uncontrolled environment. Hence to targeted ship, the image is processed by Ordered Weighted Averaging (OWA) method and produces promising results. It is also observed threshold produces by ‘at least half’, and ‘as many as possible’ linguistic quantifier are better in terms of histogram based threshold.

. TABLE OF CONTENTS

LIST OF TABLES

LIST OF FIGURES

LIST OF ABBREVIATIONS

Symbol	Description
EM	Electromagnetic Spectrum
AI	Artificial Intelligence
OWA	Ordered Weighted Averaging
LoG	Laplacian of Gaussian
SCM	Subaperture Cross correlation Magnitude
RGB	Red, Green, and Blue
CMY	Cyan, Magenta, Yellow
HSI	Hue, Saturation, and Intensity
HSL	Hue, Saturation, Lightness
HSB	Hue, Saturation Brightness
TIFF	Tagged Image File Format
JPEG	Joint Photographic Experts Group
BMP	Bitmaps
SAR	Synthetic Aperture Radar
ACO	Ant Colony Optimization
GHP	Gradient Histogram Perserving
GA	Genetic Algorithm
ANN	Artificial Neutral Network
SOFM	Self -organization of Kohonen Feature Map
WPS	Windows Per Second
HMIiOL	Human-Machine Interaction in Object Level
SLC	Simple Look Complex
SLI	Simple Look Intensity
DPCM	Differential Pulse Code Modulation
SCM	Sub-aperture Cross-Correlation Magnitude
ISCM	Improved Subaperture Cross correlation Magnitude
FFT	Fast Fourier Transfer
IFFT	Inverse Fast Fourier Transfer
GHP	Gradient Histogram Preservation

CV	Coefficient of Variations
SV	Spatial Resolution
RADAR	Radio Detection & Ranging
TCR	Target- to-Clutter Ratio

CHAPTER I
INTRODUCTION

Images are one of the ancient tools of information transformation. Single image can communicate more than thousand words. Significant progress in the development of machine vision and digital image processing or image processing technology has been made in recent past in conjunction with improvements in computer technology. Equipment for machine vision and image processing has been reduced in cost, size, and weight, can be installed in most places and is accessible for civilian use.

Machine vision and image processing are used increasingly in life sciences, materials science, photography, and other fields. Images in real world are proportional to the energy radiated by the source. Image Analysis is the collection of processes in which a captured image that is prepared by image processing is analysed in order to extract information about the image and to identify objects or its environment.

Computer vision is one of the progressing research areas that can emulate human vision in near future. Computer vision takes visual by sensors. Image analysis is the field of engineering that binds digital image processing and computer vision in common territory.

On the seminal line digital image processing refers to process the digital form of images generated by means of digital devices. Some of the techniques are enlisted here, Image acquisition, enhancement, restoration, compression, segmentation and recognition and many more. Figure 1.1 is summarizing all the important image processing techniques [18]. It is not necessary every process is applied to an image. Some methods take input as image and produces as the output, whereas some methods produce as output which is not a complete image but extracted features of image. Hence the processes shown in figure 1.1 convey an idea all the methodologies that can applied to images for different purposes and objectives. In proposed research image enhancement and segmentation techniques are analyzed, compared, and developed. Diagrammatic representation of proposed work is shown in figure 1.2.

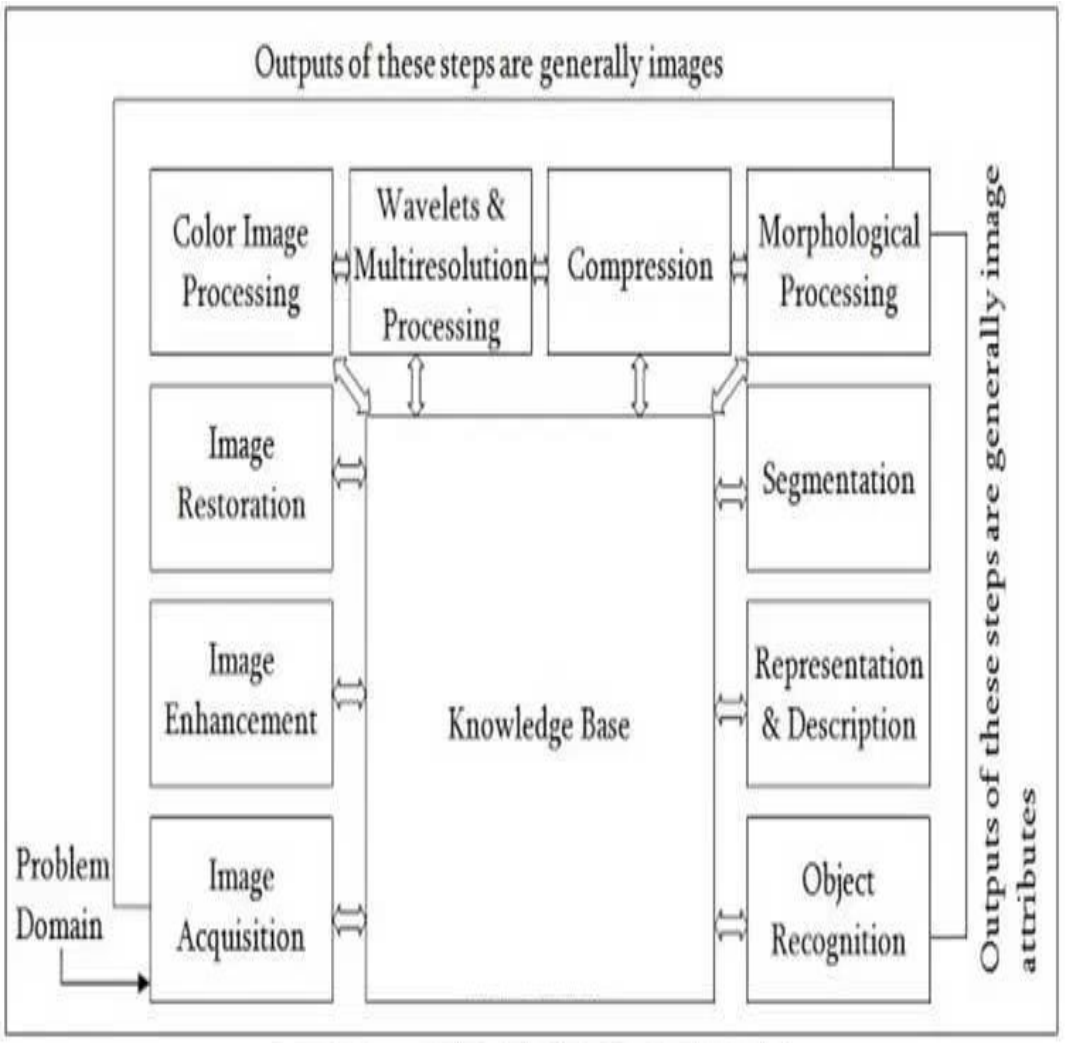

Figure 1.1 Fundamental Steps in Image Processing Techniques

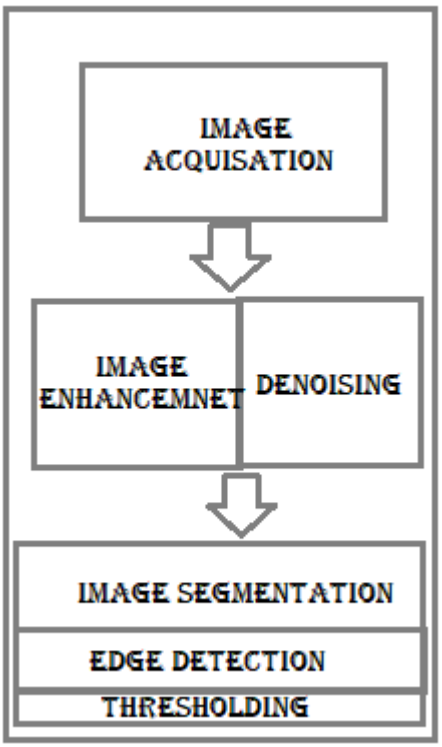

Figure 1.2 Methodologies applied to images

1.2 UNDERSTANDING OF DIGITIZATION OF REAL LIFE IMAGES

A real life picture is taken by a microscope, telescope, camera or any other optical device shows a non-discrete varying array of colour tones and shades. Camera used to produce the video images or film which are subset of all possible images and comprise a varied spectrum of intensities, that are ranging from dark to light and a variety of colours that can have just about any imaginable hue and saturation level.

Images of this type are referred to as analog image**,** because the various combinations of tonal shades and hues blend together without disruption to generate a faithful reproduction of the original scene. Illumination and reflection are two components to generate intensity. Energy radiated by image is continuous electromagnetic waves, while the machines (electronics devices) cannot understand, store and transmits analog frequency based data. Moreover, perceiving the world by using eyes is one of the most important parts of human sensory system. But, human being can see only images which are generated by sources that falls within visual band (wavelength of 700 nanometer to 400 nanometer) of Electromagnetic Spectrum (EM). EM varies

from radio waves, microwaves, infrared waves, X-rays up to gamma rays. Hence, visual wavelengths share a very small portion of entire EM.

Therefore images those are generated by a source of nonvisible energy band, should be visualize, process, and analyzed by some machine before producing in front of naked eyes. Hence, digitization of real world objects is needed.

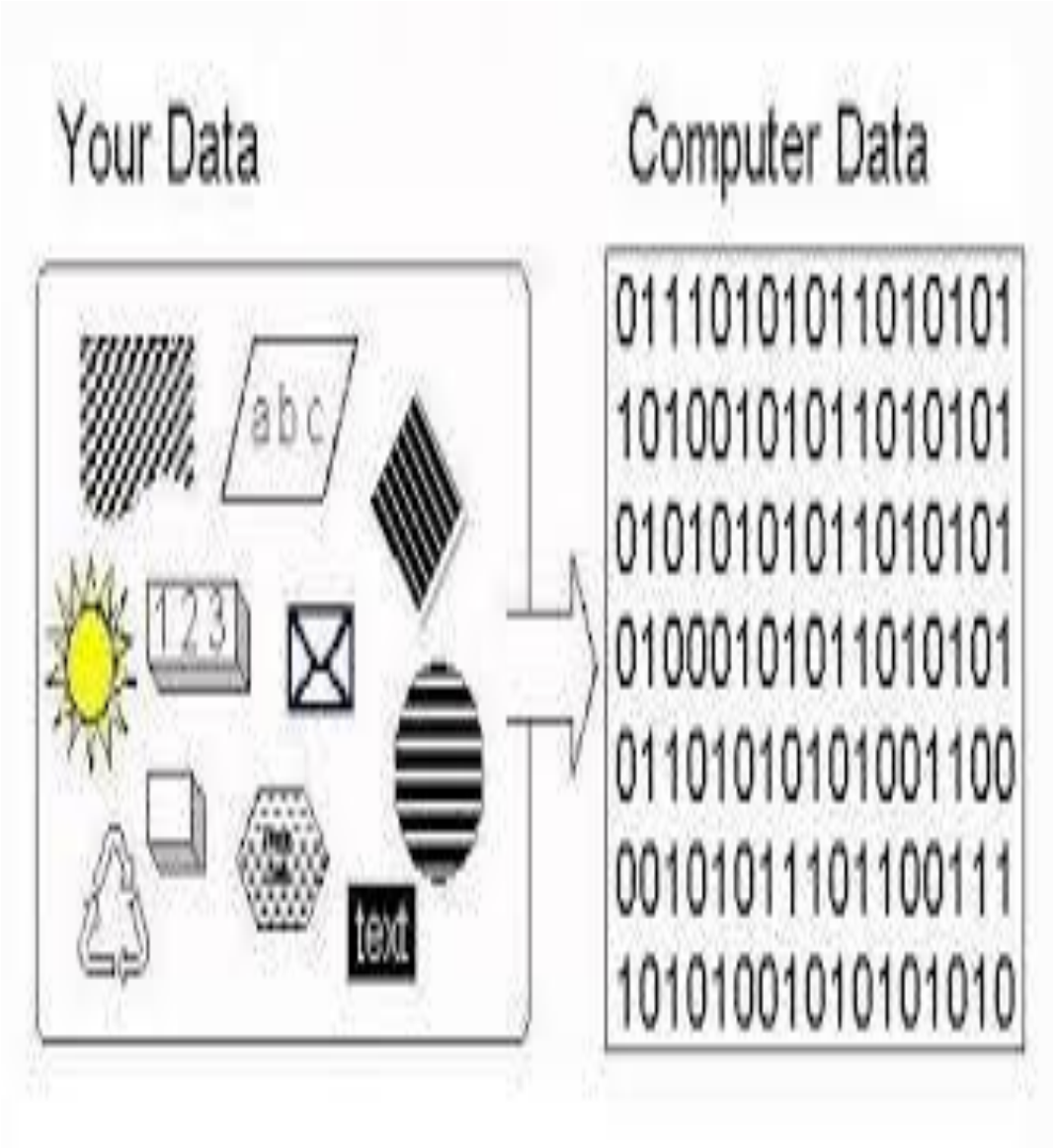

Figure 1.3 Digital Representations of Image Data

1.2.1 Basic Properties of Digital Images

The images that are continuous in nature generated by electronic instruments, analog and optical devices, which precisely record image data by numerous methods, like as

variations in electrical signal or variations in chemical properties of a film emulsion that changes over all dimensions of the image continuously. Analog image must be transformed into a digital format or computer-readable form in order to be processed and displayed by a computer. Therefore images are defined by two dimensional or three dimensional array in digital devices.

This process of digitization is applied to all images, irrespective the complexity and origin and whether they exist as white (grayscale) or full colour and black colour. Due to simplicity of grayscale images, these images will serve as a primary model.

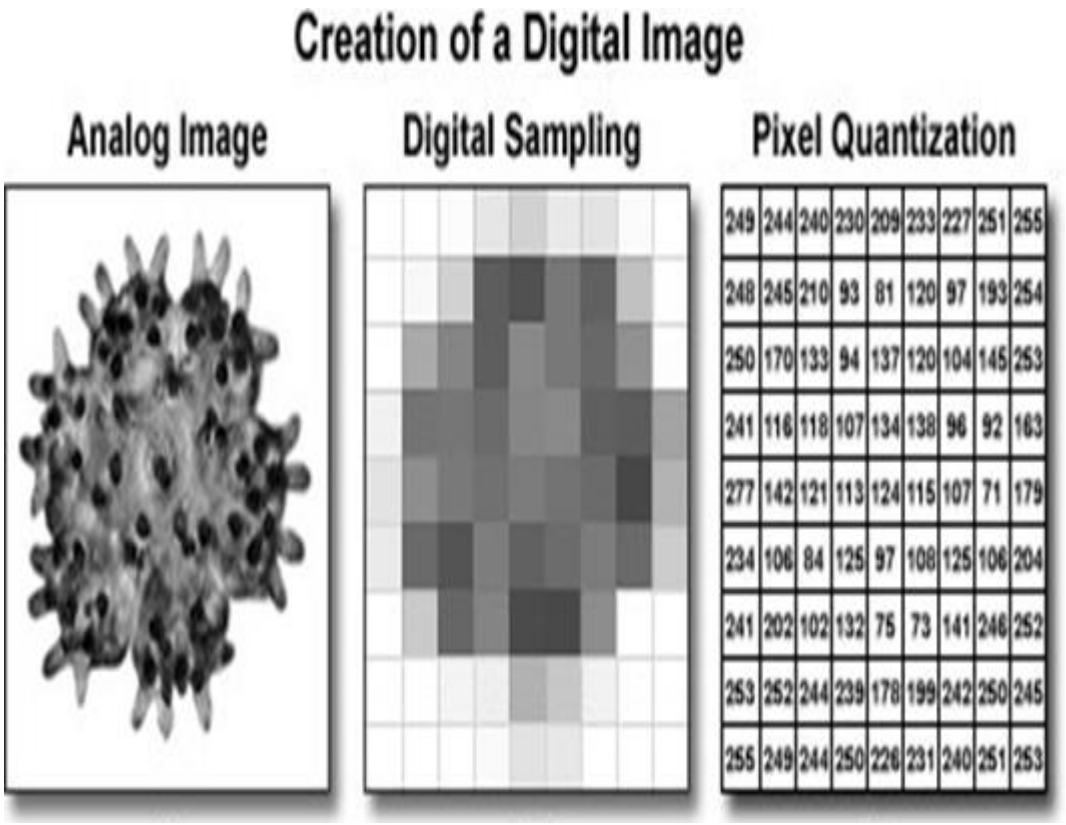

Figure 1.4 Creation of Digital Image

To obtain a digital format of a continuous time image, two operational processes known as sampling and quantization are used to convert the analog image into individual brightness values as shown in figure 1.5. The miniature young starfish captured with the help of an optical microscope is shown in analog form in figure 1.5 (a).

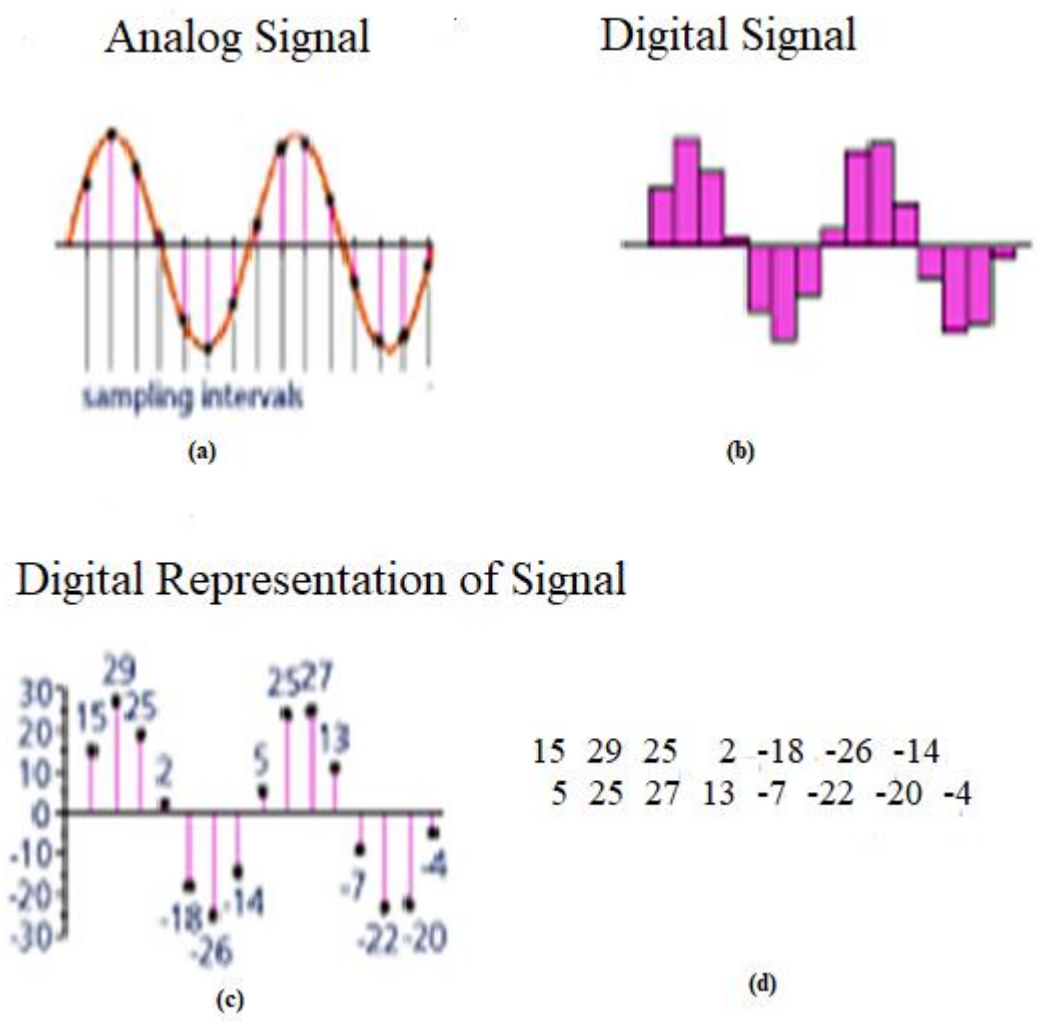

Figure 1.5 Sampling and Quantization of Image Data

After sampling process digital form of analog signal is represented in figure 1.5 (b) and then figure 1.5 (c) represents two dimensional array, the level of brightness at particular points in analog image are obtained and then converted into integers in quantization process shown in figure 1.5 (d). With the help of this process the image is converted into an array of discrete points that every point exhibits particular information about tonal range and brightness and can be represented by a particular digital data value in a specific place.

The intensity at successive locations in the image is measured by sampling process and it produces a two-dimensional array having small rectangular blocks which is representing the intensity information. After completion of sampling process the

resulting information is quantized to allocate a particular digital brightness value to sampled information which is changing from black to white through all intermediate gray levels. This process resulted in intensity in the form of numerical representation, which is generally mentioned as pixel or picture element for each sampled information point in the array.

Because in general, images are either rectangular or square, hence each pixel resulted from image digitization is represented in a Cartesian coordinate system, denoted by a coordinate-pair with particular x and y values. The x coordinate of the pixel represents the column location or horizontal position, while the y coordinate of the pixel represents the vertical position or row number. By convention, the picture element or pixel located at coordinates (0,0) is placed in the upper left-hand corner of the array, while a pixel Px placed at (1,3) would be positioned where the 1st column and 3rd row intersect each other.

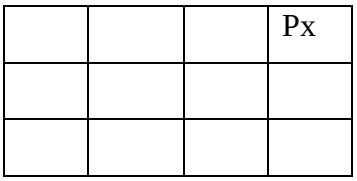

Figure 1.6 Representation of Image in 2-D Array Form

In most of cases, the pixel number is represented by x location and the line number is represented by y location. Hence, a digital image is consisting of a square or rectangular picture element or pixel array denoting a sequence of intensity values and arranged through an (x,y) coordinate system. In actual, the image is represented by a large sequence of data values or array of numbers so that computer can interpret the array which is used to produce a digital representation of the original scene.

The image resolution, representing the quality of a digital image, is determined by the range of brightness values available for every pixel and number of picture elements or pixels used in the image. The image resolution is represented as the capability of the digital image to regenerate fine details presented in the actual analog image. The number of pixels used in construction and rendering a digital image is termed as spatial resolution generally. Spatial resolution depends upon how minutely the image

is sampled in the process of acquisition or digitization, the images having higher spatial resolution represents a greater number of pixels comprise in the same physical space or dimensions. Hence, if the number of pixels acquired in the sampling and quantization process of a digital image increases, then spatial resolution of the image increases.

The number of pixels used to produce a digital image or sampling frequency is determined by matching the electronic and optical resolution of the imaging instrument and computer system used for the visualization of the image. In the process of sampling and quantization a sufficient number of pixels should be generated so that a faithful representation of the optically acquired or original scanned image can be done. A substantial amount of detail can be lost, if the analog images are not properly sampled, as shown in figure 1.7. Either a scanned image or a photograph can be represented as original analog signal as shown in figure 1.7 (a). Before sampling and digitization the continuous intensity variations plotted as a function of sample position are displayed by the original image. As illustrated in figure 1.7 (b), when the size of digital samples taken is 32, most of the characteristic intensities and spatial frequencies that were present in the original analog image, are retained in the resulting image.

If the sampling frequency is decreased as shown in (figure 1.7 (c) and figure 1.7 (d)), some information like characteristic intensities and spatial frequencies that were present in the original analog image are now lost or missed in the conversion from analog to digital and a phenomenon commonly known as aliasing starts to occur. As shown in figure 1.7 (d), the digital image with the lowest number of samples taken as 8, aliasing has occurred and it produced a loss of high spatial frequency data. Simultaneously aliasing has introduced spurious lower frequency data that was not present actually. When the original analog image is compared to the digital image in figure 1.7 (d), this effect is exhibited by the loss of peaks and valleys in between position 0 and 16. Also the peak present at position 3 in the original analog image has now become a valley as shown in figure 1.7(d), while the valley at position 12 has now become as the slope of a peak in the lower resolution digital image.

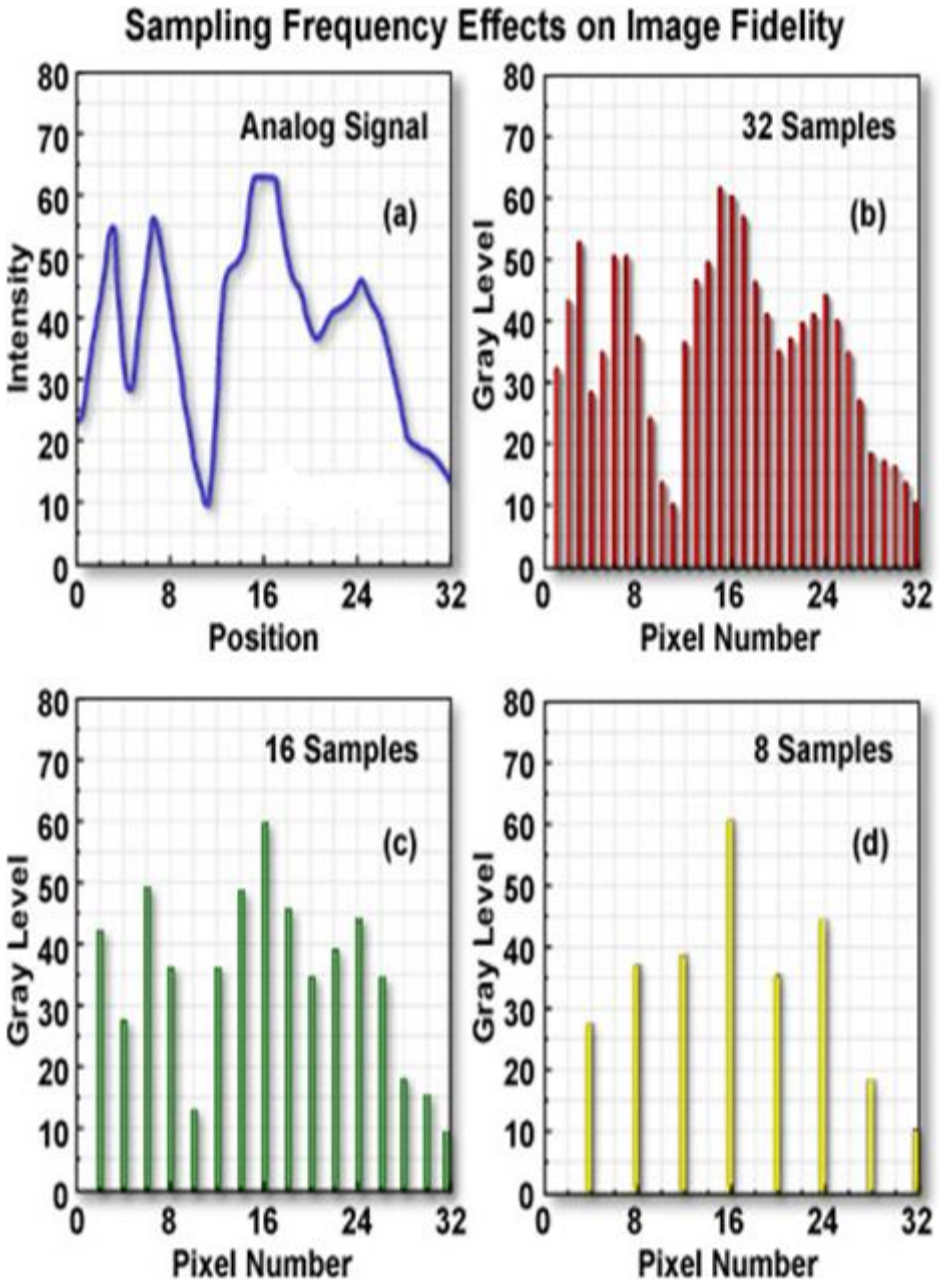

Figure 1.7 Sampling Frequency Effects on Image Fidelity

The optical resolution of the microscope or other optical instruments which are used to take the image and the spatial density of the image are associated to the spatial resolution of a digital image. The accuracy of the electronic device used for digitization depends on the distance between each pixel or sampling interval and the number of pixels confined in a digital image. The optical resolution is related to the quality of the image sensor, electronics and optics, which is a measurement of the ability of the optical lens systems (microscope or camera) that is used to resolve the

details existing in the original scene. The optical resolution used to determine the overall spatial resolution of the image in conjunction with the spatial density i.e. number of pixels in the digital image. In scenario where the optical resolution of the optical imaging system is better to the spatial density, then the spatial resolution of the resulting digital image is determined only by the spatial density.

A digital image primarily consists of image elements or pixels. Every image elements contain details ranging from very coarse to extremely fine which are composed of brightness transitions that cycle between various levels of light and dark. The cycle rate amongst brightness transitions is known as the spatial frequency of the image wherein higher rates corresponds to higher spatial frequencies. Varying levels of brightness in microscopic specimens observed through the microscope are common with the background usually consisting of a uniform intensity and the specimen exhibiting a spectrum of brightness levels. The spatial frequency varies only slightly across the view field in areas where the intensity is relatively constant (like in background). Then again, many specimens often exhibit details with extremes of light and dark having a wide gamut of intensities in between.

For an image to be processed suitably on computer, it must be digitalized spatially as well as in amplitude. Digitization of the spatial coordinates is called image sampling and the distance between pixels is known as sampling interval. The accuracy with which a digital camera is able to capture details accurately, specifically related to spatial frequency, is dependent upon the sampling interval. The numerical value of each pixel in the digital image represents the intensity of the optical image averaged over the sampling interval. Thus, background intensity will consist of a relatively uniform mixture of pixels, while the specimen will often contain pixels with values ranging from very dark to very light. Features seen in the microscope that are smaller than the digital sampling interval (have a high spatial frequency) will not be represented accurately in the digital image. The Nyquist criterion requires a sampling interval equal to twice the highest specimen spatial frequency to accurately preserve the spatial resolution in the ensuing digital image. An equivalent measure is Shannon's sampling theorem, which states that the digitizing device must utilize a sampling interval that is no greater than one-half the size of the smallest resolvable feature of

the optical image. In order to to capture the smallest degree of detail present in a specimen, two samples need to be collected for each feature so that sampling frequency is sufficient thereby guaranteeing that both light and dark portion of the spatial period are gathered by the imaging device.

The final digital image containing details with high spatial frequency will not have required accuracy, if sampling of the specimen occurs at an interval beneath that required by the Nyquist criterion or Shannon theorem. In the optical microscope, the Abbe limit of resolution for optical images is 0.22 micrometers, meaning that a digitizer must be capable of sampling at intervals that correspond in the specimen space to 0.11 micrometers or less. A digitizer that samples the specimen at 512 points (or pixels) per horizontal scan line would produce a maximum horizontal field of view of about 56 micrometers (512 x 0.11 micrometers). If fewer pixels are utilized in sample acquisition, then all of the spatial details comprising the specimen will not get representation in the final image. Conversely, if too many pixels are gathered by the imaging device (often as a result of excessive optical magnification), no additional spatial information is afforded, and the image is said to have been oversampled. The extra pixels do not theoretically contribute to the spatial resolution, but can often help improve the accuracy of feature measurements taken from a digital image. To ensure adequate sampling for high-resolution imaging, an interval of 2.5 to 3 samples for the smallest resolvable feature is suggested.

Most of the digital cameras that are coupled to modern microscopes and other optical instruments have a fixed minimum sampling interval, which cannot be adjusted to match the specimen's spatial frequency. It is important to choose a camera and digitizer combination that can meet the minimum spatial resolution requirements of the microscope magnification and specimen features. If the sampling interval exceeds than necessary for a particular specimen, the resulting digital image will contain more data than is needed, but no spatial information will be lost.

Generally an entry-level digital camera produces digital image size of 640 x 480 pixels, which equals 307,200 individual sensor elements. Most of these entry-level digital cameras are designed to be coupled to an optical microscope containing an image sensor having pixel dimensions around 7.6 square microns, which produces a

corresponding image area of 4.86 x 3.64 millimetres on the surface of the photodiode array when the sensor is operating in VGA mode. The ultimate resolution of a digital image sensor is a function of the number of photodiodes and their size relative to the image projected onto the surface of the array by the microscope optics. A specimen imaged with a digital microscope with acceptable resolution can only be achieved if at least two samples are made for each resolvable unit. The numerical aperture of lower-end microscopes ranges from approximately 0.05 at the lowest optical magnification (0.5x) to about 0.95 at the highest magnification (100x without oil). Considering an average visible light wavelength of 550 nanometers and an optical resolution range between 0.5 and 7 microns (depending upon magnification), the sensor element size is adequate to capture all of the details present in most specimens at intermediate to high magnifications without significant sacrifice in resolution. A serious sampling artefact, known as spatial aliasing, occurs when details present in the analog image or actual specimen are sampled at a rate less than twice their spatial frequency. This phenomenon, also commonly termed under sampling, typically occurs when the pixels in the digitizer are spaced too far apart compared to the high-frequency detail present in the image. As a result, the highest frequency information necessary to accurately render analog image details can pretence as lower spatial frequency features that are not actually present in the digital image. Aliasing usually occurs as an abrupt transition when the sampling frequency drops below a critical level, which is about 1.5 times that of repetitive high-frequency specimen patterns, or about 25 percent below the Nyquist resolution limit. Specimens containing regularly spaced, repetitive patterns often exhibit moir Ã fringes that result from aliasing artefacts induced by under sampling.

1.3 IMAGE BRIGHTNESS AND BIT DEPTH

Brightness and grey level of any pixel are two important parameter of any image. Both are function of energy radiated by any particular pixel. Brightness of any image is function of pixels is relative intensity values after digitization. Digitization is done by an analog-to-digital converter.

Brightness should not be resembled with grey level or degree of energy truly reflected from object. Discrete version of analog image explain brightness more properly

described, “it is measured intensity of all the pixels comprising an ensemble that constitutes the digital image after it has been captured, digitized, and displayed”. Pixel brightness is significant component in digital images, because it is used by processing techniques to quantitatively adjust the image.

After an image has been digitized i.e. quantized and sampled, each discrete unit is represented either by a digital integer or by an analog grey level value on CRT. Brightness is represented by continuous tone intensity within the specimen into a digital value.

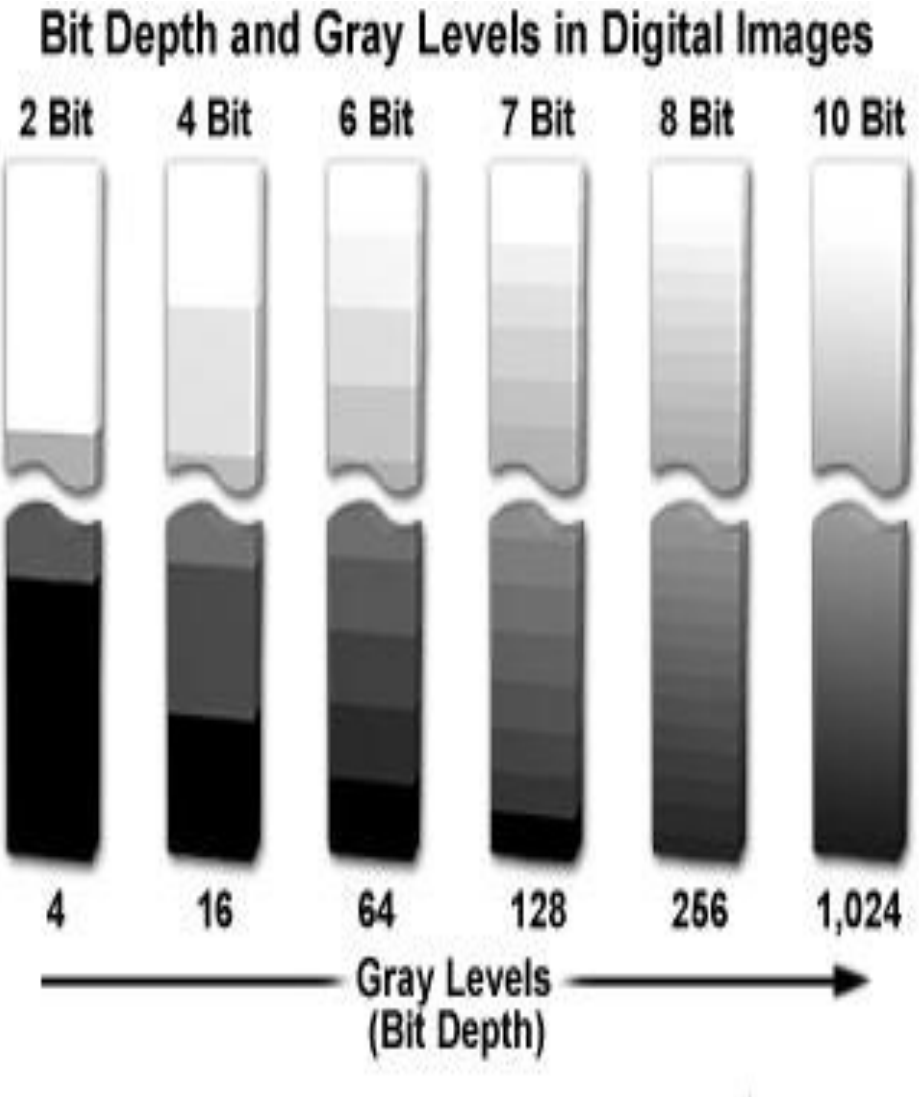

Figure 1.8 Bit Depth and Gray Levels in Digital Images

Accurate representation of real time image in to its machine version depends upon bit depth of the digitizing device or simply number of bits going to store one pixel. So, bit depth is function of number of bits that are using to store single pixel. Higher order bit depth represents clearer image of any object. If image has 3 bits it represents by 8 brightness levels, where as 4 bits have 16 brightness levels, as shown in figure 1.8. Lowest bit depth represents black, while the upper level represents white colour. Moreover each intermediate level corresponds to different shades of gray level.

Table 1.1 shows relation between gray levels and bit depth very clearly. An upper quantity of bit depth results in to better pixel intensity and facilitates accurate representation of real time picture. It should be kept in mind; combination of black, white, and gray brightness levels constitutes the variation in brightness of the image.

Table 1.1 Bit Depth, Gray Levels and Sensor Dynamic Range

Bit Depth	**Grayscale Levels**	**Dynamic Range (Decibels)**
1	2	6 dB
2	4	12 dB
3	8	18 dB
4	16	24 dB
5	32	30 dB
6	64	36 dB
7	128	42 dB
8	256	48 dB
9	512	54 dB
10	1,024	60 dB
11	2,048	66 dB
12	4,096	72 dB
13	8,192	78 dB
14	16,384	84 dB
16	65,536	96 dB
18	262,144	108 dB
20	1,048,576	120 dB

Colour images are combination of three colours red, green, and blue (RGB). RGB based images have different intensity levels consisting of varying brightness levels for each colour. To represent ultimate image a fixed ratio of RGB colour combined within each pixel. Hence RGB colours are known as primary colours. Colour image representation will be discussed shortly.

In digital devices ‘bit’ is the smallest unit of information. That makes Byte, Kilo Bytes, Mega Byte and Tera Bytes. In binary number system different numbers are represented by only two digits i.e. 1 and 0. Black and white image has 1-bit resolution and 2 bit depth. To, digitized image the effect of grey level, bit depth and processing speed must be understand.

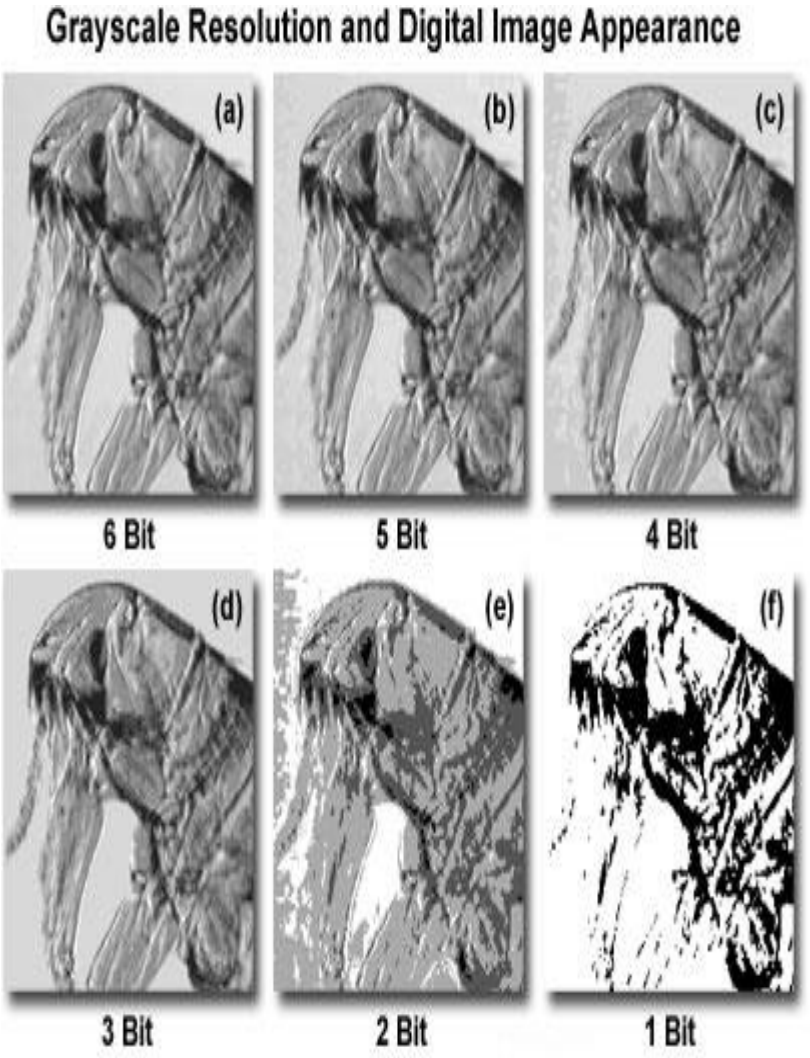

Figure 1.9 Trade Off Between Resolution And Appearance

Lower depth level of bits is resulting in loss of important information. To, understand this, an specimen of common flea is shown in figures 1.9 (a) to 1.9(f). The specimen is represented by 6-bit (Figure 1.9 (a)) to 1-bit 1.9 (f). Figure 1.9 (a) has highest resolution and displaying maximum details. Figure 1.9 (c) has 4 bit it means 16 gray levels; start to attain loss in visual. Figures 1.9 (d) – 1.9 (f) resolution of grey level is gradually decreasing and inadequate to represent information.

For a majority of the online visual applications, present on output screen used six or seven bit resolution. It is typically adequate for displaying digital images on computer screen by eight or sixteen bits.

Finally, the judgment on number of pixels and variety of intensity are essential to satisfactorily illustrate an appearance of image is dictated by the materialistic attributes of the original scene (or accusation methods.).

Many low contrasts, high-resolution images require a higher quantity of pixels and variety of intensities to construct acceptable image, while other high contrast and low resolution images (simple geometric objects) can be sufficiently represented with a considerably small number of pixels as well as low gray level.

Finally, there is a trade-off in processing speed among contrast, number of bits to store one pixel, bit depth, and the transmission speed. Images having variations in colour depth will involve more CPU cycles than those having fewer pixels and gray levels. However, any advanced machine or electronic devices is proficient in processing complex calculations on digital images in general sizes (six hundred forty x four hundred eighty through Twelve hundred eighty x One thousand twenty four) speedily.

Images generated by photoshop, Corel draw are larger in size and containing many layers, may diminish performance, but can still be processed in less time by using high processing power machine as well as personal computers.

Til now resolution of Gray images has been discussed. A gray image has various shades of gray. If 8 bits are used to store gray images, it can generate 256 shades of

gray. In next subsection different types of colour level of images are going to be discussed.

1.3.1 Colour Space Models

Colours are most important components of our life. Without colour nature cannot be imagine. A colourful image speaks a lot. So, it is very important to digitized colour images also. Digital images produced in colour are involved sampling, quantization, spatial resolution, bit depth, and dynamic range that apply to their grayscale counterparts.

Colour model or colour space model can be divided into three types:

(i) RGB model

(ii) CMY model

(iii) HSI model.

In this section these three models will be discussed in brief.

RGB Model:

RGB model shown in figure 1.10 represents into three axis. Red colour is represented by x axis, Green colour is represented by y axis, whereas Yellow colour represented by z axis of three dimensional space.

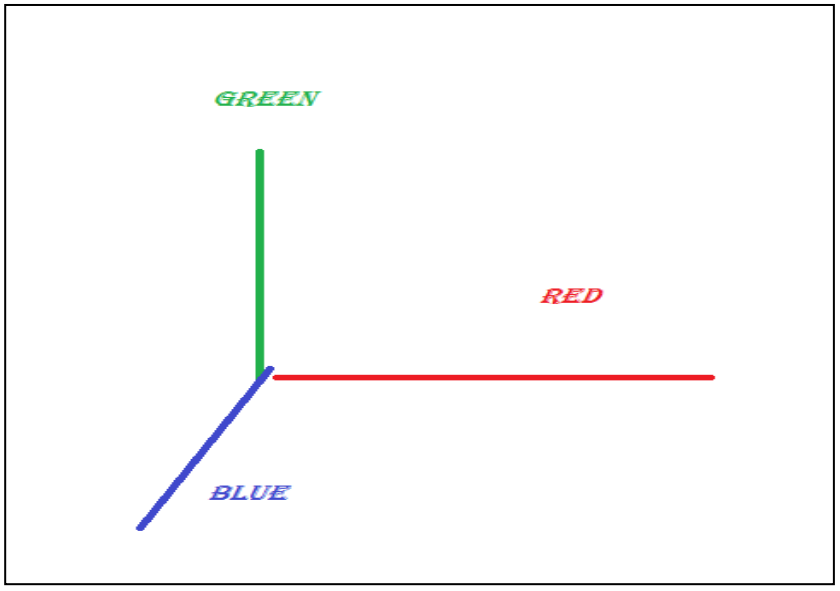

Figure 1.10 RGB Space Model

These three primary colours, red, green, and blue, can be selectively combined to produce all of the colours in the visible light spectrum. Together, these primary colours constitute a colour space (commonly referred to as a colour gamut) that can serve as the basis for processing and display of colour digital images.

In general, the RGB colour space is utilized like display screen, LED, TFT monitor and image sensors. Hardcopy devices required another model to represent colour.

CMY Model

If a digital image must be printed, it is first acquired and processed as an RGB image, and then converted into the cyan, magenta, yellow (CMY) colour space necessary for three-colour printing, either by the processing software application, or by the printer itself shown in figure 1.11.

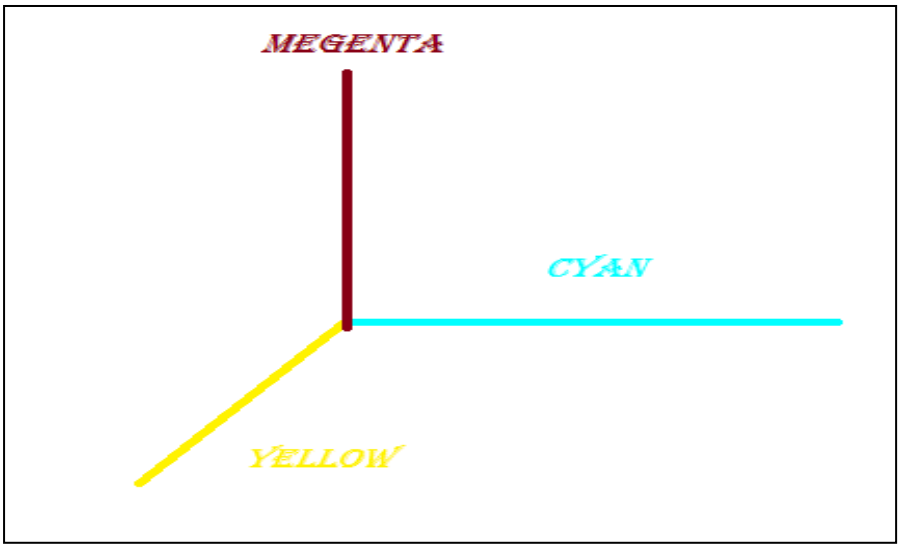

Figure 1.11 CMY Space Model

HSI Model

In some cases, an alternate colour space model is more appropriate for specific algorithms or applications, which requires only a simple mathematical conversion of the red, green, and blue (RGB) space into another colour space. For example, if a digital image must be printed, it is first acquired and processed as an RGB image, and

then converted into the cyan, magenta, yellow (CMY) colour space necessary for three-colour printing, either by the processing software application, or by the printer itself.

HSI Colour Model

The most popular alternative colour-space model is the hue, saturation, and intensity (HSI) colour space, which represents colour in an intuitive way (the manner in which humans tend to perceive it). Instead of describing characteristics of individual colours or mixtures, as with the RGB colour space, the HSI colour space is modelled on the intuitive components of colour. For example, the hue component controls the colour spectrum (red, green, blue, yellow, etc.), while the saturation component regulates colour purity, and the intensity component controls how bright the colour appears.

Numerous derivatives of the HSI colour-space model have been devised.

a) hue, saturation, lightness or (HSL) model
b) hue, saturation, brightness (HSB), model

The terms brightness, lightness, value, and intensity are often used interchangeably, but actually represent distinctively different manifestations of how bright a colour appears. Each colour-space model provides a colour representation scheme that is tailored for a particular application.

1.3.2 Digital Image Storage Requirements

Individual pixel coordinates of digital images are not stored in common computer file formats, to save storage resources. The reason behind this is that images are digitized in sequential order by raster scanning or array readout of either an optical or analog image by the digitizing device (CCD, scanner, etc.), which then transfers data to the computer in a serial string of pixel brightness values. According to the established image vertical and horizontal dimensions, which are usually recorded in the image file header, the image is then displayed by incremental counting of pixels.

There are several ways to express the features of digital images. For example, the pixel array size (for example, 640 x 480) can be utilized or the number of pixels in a given length dimension (such as pixels per inch) can be specified. As an alternative, the computer storage file size or the total number of image pixels also provides an indication of the image sizes. File sizes, in bytes, can be determined by dividing the pixel dimensions by 8 (the number of bits per byte) and multiplying that number by the bit depth. For example, a 640 x 480 (pixel) image having 8-bit resolution will require 302 kb of computer memory as represented in Table 2. Likewise a high-resolution 1280 x 1024 true colour image with 24-bit depth will require over 3.8 mb of storage space.

Table 1.2 represents Digital image file size as a function of pixel dimensions, format, and bit depth is presented for a wide range of images. Uncompressed file formats, such as "Windows" Image Bitmaps (BMP) and Tagged Image File Format (TIFF) require huge space when encoded in full colour though they have a better Image quality. In contrast, common compression algorithms, including the popular Joint Photographic Experts Group (JPEG) technique, can significantly reduce storage requirements while maintaining a reasonable degree of image quality. In determining how digital images should be stored, the significant factors like target output and the pixel depth requirements are also considered. For Instance, images destined for printed media require high pixel resolutions (frequently exceeding 300 pixels per inch), whereas those intended for distribution over the Internet benefit from reduced file size and resolution (around 72 pixels per inch).

With the advent of relatively low-cost computer memory (RAM), coupled with dramatically improved capacity and speed, storage of digital images is not as big an issue as it used to be in the past. The personal computers can now be utilized to store and manipulated the huge digitized arrays, up to 1024 x 1024 pixels with 10, 12, or 16-bit depths at high speeds. In addition, dozens of smaller (640 x 480, 8-bit) images can be stored as stacks and quickly accessed for playback as video-rate movies utilizing for simultaneous image processing or commercially available software.

Multiple digital images acquired via optical section confocal and multiphoton microscopy techniques or taken in orders using CMOS or CCD image sensors, can be

Table 1.2 Digital File Format Memory Requirements

Pixel Dimensions	**Grayscale (8-Bit)**	**Bitmap (24-Bit)**	**JPEG (24-Bit)**	**TIFF (24-Bit)**
16 x 16	2k	2k	2k	2k
64 x 64	6k	13k	5k	13k
128 x 128	18k	49k	12k	49k
256 x 256	66k	193k	22k	193k
320 x 240	77k	226k	24k	226k
512 x 512	258k	769k	52k	770k
640 x 480	302k	901k	56k	902k
800 x 600	470k	1,407k	75k	1,408k
1024 x 768	770k	2,305k	104k	2,306k
1280 x 1024	1,282k	3,841k	147k	3,842k
1600 x 1200	1,877k	5,626k	161k	5,627k
2250 x 1800	3,960k	11,869k	276k	11,867k
3200 x 2560	8,002k	24,001k	458k	24,002k
3840 x 3072	11,522k	34,561k	611k	34,562k

quickly presented and manipulated. To visualize a pseudo 3-dimensional performance of a microscopic scene, common stereo pair is used generated by projections of an

optical section stack alongwith two properly tilted axes. A number of display techniques to be utilized to imagine objects by pseudo colour assignments or intensity-coded, are allowed in latest digital image processing software packages. In successive time slots if multiple images are recorded then images can be presented as 2-dimensional "movies" or if combined to produce 4-dimensional images then in this a 3-dimensional object is represented as a function of time.

The significant images of 3-dimensional objects are generated by using advanced digital image processing techniques and display operation which may execute an object with suitable colouring, shading and depth cues. Generally there are two techniques i.e. surface rendering and volume rendering, which are utilized to render the optical segments for display in 3-dimensions. In surface rendering of an optical image set, only the surface pixels which represent the outside surface of the specimen are used and due to the opacity of surface the inner structure is not visible. For the production of a visually acceptable performance perspective, depth cues and lightening are necessary. In volume rendering of an optical image set, intensity information and the 2-dimensional pixel geometry is clubbed with the known focal displacements used to produce volume elements, known as voxels. The voxels produced are then properly shaded and projected to give an outlook of the specimen volume with connected lighting and perspective to generate a 3-dimensional picture.

1.4 TYPES OF IMAGE SEGMENTATION

Segmentation of the image is the first step in image analysis which divides an image into its constituent parts. Image segmentation is a fundamental process in many image, video, and computer vision applications. It is often used to partition an image into separate regions, which ideally correspond to different real-world objects. It is a critical step towards content analysis and image understanding.

Broadly, there are two types of segmentation techniques:

- Discontinuity based segmentation techniques
- Similarity based segmentation techniques

In the first technique, the methodology is to partition of an image based on unexpected variations in gray-level image. Threshold and region growing are the bases of the second technique.

1.4.1 Discontinuity Based Detection

Discontinuity detection is defined as partitioning an image based on abrupt changes in intensities of gray-level images.

Edge Detection:

Edge detection is an important tool which is used in image processing applications to acquire information from image. Edges and region boundaries are closely related to each other, as sharp change in intensity occurred at the region boundaries. Therefore edge detection techniques are also used as the base for the segmentation methods. The edges are frequently disconnected which are found by edge detection techniques. However the closed region boundaries are required to segment an object from an image. Boundaries between objects and the background in the image and outlines of an object are detected by edge detection technique. The look of blurred image can be improved by using the edge detection filter.

1.4.2 Similarity Based Segmentation Techniques

The gray levels of pixels belonging to the object are entirely different from the gray levels of the pixels belonging to the background in many applications of image processing. Thresholding becomes then a simple but effective tool to separate those foreground objects from the background. We can divide the pixels in the image into two major groups according to their gray-level. These gray-levels may serve as "detectors" to distinguish between background and objects and is considered as a foreground in the image [2]. Select a gray-level between those two major gray-level groups, which will serve as a threshold to distinguish the two groups (objects and background). Image segmentation is performed by such as boundary detection or region dependent techniques. But the thresholding techniques are more perfect, simple and widely used [3].

Types of Thresholding Techniques:

Thresholding based image segmentation can be divided broadly into two categories

- **Global Thresholding Technique**
- **Local Thresholding Technique**

1.4.2.1 Global Thresholding Technique

Global methods apply one threshold to the entire image while Local Thresholding sometimes used to segment the item from the background to read and identify the image correctly. For this purpose there are two techniques of segmentation, similarity detection technique and discontinuity detection technique.

During the thresholding process, individual pixels in an image are marked as “object” pixels if their value is greater than some threshold value (assuming an object to be brighter than the background) and as “background” pixels otherwise.

1.4.2.2 Local Thresholding Techniques.

In Local Thresholding technique, a threshold T(x, y) is calculated for each pixel based on some local statistics such as range, variance, or surface-fitting parameters of the neighborhood pixels within a local block of size w×w. Consider a grayscale document image in which I(x, y) be the intensity of a pixel at location (x , y) In local adaptive thresholding techniques, the aim is to compute a local threshold T(x , y) for each pixel such that the intensity of a pixel at location (x, y) of the image must be greater than predefined threshold T.

1.5 MOTIVATION OF STUDY

Object detection and tracking is an important task within the field of computer vision, due to its promising applications in many areas, such as video surveillance, traffic monitoring, vehicle navigation etc. The availability of high quality and inexpensive video cameras and the increasing need for automated video analysis has generated a great deal of interest in the areas of motion detection, object tracking and gesture analysis. Thus on a very high-level, it’s possible to identify three key steps in video analysis: detection of interesting moving objects, tracking of the detected objects from frame to frame, and analysis of the object tracks to recognize their behavior.

Object detection is a computer technology related to computer vision and image processing that deals with detecting, in digital images and videos, instances of semantic objects of a certain class, such as:- humans, buildings, cars, etc.

Well-researched domains of object detection include face detection and pedestrian detection. Object detection has applications in many areas of computer vision, including image retrieval and video surveillance.

In computer vision, the process of partitioning a digital image into various segments or sets of pixels known as super pixels is called as segmentation. With the objective to obtain something more meaningful and easy to analyse, segmentation technique is used to simplify and/or change the appearance of an image. To locate boundaries such as lines, curves, etc. and objects in images, the image segmentation technique is generally utilized. Therefore, assigning a label to each and every pixel in an image so that pixels with the same label have certain or a specific visual characteristic is called image segmentation.

1.6 OBJECTIVES OF RESESRCH

The applications of computer vision are ranging from biometric identification to object recognition. The problem is rather challenging, since a ship may generate innumerable images with diverse appearances, poses, viewpoints and illumination. The complicated sea background with flooding waves makes this image worse as well. Recently, image segmentation is proven as one of the dominated tool to detect objects. Therefore image segmentation is applied in proposed work to detect abandoned ship in sea as a task of computer vision.

Proposed research is divided in three levels that logically overlap over digital image processing, computer vision and image analysis. In first level noisy images are taken as input and produces clear output. In second level, images are segmented on the basis of attributes (edges or thresholding) for the purpose of partitioning the object of interest from the background. At the final stage or third level individual object is recognized by analysing subset of the available aperture.

The objective of the present research work is to study the performance of various object detection track algorithm and its image processing that appeared in the literature and to modify the possibilities of enhancements for the existing model and further to apply fuzzy on the mode. The objectives are ---

1. Analysis and development of Object Detection Algorithm.
2. To analyse Object Track algorithm using infrared red detection technique.

3. To explore the Strategies in Ship Detection with the Sub Aperture Cross-Correlation Magnitude.
4. To analyse a modified Ant Colony Optimization Based Approach for Image Edge Detection.
5. To analyse Application of Noise-resistant Algorithm for Edge Detection.
6. Comparison of used Object Detection Algorithms.

1.7 RESEARCH METHODOLOGIES

The images of ship from sea water are affected by sparsely occurring white and black pixels. Moreover clarity of sea water images can be affected by sharp and sudden disturbances in the image signal. This rippling character of ocean water waves helps in hiding small ships. Moreover leads to piercing in security by enemy and smugglers.

These sharp and sudden disturbances in the image signal are known as impulse noise. Median filter is well known filter to remove this noise, but it is failed in some case, where pixels intensity are at diversify. This phenomena triggers search of new filters that ends at aggregation operators based filter.

Object detection is the task of finding a given object in an image or video sequence. Humans recognize a multitude of objects in images with little effort, despite the fact that the image of the objects may vary somewhat in different viewpoints, in many different sizes / scale or even when they are translated or rotated. Objects can even be recognized when they are partially obstructed from view. This task is still a challenge for computer vision systems in general. Other methodologies are based on image segmentation. Image segmentation is used to detect tough man-made objects in sea water by using infrared images and Radar images.

To detect edges of small boat, fuzzy membership function Ant System based algorithm is used and compared with fuzzy mean based ACO edge detection algorithm.

1.8 DESCRIPTION OF THESIS CHAPTERS

In this thesis chapter 2 is Literature Review which consists of literature survey. Related work of this chapter will be divided into four parts,

(i) Image Segmentation: This part content all the literature related to image segmentation based on similarity like thresholding technique.

(ii) Image segmentation based on discontinuity: There are various attributes that exists in image to extract object of interest or sub part of the image. One of the kinds of feature is abrupt change in intensity of pixel. This characteristic of pixel is helpful in identification of edges of object of interest. This part throws light on conventional and new methods of edge detection.

(iii) This part is dedicated on litterateur survey of various method of noise removal in an image.

(iv) Soft Computing based Techniques

Due to high sensitivity of strategically importance of sea border, detection of motion of enemy's military troops and arms may play a crucial role. Attack of 26, November, 2008 on Mumbai, commercial capital of India, is the result of such type of piercing of water territory. Hence, in this paper a Threshold based new method proposed to detect ship in sea environment. Infrared images of ship in sea water are used as input. To, specify appropriate threshold Yager's Linguistic quantifier 'most', 'at least half', and 'as many as possible' are used. Moreover edge based segmentation of thresholding images is carried out by using Laplacian operator. It is observed that threshold generated by 'at least half' and 'as many as possible' quantifier are closer to visual heuristic threshold. It is also found linguistic quantifier based thresholding has generated clear edge to separate ship from background along with digital approximation of Laplace operator than other methods. Hence, proposed research, Chapter 3 is dedicated to analyzed detection of Small Object in Infrared Images.

Image de-noising has been an active area in image processing in recent past. Therefore chapter 4 applied ordered weighted averaging (OWA) based linear objective function is used to remove impulse noise to get a clear image of ship in a sea

environment. Moreover, Salt & Pepper/Impulse noise may be introduced into images during acquisition, transmission, and flooding waves. Salt & Pepper and Impulse noise both are same types of noise, hence in rest of the article are used interchangeably. Therefore, chapter 4 covered De-noising of Infrared Image of Ship under Sea Water.

Improved version of Sub-aperture Cross-Correlation Magnitude (SCM) is used to detect small ship targets in synthetic aperture radar (SAR) images of sea water. Spectrum shifted to zero azimuth frequency. An pre-processed SAR image is taken as input, Azimuth bandwidth reduction, Sub-band extraction, Up-sampling, Hermitian inner product, Low pass filter, Down-sampling, and Local Averaging are the steps to produce clear image. All these things are covered in chapter 5.

Image segmentation is one of the most nontrivial tasks of machine vision to detect abandoned ship in sea. Point, Line and Edge detection are example of discontinuities Based Segmentation. Edge detection is in particular one of the staple and popular segmentation techniques. It is seen conventional edge detection technique results low performance in terms of time complexity if the size of image is increased. Moreover, situation becomes more venerable in the presence of discontinuities between the edge's pixels. Hence, in proposed work one of the bio inspired technique Ant Colony Optimization (ACO) based approach is used to detect edges of a ship in sea environment. To improve time complexity triangular fuzzy member ship function is used. The outcome of proposed work shows clear edges of small and partial objects. Therefor Image Edge Detection Based on modified Ant Colony Optimization is done in chapter 6.

Chapter 7 explains the differences and comparison of some famous edge detection algorithms and evaluates them on the basis of their results to different images. Gradient based edge detectors like Prewitt and Sobel are relatively simple and easy to implement, but are very sensitive to noise. LoG tests wider area around the pixel and find the edges correctly, but malfunctions at corners and curves. It also does not find edge orientation because of using Laplacian filter. Cannys algorithm is an optimal solution to problem of edge detection which gives better detection especially in presence of noise, but it is time consuming and requires a lot of parameter setting.

Chapter 8 concluded the research. This chapter future direction for further exploring the proposed work is also discussed. In proposed research small objects like ship in sea water are detected by using two methods. There are two main technique is used to detect small objects. Proposed Object Track algorithm is better if input images are infrared images; this technique is also capable to capture movement of enemy troops due to its heat sensing property, whereas SCM version of ship detection is useful when input image is taken from RADAR in highly agitated sea water.

- Object Track algorithm using infrared red detection technique.
- Sub-aperture Cross-Correlation Magnitude based technique.

Infrared image of ship is segmented from background i.e. sea water using global thresholding to identify the location of ship. Infrared image is taken as input due to its high heat signature.

Results produced by 'at least half ', and 'as many as possible' linguistic quantifier are much closer to visual inspection. The output of Sobel object detection is not very clear. OWA operators are used for segmenting ship in static images, In future same methodology can be used for moving ship and it is accepted to produce good results.

Further infrared image of ship in sea is de-noised from Impulse noise. Impulse noise may be introduced into thermal images either due to flood waves in sea water or during acquisition and transmission.

Results generated by proposed method, which is application of OWA operator, shows quite satisfactory performance. In future more fuzzy quantifier like 'as many as possible', 'at least half' can be used to de-noising the image. The filtered image can be used for tracking of ship or movement of military troops in the water territory by using different segmentation techniques.

ACO search methodology based on a triangular membership function based heuristic to detect edges of ship under sea water. The general idea underlying the Ant Colony System paradigm is that ants are directed by quantity of pheromone on the various path. Higher quantity of pheromone on any path from source to destination is indicated that, it was followed by a good number of ants and may leads to shortest path. To construct final pheromone matrix threshold is used. Proposed work gives better results as compared to other conventional methods of edge detection.

1.9 Contribution

In proposed research images of ship under sea water are de-noised by impulse noise. For de-noising images aggregation operators are used, and compared with well-established median filter. Results generated by OWA filter are quite satisfactory.

Further different types of edge detection techniques are analyzed and their advantages and disadvantages are outlined.

Moreover, to detect image of ship from the sea water ACO based edge detector is developed and analysed. It is found in less computing time more clear edges are plotted by fuzzy based heuristic. Proposed work gives better results as compared to other conventional methods of edge detection.

As a next step ship is segmented on the basis of fuzzy linguistic thresholding. Performance of three fuzzy operators is compared.

Detection of difficult man-made targets with low backscattering coefficients and low contrast to the background sea clutter is done by using cross-correlation of sub-aperture measurements. Radar images of sea under sea water are treated as input images.

CHAPTER II
LITERATURE REVIEW

2.1 INTRODUCTION

Digital Image Processing is a domain that process and improve images by using machines for human interpretation. There are various digital image processing techniques that can be applied to images for different purposes. Digital Image Processing related to the preparation of an image which can analyse and use further for the images captured by a camera or similar techniques which are not necessarily in a form that can be used by image analysis routines. Some may need improvement to reduce noise, others may need to be simplified, and still others may need to be enhanced, altered segmented, filtered, with some objective or analysis purpose. Image processing is the collection of routines and techniques that improve, simplify, enhance, or otherwise alter an image. Recognizing objects and their background in real life applications can be managed by segmentation in computer vision.

2.2 LITERATURE SURVEY

Proposed research is divided in three levels that logically overlap over digital image processing, computer vision and image analysis. In first level noisy images are taken as input and produces clear images as outputs. In second level images are segmented on the basis of attributes (edges or thresholding) for the purpose of partitioning object of interest from the background. At the final stage or third level individual objects are recognized by analyzing subset of the available aperture. Which leads division of literature survey into four fragments as mentioned below:

(i) Segmentation based on similarity
(ii) Noise removal
(iii) Segmentation based on dissimilarity
(iv) Soft Computing based Techniques

2.2.1 Segmentation Based on Similarity

This part contains all the literature related to image segmentation based on similarity like thresholding technique. In the past decades, image semantic segmentation has

been usually established by using supervised neural network [3-11].Techniques based on Supervised Neural Network are not only effort exhaustive but also slow. As a consequence, a promising solution is required to explore segmentation methods with no supervision.

Yuan et al. [6] presented graph-based ranking and segmentation algorithms for traffic sign detection. However, the aforementioned methods are all built on the basis of having sufficient pixel-wise annotated samples for training. As the output of existing automatic systems is far from satisfaction, the vast majority of these annotations are obtained manually, which is labor intensive and time-consuming. Accordingly, the fully supervised networks are typically un-adaptable to general application in the reality. On the other side, there are some unsupervised semantic network based segmentation methods that utilize image data without any annotation for training [11]. Instead of the ground truth of each pixel, weakly supervised semantic segmentation approaches [12-14] often required image level annotations for training. Besides, in [13]author built a model based on convolution neural network with the constraint of putting more weight on the helpful pixels for image classification during training. Among these methods, [14] is an exceptional one since it utilizes object bounding boxes as supervision.

Dai et al. [14] iteratively updated a pool of region proposals and assign them labels by training convolution networks whereas in [15] inference for a test image is used for the optimal solution. Supervised network is used in [16], and [17] for data representation by using subspace learning, and for large-scale image retrieval. However, their final target is the trained network while our aim is to construct fuzzy granule based method with even less supervision.

Infrared imaging information processing technology has attracted attention and is researched deeply. Thresholding, region growing, region splitting and merging are example of similarity Based Segmentation. Global Thresholding is most popular segmentation technique due to its simplicity and speed [18].

Segmentation has central role in autonomous image processing, image analysis, and computer vision, detail literature is reported in Shaprio and Stockman [19] Several model of image processing have been already proposed. However, they are mainly proposed for image recognition [20], indexing [21], or coding [22] rather than for

identification. A good appreciation to rapid object detection [23] and high altitude of projectile location measurement using multi-screen target method [24] in the literature attention towards Infrared imaging information processing technology and they researched deeply. In Infrared image technology the basic research is related to description of infrared background. The infrared detectors inner noise is lowest by the amelioration and development of infrared detection manufacture technology, in some conditions; the obstacle of infrared detection is the jamming of background [25-26].

In web searching, OWA was used by the user to find the importance of weight for each of the document [27]. With different aggregation techniques introduced in fuzzy information processing tasks [28], detailed description of OWA operators [29], has been applied in many applications like lossless DPCM image compression [30], decision making [31,32], fuzzy logic controller [33]. With the use of fuzzy numbers OWA operators, the environmental indices were developed, for finding similarity with multiple linguistic parameters as inputs [34,35].

Sometimes images are corrupted by different unwanted elements. To, get clear image of targeted object there are various methods reported. In next subsection these methods are mentioned.

2.2.2 Survey on Noise Removal Technique

This part is dedicated to literature survey of various method of noise removal in an image. In the task of removing impulse noise, various successful techniques have been reported in recent years. Among them 'Block Matching Three Dimensional filtering technique' shows exceptional performance [36]. Moreover the sparsity based regularization has achieved great success in various image processing applications such as image de-noising [37], image restoration using Non-local sparse models [38], image restoration utilizing centralized sparse representation [39], Non-locally centralized sparse representation method for image restoration [40], image de-blurring [41], and super resolution [42].

Although local and global intensity are applied to remove noise, very less number of effort have been made by considering manifold structure of images. In [43], removal of noise from image is done by filter diffusing technique; moreover, the author has

used neighborhood similarity based information of patches to construct a manifold structure to construct a global diffusion energy function and de-noising the image. In, [44] authors proposed a new understanding of the influence of noise on the eigenvectors of the graph Laplacian of a set of image patches, and an algorithm to estimate a de-noised set of patches from a noisy image. However in [45], an efficient noise removal technique is reported, which is based on non-local similarity of pixels.

In, [46] authors proposed a Gradient Histogram Preservation (GHP) based image de-blurring method, where the reference histogram is parameterized by Hyper-Laplacian distribution. Considering the complexity of blurring process, a Bayesian non-parametric method, Gaussian Processes regression, is utilized for estimating histogram parameters. The experiments demonstrate that, the histogram parameter estimation method is effective, and the proposed GHP based image de-blurring method can well restore image textures and improve image quality. Authors introduce a local image statistic for identifying noise pixels in images corrupted with impulse noise of random values. The statistical values quantify how different in intensity the particular pixels are from their most similar neighbors. We continue to demonstrate how this statistic may be incorporated into a filter designed to remove additive Gaussian noise [47].

However, the impulse noise makes the de-noising problem more complicated. Many existing de-noising techniques usually first detect impulse noise and then remove noise. This two-step procedure of de-noising technique is very sensitive if the level of impulse noise nurtures the computational proficiency and de-noising effect decay. In, [48] fuzzy impulse noise detection and reduction method algorithm is developed for decreasing all classes of impulse noise. Detection of hybrid noise has been done by using sparse coding based methods in [49], [50]. Nonetheless, the weight introduced in [51] depends upon residual of data fidelity on the uncorrupted pixels. These methods have limitations as noise level increases. The ‘median filter’ yields excellent results for images corrupted by impulse noise or salt pepper noise [18]. Thus, it is necessary to recover the pixel intensity that is robust against impulse noise, as well as preserve the image feature, rather than detecting impulse noise.

One of the kinds of feature is abrupt change in intensity of pixel. This characteristic of pixel is helpful in identification of edges of object of interest. Hence next sub-part throws light on conventional and new methods of edge detection.

2.2.3. Segmentation Based on Dissimilarity

There are various attributes that exists in image to extract object of interest or sub part of image. In the last years, based on the techniques that include geometry, statistics, wavelet, and neural theory, several new edge detectors have been derived in [52,53,54,55,56 57,58] Some of those methods [59,60] were adapted not only to single grayscale images but also to colour or multispectral ones. Even if their performance might be better than the classic ones, they are not very commonly applied. Most common implementations are still the mask-based ones [61] In the seminal line in [62] authors proposed a new edge detection method based on estimating the difference between two regions as a measure of edge information, including strength and orientation. The authors of [63] proposed methodology by associated each pixel with the resulting force of the gravitational forces exerted on it by the surrounding. Edges may also be regarded as a set of points separating two adjacent homogeneous regions.

Detection of edges therefore denotes the process of finding the boundary. Imran et al [64] implemented f similarity in f- geometric objects. Abdul Rahman, et al. [65] introduced few f-theorems used for estimating the membership value of f-objects in f-geometry. These f-objects play important role in identifying clues in computational forensic**.** Liping Lu'[66] designed the infrared object tracking detection system to attain the information of object far away**.** Camilla Brekke, et al. [67] proposed a method to mitigate an antialiasing filter. R. Rajeshwari et al [68] discussed a modified ACO-based approach to detect edges. Xikui Sun et al. [69] suggested a new edge detection method based on estimating the difference between two regions especially under noisy conditions.

There are various approaches to detect edges in images based on gradients [70]. But the limitation of these conventional approaches is that as the size of the image increases the computation time also increases quickly [71]. Moreover these approaches result in edges with discontinuities [72]. Ant Colony Optimization (ACO) is a bio-inspired optimization algorithm [73, 74, 75, 76] which is based on the natural foraging behaviour of ant species. ACO has been used to solve a number of optimization problems. Several ACO-based approaches have been proposed for edge detection [77], [78], [79],[80] and [81]. The approaches proposed in [77], [78] are used to enhance the edge information obtained using conventional techniques. The pure ACO based methods proposed in [79]–[81] show that ACO-based approaches based on Ant System [72],[75] and Ant Colony System [73], [74], [76] and [77] can be used to directly detect edges. In [82] ant-density algorithm was introduced whereas ant-quantity algorithms design by authors in [83]. In [84] an ant cycle algorithm was implemented.

2.2.4 Soft Computing Based Techniques

Three different soft computing approaches to edge detection for image segmentation are most frequently used. These are (1) Neural Network based Approach [85], (2) Fuzzy based Approach [86] and (3) Genetic Algorithm based approach [87]. Neural networks are made by numerous elements that are connected by links with variable weights [88][89]. Artificial neural networks (ANN) are usually applied for pattern recognition [90]. Their processing nonlinear and potential characteristics are used for clustering [91-92]. Self -organization of Kohonen Feature Map (SOFM) network is a powerful tool for clustering [93]. This approach finds the watershed segmentation of luminance component of colour image [94], [90]. Ji and Park proposed an algorithm for watershed segmentation based on SOM [95]. This approach comprises of two independent neural networks one each for intensity and saturation planes [96],[97].

Edge detection method is based on defining a membership function indicating the degree of edginess in each neighborhood [98].This approach can only be regarded as a true fuzzy approach if fuzzy concepts are additionally used to modify the membership values [99]. Significant work on GAs within edge detection is described in [100]. Recently, researchers have studied the use of genetic algorithms into the image

segmentation problem [101].The membership function is estimated heuristically. It is fast but the performance is inadequate [102]. By means of suitable fuzzy if-then rules, one can develop specific or general edge detections in pre-defined neighborhoods [103]. Homogeneity is a measure to test the similarity of two regions during the segmentation procedure under consideration [104],[105]. Advantage of using general pattern recognition approach is mainly related with the GA ability to deal with large, complex search spaces in situations where only minimum knowledge is available about the objective function [106]. This ability led authors to adopt a GA to determine the parameter set that optimize the output of an existing segmentation algorithm under various conditions of image acquisition and is namely Phoenix segmentation algorithm [106]. Another situation wherein GAs may be useful tools is illustrated by the work of George Karkavitsas and Maria Rangoussi [107].

AdaBoost was proposed by Freund and Schapire [108]. The connection between AdaBoost and SVMs was discussed by Freund and Schapire [109]. The difference between the two methods in this regard is that SVM corresponds to quadratic programming, while AdaBoost corresponds only to linear programming. Quadratic programming is more computationally demanding than linear programming. AdaBoost is one of the approaches where a “weak” learning algorithm, which performs just slightly better than random guessing, is “boosted” into an arbitrarily accurate “strong” learning algorithm.

Sung and Poggio [110] applied the following ‘bootstrap’ strategy to constrain the number of non-face examples in their face detection system. They incrementally selected only those non-face patterns with high utility value.

Schapire and Singer [111] described several improvements to Freund and Schapire’s original [108] AdaBoost algorithm, particularly in a setting in which hypotheses may assign confidences to each of their predictions. More precisely, weak hypotheses can have a range over all real numbers rather than the restricted range [-1, +1] assumed by Freund and Schapire [109].

Lienhart and Maydt [112] added a set of classifiers, same as those proposed by Viola, but they are all rotated 45 degrees. They claimed to gain a 10% improvement in the face detection rate at any given hit rate when detecting faces.

Viola and Jones [113] proposed some modifications to their original machine, to improve its speed. In the first modification they change the weight for classifiers, but report that gains obtained at the beginning were compensated for later on when more classifiers were added.

Froba, Stecher, and Kublbeck [114] elaborated on a face verification system. They recognized a particular person based on his/her face. The first step in face verification is face detection. The second is to analyze the detected sample and see if it matches one of the training examples in the database.

Howe [115] looked at boosting for image retrieval and classification, with comparative evaluation of several algorithms. Boosting was shown to perform significantly better than the nearest neighbour approach. Two boosting techniques that were compared based on feature and vector based boosting. Feature based boosting was the one used in Viola [116]. Vector based boosting worked differently.

Jones and Viola [116] built one face detector for each view of the face. A decision tree was trained to determine the viewpoint class (such as right profile or rotated 60 degrees) for a given window of the image being examined. The appropriate detector for that viewpoint can then be run instead of running all of the detectors on all windows.

McCane and Novins [117] described two improvements over the Viola [118] training scheme for face detection. The first one was a 300-fold speed improvement over the training method, with an approximately three times slower execution time for the search. Instead of testing all features at each stage (exhaustive search), McCane and Novins proposed an optimization search, by applying a ‘downhill search’ approach. The second improvement in McCane and Novins was a principled method for determining a cascaded classifier of optimal speed. However, no useful information is reported, except the guideline that the false positive rate for the first cascade stage should be between 0.5 and 0.6.

Viola [118] involved different stages of operation in face detection. He had three major contributions: integral images, combining features to find faces in the detection

process and use of a cascaded decision process when searching for faces in images. This machine for finding faces is called cascaded AdaBoost.

Treptow et al [119] described a real-time soccer ball tracking system, using the described AdaBoost based algorithm by Viola [118]. They added a procedure for predicting ball movement.

Kolsch and Turk [120] described and analyzed a hand detection system. They created a training set for each of the six posture/view combinations from different people's right hands. The training and validation sets were rotated and a classifier was trained for each angle. In contrast to the case of the face detector, they found poor accuracy with rotated test images for as little as a 4° rotation. They then added rotated example images to the same training set, showing that up to 15° of rotation can be efficiently detected with one detector.

Le and Satoh [121] observed AdaBoost advantages and drawbacks, and proposed to use it in the first two stages of the classification process. The first stage was a cascaded classifier with sub windows of size 36x36, the second stage was a cascaded classifier with sub windows of size 4x24. The third stage was a SVM classifier for greater precision.

Levi and Weiss [122] added a new perspective of detection upright, forward facing faces. They added an edge orientation feature that the machine can be trained on. They also experimented with mean intensity features, which mean taking the average pixel intensity in a rectangular area. They claimed that using edge orientation histograms, they are able to achieve higher detection rates at all training database sizes.

Li, Wang and Sung [123] proposed an active learning approach, to select the next unlabelled sample which is at the minimum distance from the optimal AdaBoost hyperplane derived from the current set of labelled samples. The sample is then labelled and entered into the training set.

Yen and Tretter [124] introduced an automatic redeye detection and correction algorithm which used machine learning in the detection of red eyes. They used an adaptation of AdaBoost in the detection phase of redeye instances.

The authors [125] used histograms of Gabor and Gaussian derivative responses as features for training, and applied them for face expression recognition with AdaBoost and SVM. Both approaches show similar results and AdaBoost offers important feature selections that can be visualized.

Le and Satoh [126] maintained that the pure SVM has constant running time of 554 Windows Per Second (WPS) regardless of complexity of the input image, the pure AdaBoost (cascaded with 37 layers-5,924 features) has running time of 640, 515 WPS. They claimed that cascaded AdaBoost is 1000 times faster than SVMs.

Stojmenovic M.[127] described a new type of the AdaBoost based learning algorithm, in which a strong classifier is generated by incremental addition of weak classifiers so that the error can be minimized for the already selected weak classifiers.

Felzenszwalb, Pedro F [128], investigated Deformable models for object detection including Fast matching algorithms and - Learning from weakly-labeled data and Leads to state-of-the-art results in PASCAL challenge.

Jayanta Kumar Basu et al [129], described the strategies for Pattern Recognition using Artificial Neural Network.

Gualdi et al [130], generated grid-distributed patches, at all possible positions and sizes, which were evaluated by a binary classifier: The tradeoff between computational burden and detection accuracy was the real critical point of sliding windows; several methods have been proposed to speed up the search such as adding complementary features. They proposed a paradigm for object detection into a statistical-based search using a Monte Carlo sampling for estimating the likelihood density function with Gaussian kernels.

Beaugendre, A., et al [131] proposed enhanced moving object detection tracking system for video surveillance purposes. The method can also speed up the tracking by creating a link between a tracker and a blob to avoid unnecessary processing in some situations.

Lan, J. et al [132] presented a novel embedded target detection system built upon a visible image sensor which can detect both static and dynamic targets under difficult

situations. It was small in size, light in weight, had low power consumption, and can be embedded into the system of robotics and intelligent systems.

Oreifej, Omar ; Li, Xin ; Shah, Mubarak [133], proposed a novel three-term low-rank matrix decomposition approach in which they decomposed the turbulence sequence into three components: the background, the turbulence, and the object. They simplified this extremely difficult problem into a minimization of nuclear norm, Frobenius norm, and 21 norm.

Han, J. et al[134] developed a probabilistic computational algorithm by integrating objectness likelihood with appearance rarity. The image sparse coding representations were yielded through learning on a large amount of eye-fixation patches from an eye-tracking dataset.

Bleszynski, Elizabeth H. et al [135] proposed a method that the transmitted signal consists of a coherent train of short wide-band pulses emitted at chirped (linearly varying) time intervals. As the energy of a single pulse which has travelled a large distance in the medium is almost entirely concentrated in the precursor-type structures associated with its leading and trailing edges, the increase of the signal total energy is achieved by using trains with a large number of pulses.

Wan-Lei Zhao, Chong-Wah Ngo, [136] proposed a new descriptor, named flip-invariant SIFT (or F-SIFT), that preserved the original properties of SIFT while being tolerant to flips. F-SIFT starts by estimating the dominant curl of a local patch and then geometrically normalizes the patch by flipping before the computation of SIFT.

Tsung Han Tsai et al [137] presented a hardware-oriented foreground detection that was based on human-machine interaction in object level (HMIiOL) scheme. The HMIiOL can vary the conditions for a moving object been regarded as a foreground object. The conditions are depending on background environment and are derived from the information from human-machine interaction.

2.3 RESEARCH GAPS

After literature survey research gaps found in three levels for the analysis of object detection technique.

In the task of removing impulse noise, various successful techniques have been reported in recent years. If the level of impulse noise rises the computational efficiency and de-noising effect decline.

The median filter yields excellent results for images corrupted by impulse noise or salt pepper noise. Sometimes median filter produces noisy pixels, hence another refine aggregation filter required.

In autonomous object tracking there is no control over complex environment specifically that contains flooding wave and noise.

The key objective of thresholding is to produce a clean segmented image by eliminating the noise and flood waves. Global thresholding expected to be successful in highly control environment.

But, sea water environment is uncontrolled. Hence there is a requirement of a method that can be specifying threshold 'T'.

ACO is to determine edges by using heuristic information. However as the size of the image increases the computation time for conventional edge detection increases quickly as well as result in edges have discontinuities .

The sub aperture cross-correlation magnitude (SCM) has previously been proposed as a statistic that improves the contrast between small ship targets and the surrounding sea in synthetic-aperture-radar images.

This preprocessing technique utilizes the fast decorrelation of open-water surface ripples on the scale of the SAR wavelength relative to coherent targets such as a ship.

However, optimization of the bandwidth splitting in the sub band extraction has not received any attention.

The next five chapters are trying to bridge above said research gaps.

CHAPTER III
DETECTION OF SMALL OBJECT IN INFRARED IMAGES

3.1 INTRODUCTION

Due to high sensitivity and strategical importance of sea border, detection of motion of enemy's military troops and arms may play a crucial role. Attack of 26, November, 2008 in Mumbai, commercial capital of India ,is the result of such type of piercing of water territory. Hence, in this work, Threshold based new method is proposed to detect ship in sea environment. Infrared images of ship in sea water are used as input. To specify, appropriate threshold Yager's Linguistic quantifier 'most', 'at least half', and 'as many as possible' are used [29]. Moreover segmentation of thresholding images is carried out by using Sobel operator. It is observed that threshold generated by 'at least half' and 'as many as possible' quantifier are closer to visual heuristic threshold. It is also found that linguistic quantifier based thresholding has generated clear image of ship from background than Sobel Operator methods [65],[66].

3.2 THRESHOLDING

Thresholding, region splitting and merging, region growing are examples of Segmentation. Segmentation is one of the image processing method whose output(s) are attributes extracted from input image(s).

Thresholding is the central concept among the segmentation methods. The popularity of thresholding is due to its simplicity and speed.

The key objective of using thresholding is to produce a clean segmented image of targeted ship by eliminating the noise and flood waves. Hence there is a requirement of a method that can be specifying threshold 'T'. In proposed work, global thresholding is used. Global thresholding is expected to be successful in highly controlled environment. However to process these noises and the targeted ship, the

image is processed by Ordered Weighted Averaging (OWA) method and produces promising results.

3.2.1 Formalization of Global Thresholding

Global thresholding is simplest one, wherein by using single global threshold 'T', it segments the image.

Suppose, gray level in an image *f*(x, y), represents light objects on dark background, in a manner that both object and background pixels have gray levels which can be grouped into two dominant modes [1]. The objective is to select a threshold 'T' that splits up these modes. If for any spatial coordinate *f*(x,y)>T, then it is related to the object and if *f* (x,y) <T, then it is related to the background.

A threshold image *g(*x,y) is defined as

$$g(x,y) = \begin{cases} L & if \quad f(x,y) > T \\ 0 & if \quad f(x,y) \leq T \end{cases} \tag{3.1}$$

If, Threshold T only depends upon *f*(x, y), then it is called global.

3.3 SOBEL OBJECT DETECTION ALGORITHM ON INFRARED IMAGE

The object detection algorithm given by *Sobel* is based upon the gray level weighted computation in the neighborhood [65]. The size of which is 3×3, and the center of which is the pixel. The algorithm for detection suggested by *Sobel* is defined as:

$$S\,(x,y) = \left(f_x^2 + f_y^2\right)^{1/2} \tag{3.2}$$

Where f_x and f_y are represented as:

$$f_x = \begin{pmatrix} -1 & 0 & 1 \\ -2 & 0 & 2 \\ -1 & 0 & 1 \end{pmatrix} \tag{3.3}$$

$$f_y = \begin{pmatrix} 1 & 2 & 1 \\ 0 & 0 & 0 \\ -1 & -2 & -1 \end{pmatrix} \tag{3.4}$$

In Sobel edge detection algorithm, the calculation of weighted sum on gray of every pixel is done, which are the above point, the lower point, the left point and the right point of image. When the pixel is closer to the center of the model, the weighted value

will be higher. Similarly we can decide the threshold T and if f (x, y) >T, we say that the point f (x, y) is the object point.

3.4 ORDERED WEIGHTED AVERAGING METHOD

Yager [1] discovered the OWA operator which is basis for the information aggregation. OWA provides the aggregation method for solving the problems which includes multiple criteria of decision making. A parameterized family of aggregation operator like k-order statistics, arithmetic mean, median, maximum and minimum is provided by OWA operator. In some cases of multi criteria decision making exact -and-ness is required which produces minimum value and in some cases exact -or-ness is required which produces maximum value. The value in between these two extremes i.e. -and-ness and or-ness is provided by the aggregation operator based on OWA. These two extremes are limited for multiplication (like AND gate) and summation (like OR gate). OWA operators are taken in account in the later part and then detailed discussion was made regarding the behavior of operators as in [1]. Three steps in OWA operation are as follows – 1) Reordering of inputs, 2) Weight determination related with OWA operators and 3) Aggregation process.

3.4.1 Yager's OWA Operator Weights Method

Definition: *"*Mapping the OWA operator R from R m→ R, (where R = [0, 1]), with dimension m, has weighting vector w = $(w_1, w_2, w_3, \ldots w_m)^T$, where $w_j \in [0, 1]$ and $\Sigma w_j = 1$, the summation of individual weights will always one. Thus, for the multi-criteria of size m, the input parameter $(x_1, x_2, x_3 \ldots\ldots x_m)$, the OWA determines the f-validity in f-geometry shapes as follows".

$$OWA(x_{1,}x_{2,}x_{3\ldots\ldots\ldots\ldots\ldots}x_m) = \sum w_j\, y_i \tag{3.5}$$

$$\beta = \frac{1}{m-1}\sum_{j=1}^{m} w_j\ (m-1) \tag{3.6}$$

In this, β (*or-ness)* lies in the range [0, 1]. At every instance when β occupies maximum value i.e. 1, produces the weight vector as (1, 0, 0,...0), means that entire weight is acquired by the maximum value of x_j producing the maximum OWA operator and when β occupies minimum value i.e.= 0, produces the weight vector as (0, 0, 0,…, 1), means that the entire weight is acquired by the minimum value of x_j,

producing the minimum OWA operator. When β occupies middle value i.e. 0.5, the weight vector as (1/n, 1/n, 1/n,…, 1/n) is generated which shows that the arithmetic mean of weights are distributed evenly between the inputs [1]. The relative quantifier's membership function can be expressed as

$$Q(r) = \begin{cases} 0 & if\ r < a \\ \frac{r-a}{b-a} & if\ a \le r \le b \\ 1 & if\ r > b \end{cases} \qquad (3.7)$$

where a,b,r ∈ [0,1].[3]

The weights w_j of the OWA aggregation calculated in [1], Yager from the function Q discusses the quantifier, with m number of criteria.

$$w_j = Q\left(\frac{j}{m}\right) - Q\left(\frac{j-1}{m}\right) \qquad (3.8)$$

where j =1,2,…,m and $Q(0) = 0$.

The relative quantifiers are pictorially represented as in figure 3.1. This shows the relative quantifiers "most", "at least half" and "as many as possible" taking the parameter a and b as (0.3, 0.8), (0, 0.5) and (0.5, 1) respectively.

Now for determination of weights, we review the OWA operator models with nonlinear objective function. The next section consists of experimental work and results.

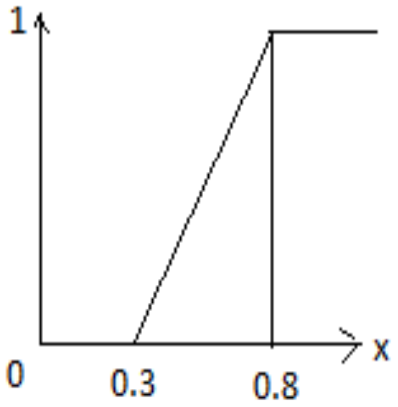

Figure3.1 (a): Linguistic Quantifier "most"

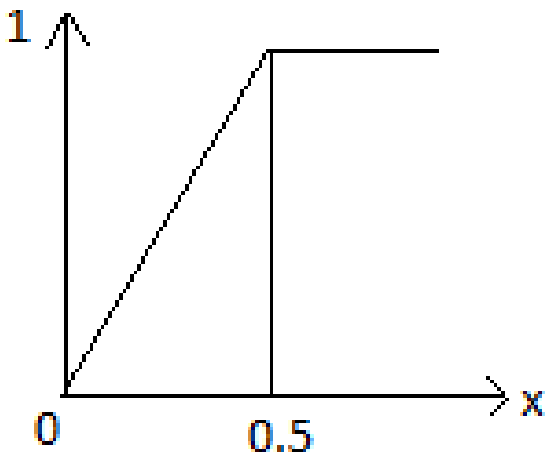

Figure 3.1 (b): Lingustic Quantifier *"at least half"*

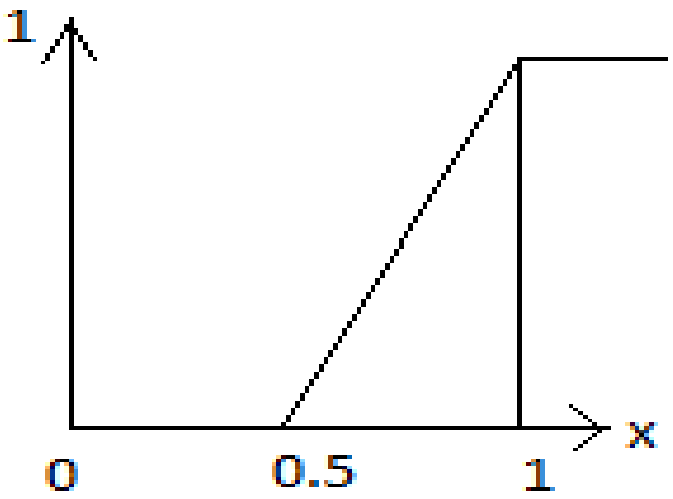

Figure 3.1 (c):Lingustic Quantifier *"as many as possible"*

3.5 PROPOSED METHODOLOGY

Proposed method is based on algorithm given below. The results of proposed method are compared with Sobel Object detection algorithm.

3.5.1 Proposed Algorithm

START

STEP 1: Read Infrared Image

STEP 2: Change image into gray scale

STEP 3: Apply histogram equalization

STEP 4: Store all distinct gray levels

STEP 5: Estimation of threshold ‘T’

3.5.1.1Arrange all gray levels in decreasing order

3.5.1.2 Estimate Weights by using linguistic quantifier by using equation (3.7) and (3.8)

3.5.1.3 Aggregate product of these weights with corresponding gray level inputs by using equation (3.5).

STEP 6: Segment the image on the basis of estimated Threshold by pixel by pixel analysis of gray level.

(a) If f(x,y) >T Then g(x,y)=f(x,y)

(b) Else f(x,y)==0

END

Based on proposed methodology the experiments are carried out and results along with experimental work are discussed in next section.

3.6 EXPERIMENTAL WORK AND RESULTS

The experimental work is carried out by taking infrared image of ship as shown in figure 3.2.

Figure 3.2 Infrared Image of Ship under Sea Water

Initially threshold is specified by using heuristic approach based on visual inspection, i.e. 129.

Figures 3.4 to 3.6 are showing results after applying ‘most’, ‘at least half ’, and ‘as many as possible’ linguistic quantifier to estimate threshold respectively.

The value of threshold ‘T’ estimated by ‘most’ linguistic quantifier is 115 whereas ‘at least half’, and ‘as many as possible’ linguistic quantifier produces 131 and 125 respectively. Values of ‘T’ produces ‘at least half’, and ‘as many as possible’ linguistic quantifier and are much closer to visual inspection i.e.129.

In Figure 3.3, output of Sobel object detection algorithm is shown that is very blur. After observing figures 3.4 - 3.6, it is found ‘at least half’ and ‘as many as possible’ producing output are much better and clearer than Sobel algorithm.

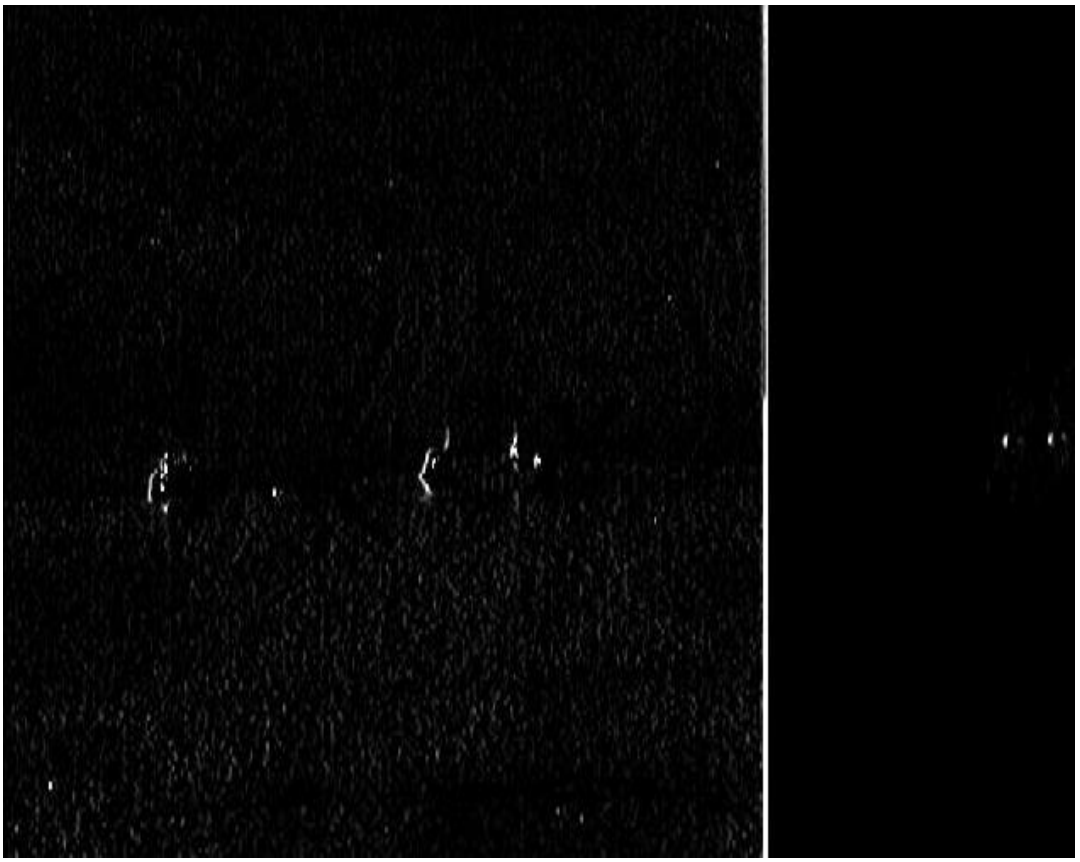

Figure 3.3 Output of Sobel object detection algorithm

The performance of ‘at least half ’, and ‘as many as possible’ are slightly better than ‘most’ quantifier. However it can be observed very clearly that both of these quantifiers have tie on the basis of visibility as well as estimated threshold value.

Figure 3.4 Output of Most Linguistic Quantifier

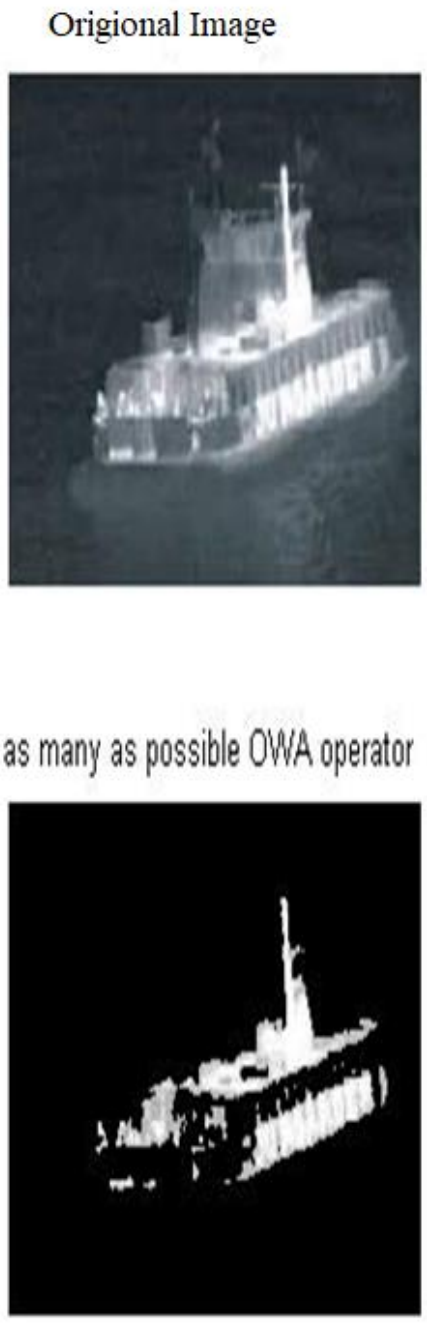

Figure 3.5 Output of As Many As Possible Linguistic Quantifier

Figure 3.6 Output of Atleast Half Linguistic Quantifier

3.7 CONCLUSION AND FUTURE DIRECTIONS

In this we have estimated global thresholding to identify the location of ship in sea water. Infrared image is taken as input due to its high heat signature. To, estimate heuristic value of threshold of histogram approach is used, and it touches half of pixel intensity of 256.

Threshold values estimated by ‘at least half’, and ‘as many as possible’ linguistic quantifier are much closer to visual inspection. The yield of Sobel detection is not very clear.

Proposed work is for static positions of ship, In future same methodology can be used for moving ship and it is expected to produce good results.

CHAPTER IV

DE-NOISING INFRARED IMAGE OF SHIP UNDER SEA WATER

4.1 INTRODUCTION

Image de-noising has been an active area in image processing in recent past. OWA based linear objective function is used to remove impulse noise to get a clear image of ship in a sea environment. Moreover, Salt & Pepper/Impulse noise may be introduced into images during acquisition, transmission, and flooding waves. Salt & Pepper and Impulse noise both are same types of noise, hence in rest of the article are used interchangeably.

To remove impulse noise, 'spatial filtering' is one of the effective tools. Median filters, Ordered Statistics Filters and Adaptive Filters are the leading filters for this problem. Median filter is based on Ordered Statistics which yields excellent results for images corrupted by impulse noise or salt pepper noise [18]. In this, linear objective function is used to remove impulse noise. The results are compared with median filter and better performance is shown by presented method. For the moment, heat sensors enhanced the images of the objects of interest and diminished the background and noise. Hence, in this work infrared image of ship is used as input. Please refer to figure 4.2 (f).

This chapter is organized as follows. The computations of median filter are introduced in Section 4.2. Section 4.3 elaborates the method called OWA based filter. Experimental work and results on removal are reported in section 4.4 and 4.5. In section 4.8, conclusion is discussed along with future directions.

Figure.4.1 Sample Images (a) Leena (b) Zelda (c) Barbara (d) Gold Hill (e) Boat (f) Cameraman

Figure 4.2 Sample Images (a) Aeroplane (b) Arctichare (c) Baboon (d) Boy (e) Cat (f) Ship

4.2 COMPUTATION OF MEDIAN FILTER

Median filters are quite popular; they provide certain excellent noise-reduction capabilities. Median filters are particularly effective in presence of impulse noise, also called salt-and-pepper noise. The median of a set of intensity values is such that, half

of the values in the set are less than or equal to median and half are greater than or equal to median. The median filtering of an image is a two-step process.

1) Select a point (pixel) in an image and then sort the pixel in question and its neighbours.
2) Determine median and assign this value to that selected point.

In this work, 3X3 neighbourhood is taken and arranged in descending order. The median is the 5^{th} element of the sorted array. For example ,sorted valuesare174,171,170,166,166,163,163,162,162. Referring Table 4.1, the median of 3X3 neighbours is 5^{th} element, i.e.166.

Table 4.1 3x3 Mask

166	166	163
174	171	170
163	162	162

Other variations of ordered statistic filters are max and min filter. Max filter finds out the brightest point whereas Min. filter is used for finding darkest point in image. Moreover, the proper aggregation of different pixel of image may generate appropriate intensity by selecting robust point. This is shown in section 4.2.

4.3 COMPUTATION OF OWABASED FILTER

Aggregation operator is the central concept of information aggregation and was originally introduced by Yager [1]. Subsequent part discloses a brief account of OWA operators, detailed discussion about the behaviour of operators in OWA is in [2].The OWA operation involves following three steps shown in figure 4.3.

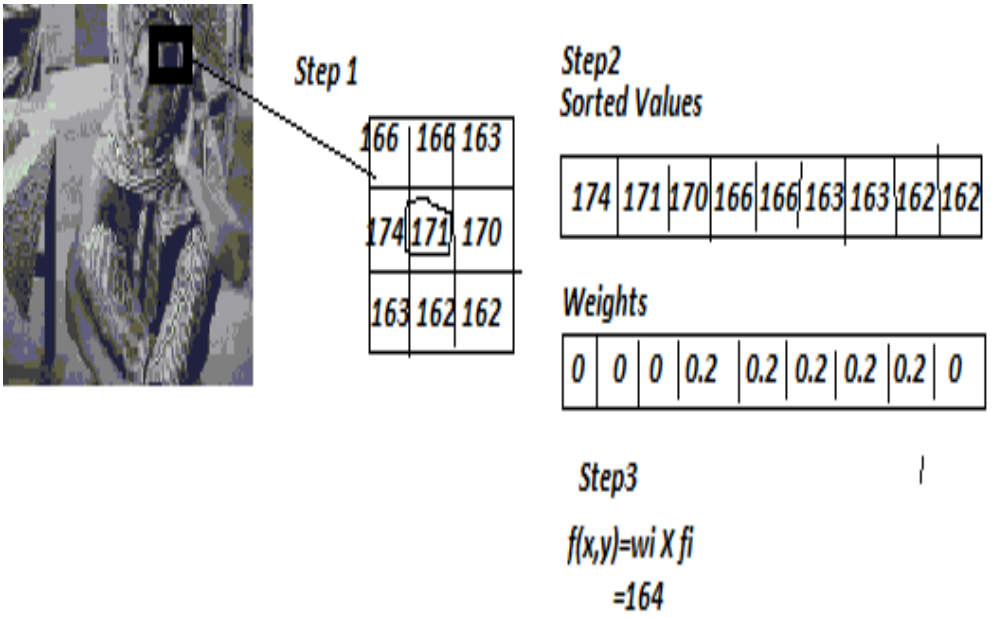

Figure 4.3 Summary of OWA Method

4.4 EXPERIMENTAL WORK

In this section, the OWA model is compared with median noise removal method. The visual performance of OWA method is higher or equal to median filter as shown in results, figures 4.4 to 4.15. The noise parameter is set 0.01 for the impulse noise.

To remove noise we have considered each and every pixel's intensities and have taken 8-neighborhoods for consideration. In Section 4.3, it is shown that OWA based filter has three steps. First step is arranging the inputs image. So we have considered the entire pixel in question and 8 pixels of neighbourhoods, and arranged them in descending order.

Table 4.2 Values of Intensities in Neighbourhoods

162	162	163
174	171	170
163	166	166

Sorted values are (174,171,170,166,166,163,163,162,162).

4.4.1 Weight Calculation

The fuzzy quantifier used for weight estimation is ‘most’. Since, the number of input parameters is nine; the value of ‘m’ is 9 for the OWA. The estimation of weights is done by step 2 for m = 9. The values of variable ‘a’ and ‘b’ are taken 0.3 and 0.8 respectively. As per our interest, we have considered an array of different size; the values are varying from 0-255. To get improved intensity aggregation process step 3 is applied.

4.4.2 Estimation of Intensity Values

To counter impulse noise, the determined weight vector is convoluted as a 3X3 mask on all pixel of image .Meanwhile, intensity of all other elements and pixel in question is improved and is j^{th} main value of intensity among other 8 elements of current pixel.

After rounding off, the value of intensity is ‘158’.

The same procedure is carried out for each and every pixel. The neighbour hoods of boundary pixels are padded with zeros.

4.5 RESULTS AND DISCUSSION

The samples images taken as input are shown in figure 4.1 and figure 4.2. First, we have applied impulse or salt and pepper noise. Then, the images are obtained after de-noising with OWA method. The results are also compared with median filter. It is observed that, the results are satisfactory.

Table 4.3 Estimation of Weight

i/m	0/9	1/9	2/9	3/9	4/9	5/9	6/9	7/9	8/9	9/9
Q(i/m)	0	0.1111	0.2222	0.333333	0.4444	0.556	0.67	0.7778	0.8889	1
Q(r)	NA	0	0	0.066667	0.2889	0.511	0.73	0.9556	1	1
weights	NA	0	0	0.066667	0.2222	0.222	0.2222	0.2222	0.04444	0

Figure 4.4 Comparative Images of Leena

Figure 4.5 Comparative Images of Zelda

Figure 4.6 Comparative Images of Barbara

Figure 4.7 Comparative Images of Camera Man

Figure 4.8 Comparative Images of Boat

Figure 4.9 Comparative Images of Gold Hill

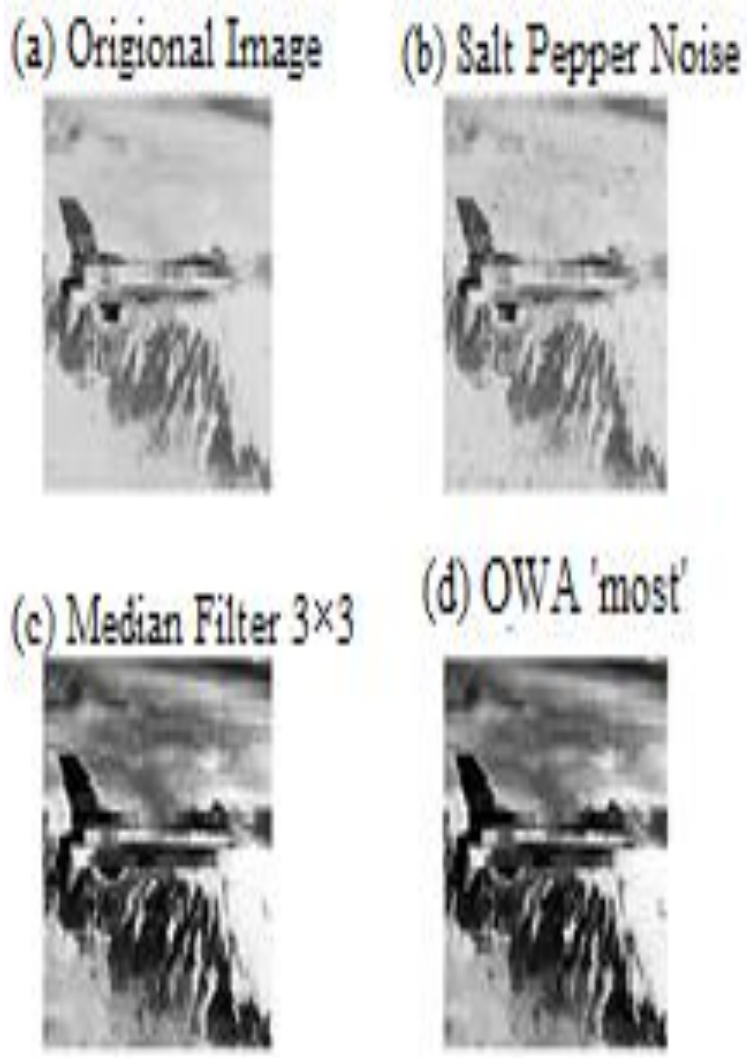

Figure 4.10 Comparative Images of Aeroplane

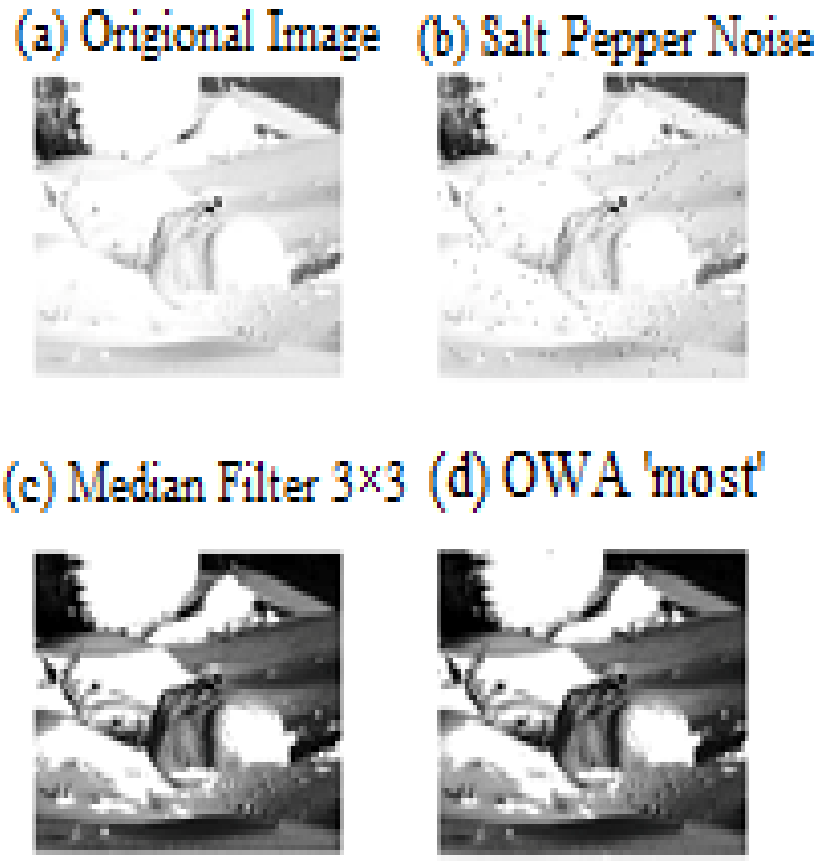

Figure 4.11 Comparative Images of Architect

Figures 4.4 to 4.15 have four parts; (a) is showing original image (b) has salt pepper noise, whereas (c) and (d) show de-noised image after applying median filter and OWA based filter, respectively. After taking a close observation of the images of figures 4.4 to 4.15, it is clear that OWA produces more clear images as compared to traditional median filter.

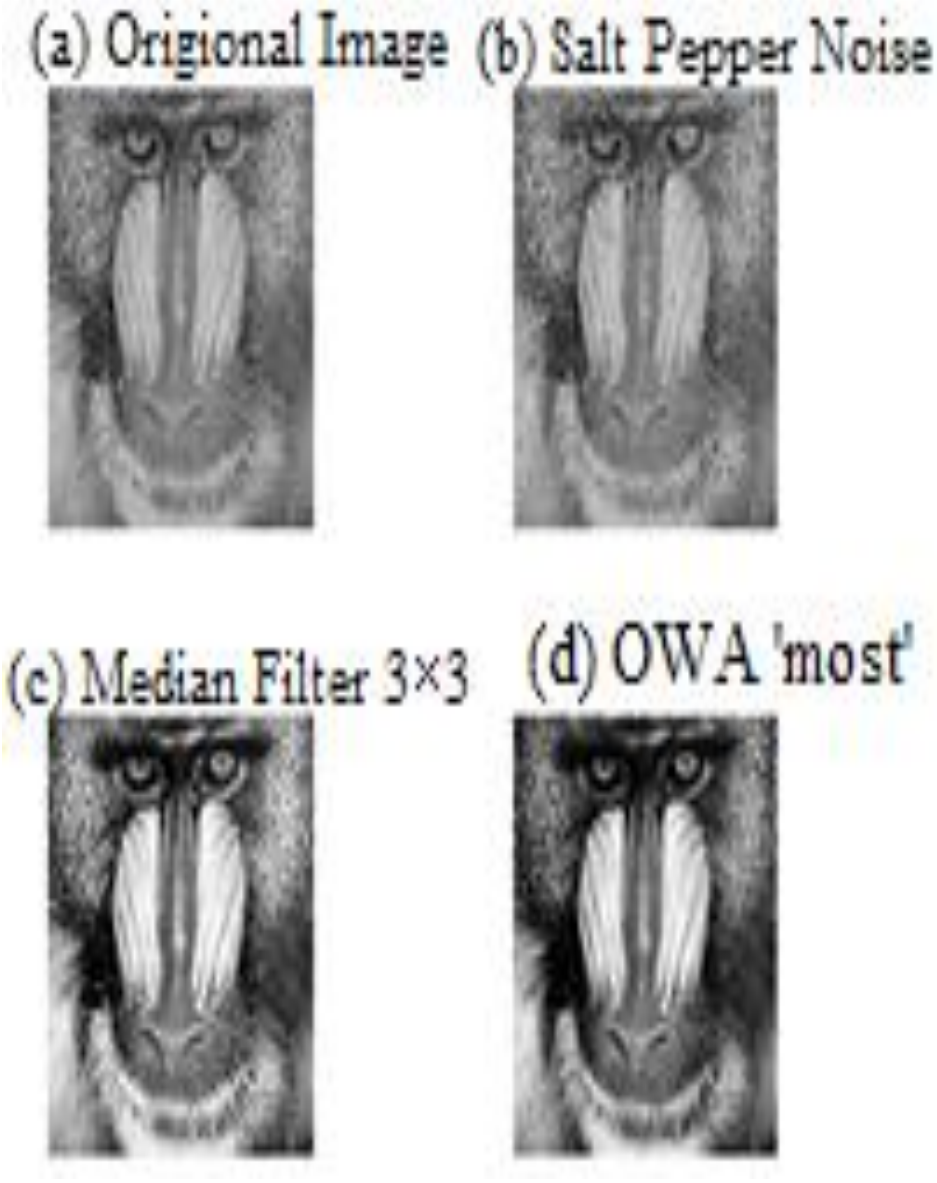

Figure 4.12 Comparative Images of Baboon

Figure 4.13 Comparative Images of Boy

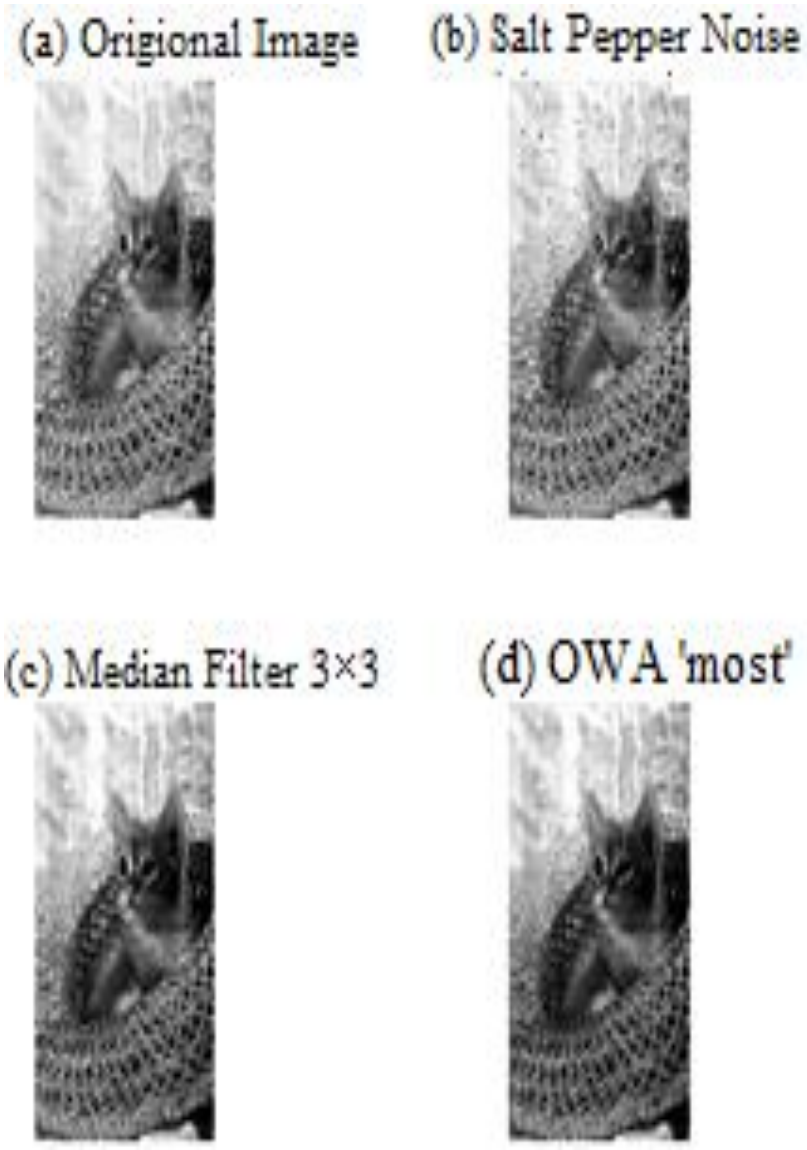

Figure 4.14 Comparative Image of Cat

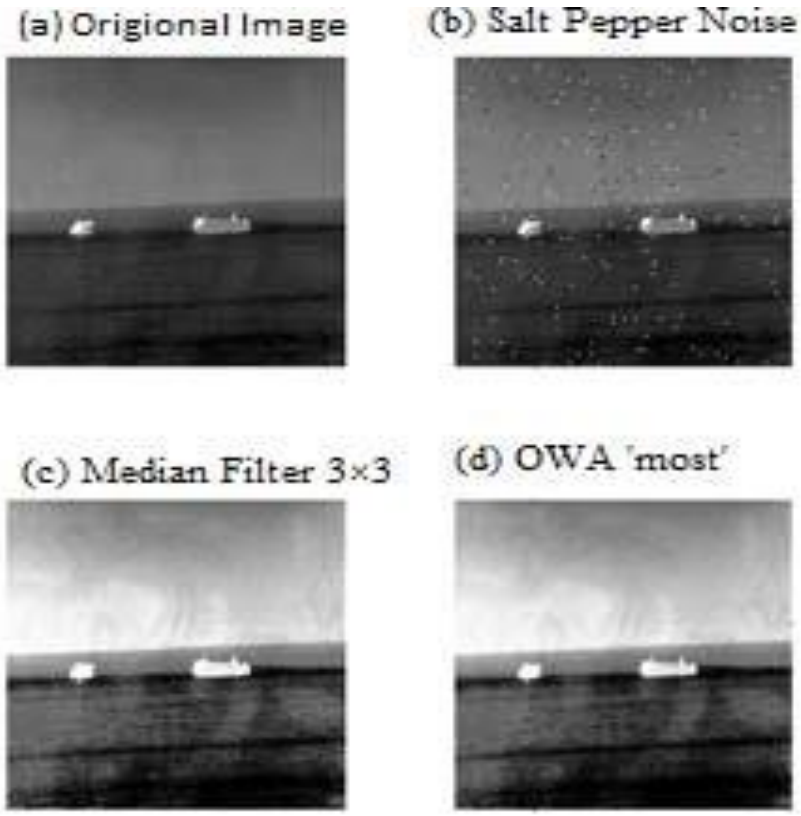

Figure 4.15 Comparative Images of Ship

4.6 ANALYSIS OF OWA FILTER WITH MEDIAN FILTER

Analysis of Noised Filter:

- A new noised filter is introduced, that is based on fuzzy linguistic quantifier ‘most’.
- This naïve filter is compared with well-established median filter.
- A mask of 3X3 is generated by OWA operator and convoluted with every pixel of images with 8 neighbors.
- Results generated by Most OWA based filter, shows quite satisfactory performance.

Performance of OWA based filter: Results generated by proposed method, which is application of OWA operator, shows quite satisfactory performance.The next section concludes the chapter. Additionally future directions also discussed.

Table 4.4 SNR of proposed Filter and Median Filter

Noise Density	SNR value	SNR value of most filter	SNR value of median filter
0.01	4.1433	4.1386	3.9897
0.02	4.614	4.609	4.4424
0.03	4.8762	4.8706	4.6969
0.04	5.3318	5.3257	5.1311
0.05	5.6092	5.6023	5.401

4.7 CONCLUSION AND FUTURE DIRECTIONS

In this work, infrared image of ship in sea is de-noised from Impulse noise. Impulse noise may be introduced into thermal images either due to flood waves in sea water or during acquisition and transmission. The proposed filter is compared with well-established median filter. A mask of 3X3 is created by aggregation operator and convoluted with 8-neighbors. In future, Results generated by more fuzzy quantifiers like ‘as many as possible’, ‘at least half’ can also be used for de-noising the image. The filtered image can be used for tracking of ship or movement of military troops in the water territory by using different segmentation techniques.

CHAPTER V

SUBBAND EXTRACTION STRATEGIES IN SHIP DETECTION WITH THE SUBAPERTURE CROSS-CORRELATION MAGNITUDE

5.1 INTRODUCTION

Higher differentiation of contrast between targets and surrounding increases the chances of spotting small targets in uncontrolled and unpredicted environment. The cross-correlation of sub aperture measurements from synthetic aperture radar (SAR) was first suggested by Arnaud [138] to spot man-made targets. SAR is based on image product that improves the detection of targets. SAR is also helpful in detecting ship in ocean because sea environment has low backscattering coefficients and low contrast to the background sea clutter.

Therefore this chapter focused in spot small vessels in oceanic water. Sub-aperture Cross-Correlation Magnitude (SCM) is used to detect small ship targets in synthetic aperture radar (SAR) images of sea water. An preprocessed SAR image is taken as input, Azimuth bandwidth reduction, Sub-band extraction, Up-sampling, Hermitian inner product, Low pass filter, Down-sampling and Local Averaging are the steps to produce clear image.

The cross-correlation of subaperture measurements from synthetic aperture radar (SAR) was first suggested by Arnaud [138] to obtain an image product that improves the detection of difficult man-made targets with low backscattering coefficients and low contrast to the background sea clutter. The concept was later elaborated by Souyris et al. [139], who referred to the format as the two-look internal Hermitian product. They extended the technique to polar metric data and provided details on the implementation.

A subaperture is defined as a subset of the available aperture, which can be extracted as a subband in the frequency domain and focused into an image of complex scattering

coefficients with degraded resolution. The subapertures are filtered out from the spectrum of full-resolution simple-look complex (SLC) data. Since they correspond to separate parts of the range or azimuth frequency band, the subapertures will originate from different time slots. The idea is to compute a cross-correlation between the complex scattering coefficients of two subapertures and to use the magnitude as a test statistic for target detection.

The underlying principle is that open water decorrelates in less than 0.05 s at C- band (< 0.1 s at L-band) [140], whereas a man- made target such as a ship should remain coherent over the time separating the acquisition of the subapertures. Therefore, the subaperture cross-correlation magnitude (SCM) is expected to provide a higher contrast between ships and open water than ordinary single-look intensity (SLI) images. This has been effectively demonstrated [139]. Other approaches have been suggested that correlate subaperture amplitude or intensity and discard the phase information [140], but not included in current literature.

The original approach of Souyris et al. [139] produced two SCM images: one based on subapertures extracted in range and a second with subapertures extracted in the azimuth direction. The magnitude values were subsequently added. However, it was found in a that azimuth band splitting is preferable because it better preserves spatial resolution and target details. In this work, SCM algorithm is studied, but limited to sub band extraction from the azimuth spectrum only.

It was suggested in [138] that the SCM technique can be adapted to different sea conditions by adjusting the width of the extracted subbands and their spectral separation. A point target may present nonstationary behavior throughout the illumination time, e.g., in cases of rough sea state. This can make the target visible only within parts of the azimuth or range spectrum. The width of the subbands might have to be reduced in agitated sea states to avoid decorrelation of the ship. It was further argued that both separation and subband width might have to be increased when the sea is calm to enhance the decorrelation of the sea.

In spite of the incitements, the subband extraction strategy has so far not been studied in the literature on SCM applied to ship detection. Hence, this is the focus of this letter. We study the effect of splitting the azimuth spectrum into subapertures as a function of spectral bandwidth and overlap. We open for subaperture overlap to investigate the whole continuum of extraction strategies, ranging from narrow time-separated sub-apertures to full subaperture overlap. In addition, by utilizing more of the bandwidth, the loss of spatial resolution associated with subaperture processing can also be reduced.

Section 5.2 describes the details of the improved SCM (I-SCM) algorithm that allows overlap of subaperture bandwidths, the subband extraction strategies, and the performance measures used in the experimental part. Section 5.3 presents the experimental work and results. Section 5.4 discusses the performance of I-SCM. The conclusions are given in Section 5.5.

5.2 IMPROVED SCM ALGORITHM OR I-SCM

The steps of the algorithm outlined in figure 5.1 are as follows.

1) *Data*: The SLC SAR data used as input to the algorithm are converted to the frequency domain by a 2-D fast Fourier transform (2-D FFT).

2) *Spectrum shifted to Doppler centroid*: It is known that the Earth's rotation causes systematic variations of the Doppler centroid along the satellites orbit [141]. We shift the Doppler centroid f_{dc} to zero azimuth frequency f_0 to compensate for this effect. This is crucial for accurate subsequent processing.

3) *Azimuth bandwidth reduction*: A reduction of the azimuth bandwidth to ~80% of the original is done to take into account that a modified Kaiser–Bessel weighting function has been applied in the processing of the delivered Radarsat-2 SLC products [142]. The reduced bandwidth is from here on referred to as the total available azimuth bandwidth B, stretching from $f_0 - B/2$ to $f_0 + B/2$.

4) Subband Extraction: Two azimuth subbands are extracted from B, which will be used

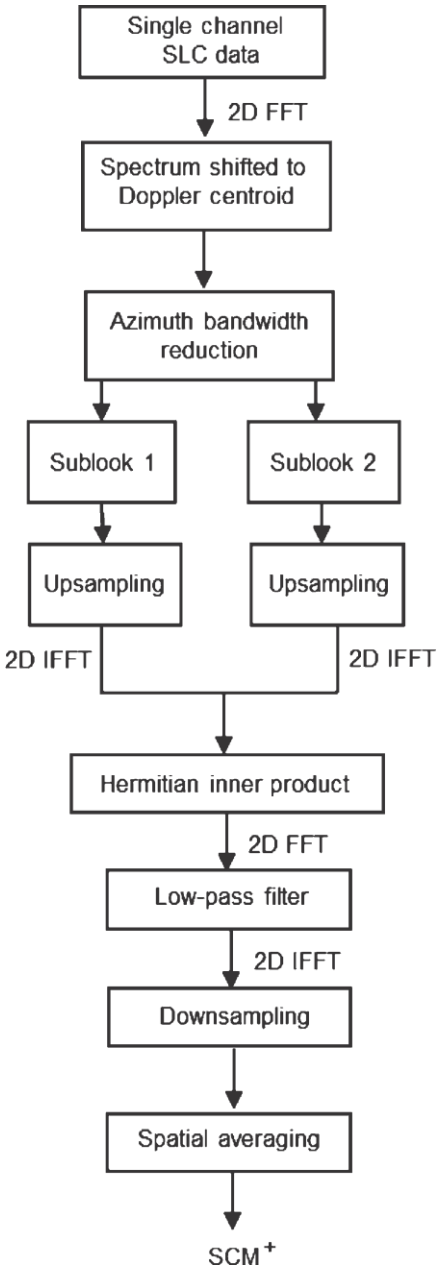

Figure 5.1 Flow Chart of the Sub Aperture Processing Algorithm

to produce the subaperture scattering coefficients S_1 and S_2 in step 6. The sub- band extraction strategies investigated in this letter are described in Section II-B.

5) Upsampling: To allow overlapping subaperture with-out introducing aliasing, both subaperture are first zero padded to double the size in both range and azimuth; then, a

low-pass filter is applied in step 7. Upsampling is done to increase the sampling frequency and avoid that unwanted components of the signal fall into the passband of the filter applied in step 7. The center frequencies of the subaperture $\mathbf{f_1}$ and $\mathbf{f_2}$ are shifted to $\mathbf{f_0}$ to avoid a frequency difference between them.

6) Hermitian inner product: A 2-D inverse FFT (2-D IFFT) is used to produce S_1 and S_2 Their complex correlation is computed as the Hermitian inner product: $S_1\ S_2^*$.

7) Low-pass filter: After a 2-D FFT, a low-pass filter (e.g., a Hanning window) stretching from $\mathbf{f_0} - \mathbf{B}/2$ to $\mathbf{f_0} + \mathbf{B}/2$ is applied in both range and azimuth direction. This shows better results when the low-pass filter is applied to the complex ρ, rather than the magnitude |ρ|.

8) Downsampling: We return to the spatial domain by a 2-D IFFT and down sample to half the size in both range and azimuth direction.

9) SCM^+ : A local averaging filter (e.g., of size 3 × 3 pixels) is applied to the complex subaperture correlation ρ. The magnitude of the data is extracted.

5.2.1 Variation of Subaperture Bandwidth

In the subband extraction stage, it is assumed that both subapertures are assigned the same fraction of the total avail- able azimuth bandwidth *B*. The bandwidth allocated to each subaperture, denoted as B_S , always starts from one end point of the azimuth spectrum and stretches towards the other, with a potential overlap with the other subaperture.

In the first limiting case, both subapertures have zero band- width. At a bandwidth of $B_S = B/2$, the subapertures together occupy the whole azimuth spectrum, but there is no overlap. A subaperture bandwidth of $B_S = B$ defines the other limiting case, where there is a total overlap between the subapertures [67].

It follows that $B_S \leq B/2$ is equivalent to no overlap, $B/2 < B_S < B$ *represents* partial overlap, and the degree of overlap in the latter region is $2B_S/B - 1$. The bandwidth definition is shown in fig. 5. 2, which shows the cases $B_S = B/4$, $B_S = B/2$, and $B_S = 3B/4$.

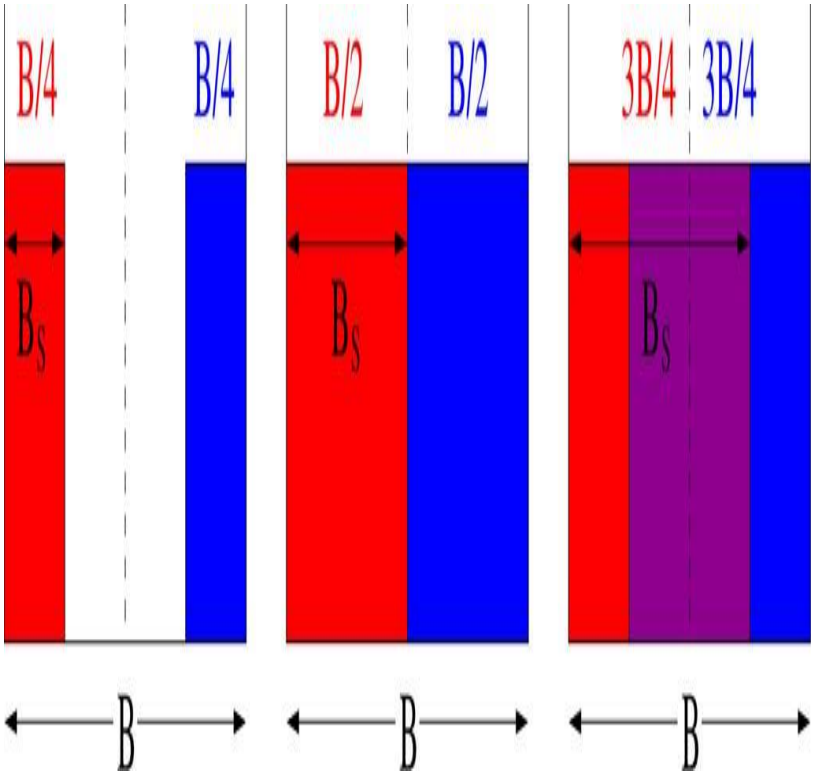

Figure 5.2. Variation of the subaperture bandwidth B_S within an azimuth spectrum with bandwidth B. (Right) Case $B_S = 3B/4$ has partial overlap between the subbands.

The SLI, which is commonly used in ship detection, is conventionally calculated as $I = S_1 \cdot S_1^*$. This is equivalent to $\rho = S_1 \cdot S_2$ with $B_S = B$ (thus $S_1 = S_2$) and no averaging. Hence, unless countermeasures are taken, the quality of the SLI data will also be reduced by aliasing, as for the SCM product. To handle this, we apply the algorithm outlined in figure 5.1 for the limiting case $B_S = B$ but omit the local averaging in step 9.

5.3. EXPERIMENTAL WORK AND RESULTS

Experiments show that the investigated target is often not properly resolved for β 0.15. Hence, we limit the following analysis to $\beta \in [0.15, 1]$.

5.3.1 Results of SCM$^+$

The data set consists of three SAR SLC images and contains three acquisitions of a search-and-rescue vessel (length: 64.5 m; width: 13.8 m) in open sea. The SAR data were

recorded over the in the Norwegian Sea. Experimental results based on dataset are shown in figures 5.3 to 5.6. An area of size 200 × 200 pixels is selected for all clutter regions studied.

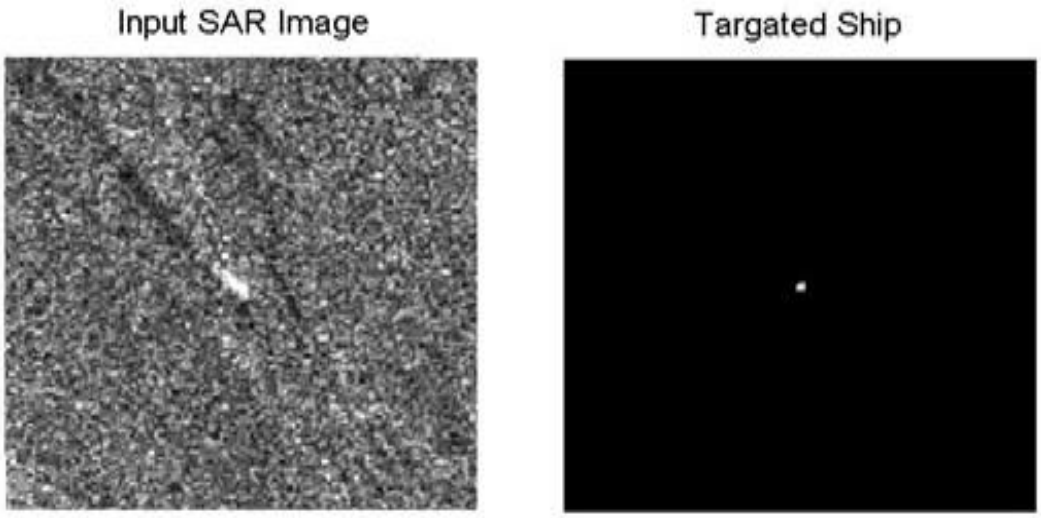

Figure 5.3 (a) Input image of SAR data set 1 (b) Output of SAR data set 1

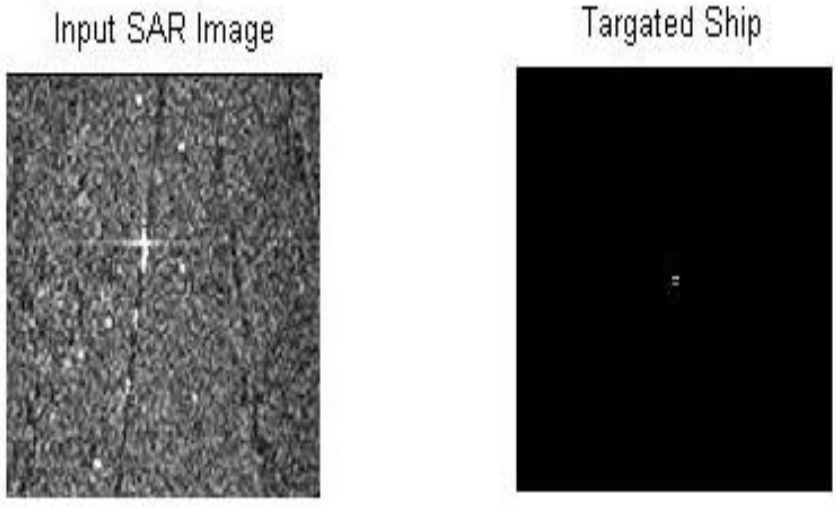

Figure 5.4 (a) Input image of SAR data set 2 (b) Output of SAR data set 2

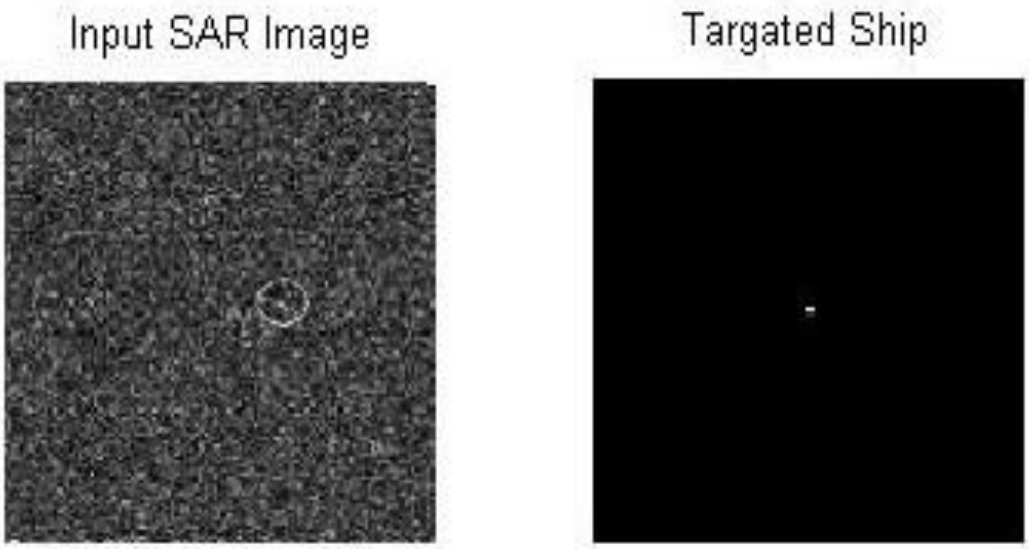

Figure 5.5 (a) Input image of SAR data set 3 (b) Output of SAR data set 3

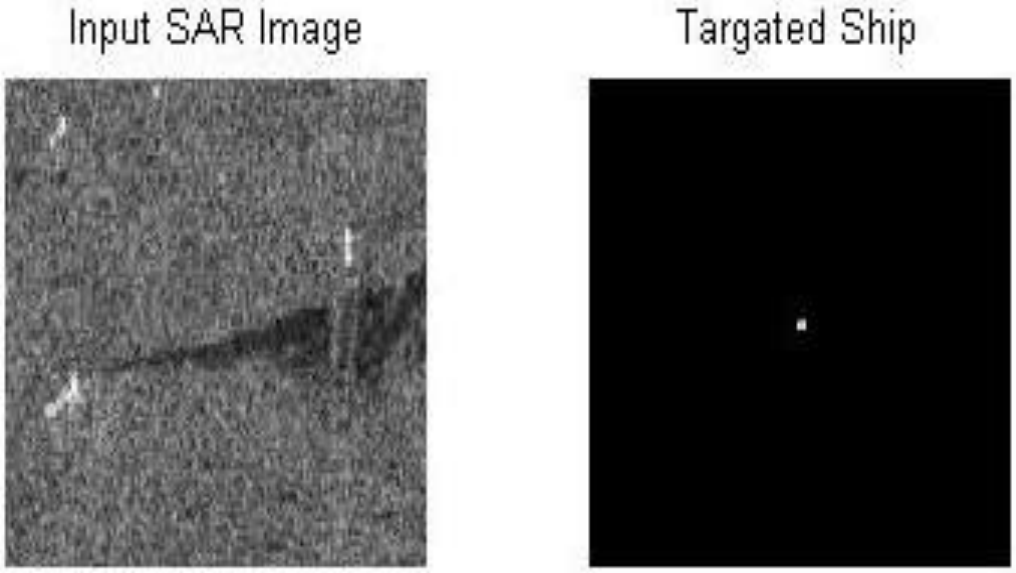

Figure 5.6 (a) Input image of SAR data set 4 (b) Output of SAR data set 4

5.4 PERFORMANCE ANALYSIS OF IMPROVED SCM OR I- SCM

In Section 5.3, we compare SCM^{+} to SLI^{+} with respect to measures of the speckle level and the contrast between the target and the surrounding background. Specifically, we investigate the coefficient of variation (CV) and the target- to-clutter ratio (TCR). These parameters are measured as a function of the normalized sub aperture bandwidth, which is defined as $\beta = B_S/B$. Hence, it ranges from 0 to 1, whereas the region where the sub apertures overlap goes from 0.5 to 1.

The performance of I-SCM is analyzed in the following terms:

Coefficient of variations (CV)

Spatial Resolution (SV)

5.4.1 Coefficient of Variations (CV)

CV is the measure of heterogeneity between targeted ship and background (open sea environment) of received SAR images. The highest pixel resolution that can be obtained is inversely proportional to the subaperture bandwidth. Thus, as β is raised, the CV is calculated from image data with steadily increasing resolution.

$$CV=\sigma_c/\mu_c$$

Here σ_c is standard deviation of pixel intensity of any given area in SAR image.

μ_c mean of pixel intensity of any given area in SAR image.

- The μ_c and σ_c contribute as a divisor and a dividend to the CV.
- The explicit decomposition is useful to interpret the variation of the CV.
- If the resolution kept same and the target is stationary. Then following observations are concluded.
- For $\beta > 0.5$, Mean value would stay same, whereas standard deviation would decreases, and speckle in images improved in terms of CV.

Table 5.1 Performance of SCM –I in terms of Coefficient of variations

β	Mean	Deviation	CV
0.5	0.0987	3.7858	38.3566
0.6	0.0733	3.1899	43.5184
0.75	0.0751	3.1855	42.4433

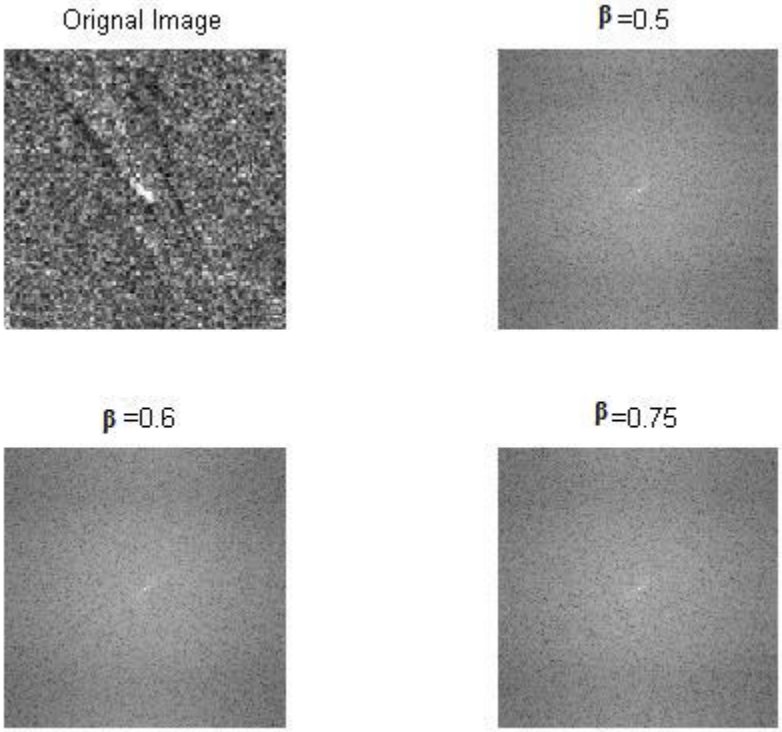

Figure5.7 Influence on spatial resolution for β>0.5

5.4.2 Spatial Resolution (SV)

- Increment in sub aperture bandwidth for β>0.5 not have any influence on the spatial resolution.

- β=0.6 we can observed we can observe peak point of CV i.e. strong contrast between the targeted ship and the surrounding water and flooding waves.
- Hence it is concluded, where the sub apertures are partially overlapped provides best contrast.

5.5. CONCLUSIONS AND FUTUREWORK

This chapter introduced I-SCM Improved algorithm (Sub-aperture Cross-Correlation Magnitude for ship detection). It is used to detect small man made target in Radar Images.

For higher degree of overlapping strong contrast between the targeted and background is found. Moreover partially overlapped sub apertures provide higher level of contrast.

The proposed work detect motionless ship target in sea water. Experimental results are based on contrast enhancement and segmentation techniques.

CHAPTER VI

IMAGE EDGE DETECTION BASED ON MODIFIED ANT COLONY OPTIMIZATION

6.1 INTRODUCTION

Ant system is one of the bio inspired technique that attract research to solve many problems. Edge detection is in specific one of the indispensable problem that is taken care by ant system. Simple edge detection technique more time to detect edges if the size of image is enlarged. Besides this, of discontinuities between the edge's pixels increase problem in multi fold [68].

In this chapter Ant Colony Optimization (ACO) based approach is used to detect edges of a ship in sea environment. Application of triangular fuzzy member ship function is reduce time consumption. Proposed work shows clear edges of small and partial objects.

Edge detection is one of the staple discontinuities based segmentation algorithm to detect object in a given image. Edges of objects are detected on the basis of abrupt changes in intensity. Hence the principal approach is to identify the pixels that may be the potential candidates for drawing edge of object of interest. The property of edge pixel is sharp change in intensity value as compare to neighbouring pixels i.e. non edge pixels [68].

ACO is one of the bio inspired technique that utilized the above said feature of pixel and first select set of pixels as candidates for edge formulation. Thereafter outputs edges by using a suitable heuristic measure.

In proposed work ACO is to determine edges of ship in a sea environment. Fuzzy triangular membership function estimate degree of edginess or heuristic information, because as the size of the image increases the computation time for conventional edge detection increases quickly as well as result in edges have discontinuities.

The above said heuristic membership function based ACO shows better performance in terms of quality of edges as well as computation time.

The chapter is organized as follows. Section 6.2 provides a brief introduction to the fundamental concepts of ACO. Section 6.3 describes the proposed ACO-based approach for edge detection. Experimental results are presented in Section 6.4. Section 6.5 provides the conclusion.

Figure 6.1 Original Image of Ship under Sea Water

6.2 ANT COLONY OPTIMIZATION (ACO) BIO-INSPIRED TECHNIQUE

The ability of real ants to find shortest routes is mainly due to their depositing of pheromone as they travel; each ant probabilistically prefers to follow a direction rich in this chemical. The pheromone decays over time, resulting in much less pheromone on less popular paths. Given that over time the shortest route will have the higher rate of ant traversal, this path will be reinforced and the others diminished until all ants follow the same, shortest path the system has converted to a single solution. It is also possible that there are many equally short paths. In this situation, the rates of ant traversal over the short paths will be roughly the same, resulting in these paths being maintained while others are ignored. Additionally, if a sudden change to the environment occurs (e.g. a large obstacle appears on the shortest path), the ACO system can respond to this and will eventually converge to a new solution.

6.3 APPLICATION OF ACO ALGORITHMS

In general, an ACO algorithm can be applied to any combinatorial problem as far as it is possible to define:

Appropriate problem representation: The problem can be described as a graph with a set of nodes and edges between nodes.

Heuristic desirability of edges: A suitable heuristic measure of the "goodness" of paths from one node to every other connected node in the graph.

Construction of feasible solutions: A mechanism must be in place whereby possible solutions are efficiently created. This requires the definition of a suitable traversal stopping criterion to stop path construction when a solution has been reached.

Pheromone updating rule: A suitable method of updating the pheromone levels on edges is required with a corresponding evaporation rule, typically involving the selection of the n best ants and updating the paths they chose.

Probabilistic transition rule: The rule that determines the probability of an ant traversing from one node in the graph to the next.

In real world a team ants come out from the nest in search of food. To communicate with each other a chemical known as pheromone is evaporated by each ant on the path, which is going to be followed by that particular ant. If any obstacle appears on the path ants can choose a new path as shown in figure 6.2. The quantity of pheromone is decayed as time passes. This causes the quantity of pheromone on the shorter path to grow faster than on the longer one, and therefore the probability with which any single ant chooses the path to follow is quickly biased towards the shorter one. The final result is that very quickly all ants will choose the shorter path.

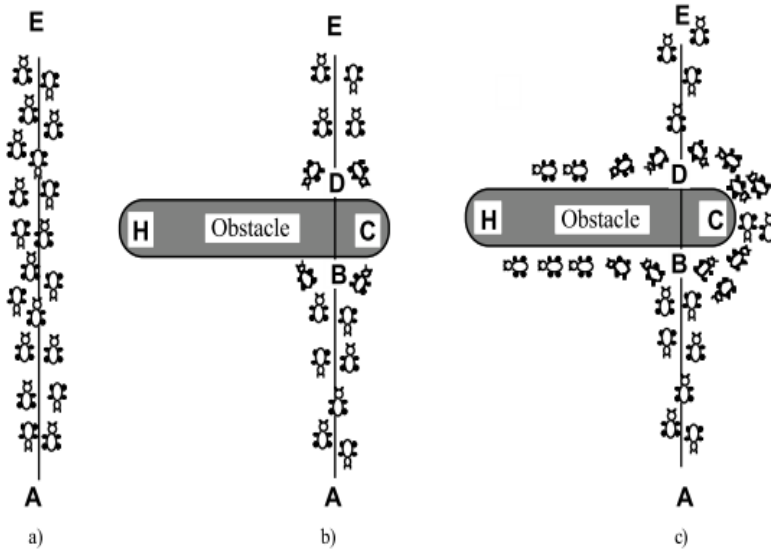

Figure 6.2 Movement of Real Ants

The selection of edge pixels task may be reformulated into an ACO-suitable problem. ACO requires a problem to be represented as a graph, here nodes represent pixels of images, with the edges between them denoting the choice of the next pixel. To search for the potential candidates for pixels an ant travels through the graph where a minimum number of nodes are visited or move of ants' satisfies the traversal stopping criterion.

Figure 6.3 illustrates this setup—the ant is currently at node and has a choice of which pixel to add next to its pixel (dotted lines). It chooses pixel b next based on the transition

rule, then c and then d. Upon arrival at d, the current set of pixels are {a, b, c, d}, and four numbers of move is used to satisfy the stopping criterion. The ant terminates its movement and outputs this traversal is a set of pixels candidate for edge formation.

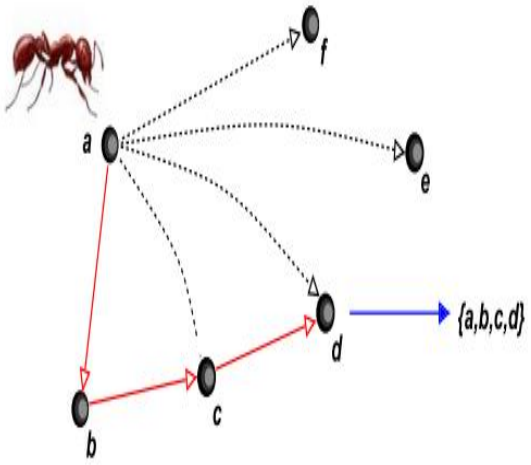

Figure 6.3 Ant Systems for Pixels Selection

6.4 EXPLANATION OF ACO

The ant colony system is derived from the study of real ant colonies. But artificial ants have some major differences with a real (natural) one [68].

- Artificial ants will have some memory,
- They will not be completely blind,
- They will live in an environment where time is discrete.

The movement of an ant in the graph is determined by the transition probabilities. This transition probability is influenced by two factors namely, the heuristic information and pheromone information. The construction of a solution to a problem contains a certain number of construction steps. Each ant tries to obtain a good solution simultaneously and individually at every construction step.

According to the [68], at the nth construction step, the k^{th} ant moves from node i to j according to transition probability. The transition Probability $^{(n)}p_{ij}$ is estimated as equation (6.1).

$$(n)_{p_{ij}} = \frac{\left\{(n-1)_{\tau_{ij}}\right\}^{\alpha}.(\eta_{ij})^{\beta}}{\sum_{j \in \Omega_j}\left((n-1)_{\tau_{ij}}\right)^{\alpha}(\eta_{ij})^{\beta}} \quad (6.1)$$

Where Ω is set of unvisited states α and β are constant to control influence of pheromone Heuristic information η is based on degree of edginess because movement of ant are trigger by greater degree of edginess it is neighbourhood.

The ant colony system allows for exploration by equation (6.2).

$$\text{j=} \begin{cases} argmax\ [\tau(i,j) * \eta(i,j)] & if\ q \leq q_0 \\ j & otherwise \end{cases} \quad (6.2)$$

Where, q is a random number, q_0 is a parameter ($0 <= q_0 < 1$) , and J is the random variable selected according to the previous probability distribution in equation 1.

At every step, based on the value of q generated an ant is moves from state I to state j. if q≤ q0 the best edge is chosen according to (6.1). The best so far solution for every construction step for entire algorithm is recorded.

If, pheromone deposited by an ant provides a positive feedback and thus reinforce the probability to find new good solution. Otherwise evaporation of pheromone acts as a negative feedback, which prevent algorithm to stop at local maxima.

The pheromone is updated twice during algorithm. The first update is performed after movement of each ant in each construction step.

$$(n)_{\tau_{ij}} = \begin{cases} (1-\rho) * \left((n-1)_{\tau_{ij}}\right)^{\alpha} + \rho * \left(\Delta_{ij}\right)^{\beta} & if\ i,j\ belongs\ to\ best\ tour \\ (n-1)_{\tau_{ij}} & otherwise \end{cases} \quad (6.3)$$

whereρ is evaporation rate.

$$(n)_{\Delta\tau(i,j)} = \begin{cases} 1/f_k & if\ ant\ k\ edges\ (i,j) \\ 0, & otherwise \end{cases} \quad (6.4)$$

Where f_k, is the tour length of k^{th} ant. This tour length depends on the nature of the problem to be solved. It's value is chosen in such a way that desirable routes have smaller tour length.

The second update is performed after all K ants have moves within each construction steps:

$$^{(n)}\tau = (1-\varphi).(^{(n-1)}\tau) + \varphi.(^{(0)}\tau) \quad (6.5)$$

here, φ is the pheromone decay coefficient

6.5. PROPOSED ACO BASED APPROACH FOR EDGE DETECTION

In proposed algorithm fuzzy membership function is used for edge detection. The heuristic information gathered by ants is very crucial for estimation of transition probability. The value of transition probability is used to decide the choice of ant to move or select a particular pixel. For segmentation of object from ground edginess property is used as heuristic information. As a final step pheromone matrix is used to determine whether a pixel is edge or not. For this purpose threshold of intensity is used. Algorithm consists of four main steps:

6.5.1 Read Image

First step is to read image 'I', and convert it into gray level image. Further, image is converted into is 2-D image matrix 'G' .

6.5.2 Initialization Process

This process consists of two steps initialization element of pheromone matrix and estimation of degree of edginess for each pixel.

(a) The initial value of each element of pheromone matrix τ_{int}=0.001.

(b) Heuristic information η_{ij} is estimated on the basis of variation of image's intensity values in neighborhood by equation (6.6).

$$\eta = \Delta/(c-b) \quad (6.6)$$

Heuristic information η is based on degree of edginess because movement of ant is trigger by greater degree of edginess at its neighborhood. A '3x3' neighborhood considered η is given by triangular fuzzy membership function as shown in figure 6.4.

$$\Delta=G(i,j) - (\sum_{k=-1\ to1} G(i+k,j+k)/8) \quad (6.7)$$

here G(i,j) is intensity of pixel at i^{th} row and j^{th} column, c = max (G(i,j)) and b = min(G(i,j))

6.5.3 Iterative Construction and Update Process

This construction step is twofold update process, in first step each ant moves individually and update pheromone matrix. The second update is performed after all K ants moved within each construction step.

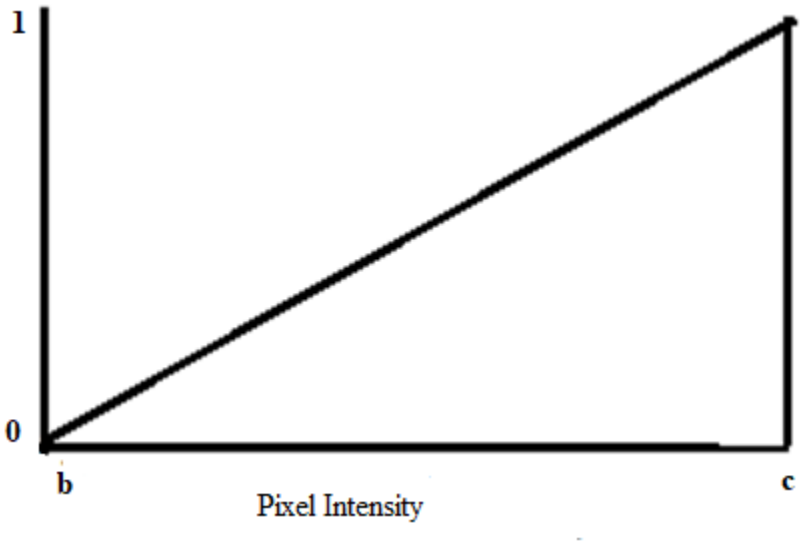

Figure 6.4 Triangular Membership Function

(a) Let, in first construction step k^{th} ant move L times. Then transition probability $^{(n)}p_{ij}$ is estimated by equation (6.1). On the basis of estimated transition probability amount of pheromone is determine by equations (6.2) and (6.3).

(b) The second update is performed in each construction step after all k ants moved within each construction step by equation (6.4).

6.5.4 Decision Process

A final pheromone matrix constructed to reflect the edge information. Each element of matrix corresponds to a pixel in image and specifies whether that pixel is an edge or not on the basis of threshold T.

6.6 EXPERIMENTAL WORK AND RESULTS

Proposed method is based on algorithm given below.

Proposed Algorithm

START

STEP 1: Read Infrared Image

STEP 2: Convert into gray level image

STEP 3: Estimation of pheromone matrix

(a) Initialize values of quantity of pheromone (τ), evaporation rate (ρ), and pheromone decay coefficient(φ) .

τ= 0.001, ρ=0.01 , and φ=0.001

(b) **)** Measure Heuristic information $\eta_{ij}$by equation (6.6).

(c) Estimate Transition Probability ($^{n)}p_{ij}$andpheromone quantity for first construction step by equations (6.1) and (6.3) .

(d) Performed second update after all K ants moved within each construction step by equation (6.4).

STEP 4: Construct final pheromone matrix reflect the edge information by pixel by pixel analysis of gray level. After iteration completion of iterative process threshold 'T' is calculated as 0.7.

(a) If f(x,y) >T

Then g(x,y)=f(x,y)

(c) Else

f(x,y)==0

END

On the basis of proposed methodology experiments are carried out and results along with experimental work are discussed in now onwards.

The experimental work is carried out by taking infrared image of ship as shown in figure 6.1. The resolution of image is 256x256 pixels. Number of ants, K=4; each ant moves N=40 construction steps. The threshold value is taken T=0.7. In first step all the values initialized as follows $\tau = 0.001$, $\rho = 0.01$, $\varphi = 0.001$. 9- Pixels (3 by 3) neighbourhood considered, to determine degree of edginess η, by applying triangular fuzzy membership function. The outcome of experimental work is shown in figure 6.5.

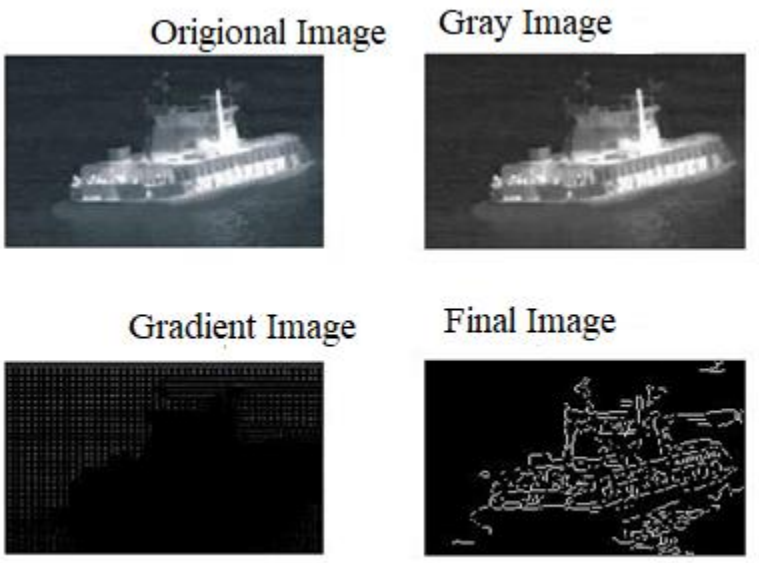

Figure 6.5 Extracted Edge Information by using Proposed Method

To check the performance algorithm work is to imagine each ant, if isolated would move with local maxima. This local guarantee only locally optimal moves and will practically always lead to formation of discontinues edges. If we now consider the effect of the simultaneous presence of many ants, then each one contributes to the trail distribution. Good parts of paths will be followed by many ants and therefore they receive a great amount of trail. On the contrary, bad parts of paths are chosen by ants only when they are obliged by constraint satisfaction these edges will therefore receive trail from only a few

ants. To verify the performance of proposed algorithm some more images are considered as shown in figures 6.6-6.8. Figures 6.6 and 6.7 displays edges of small ship and partial ship respectively. Where as in figure 6.8 edges of a girl face are shown very clearly, which are generated by proposed algorithm.

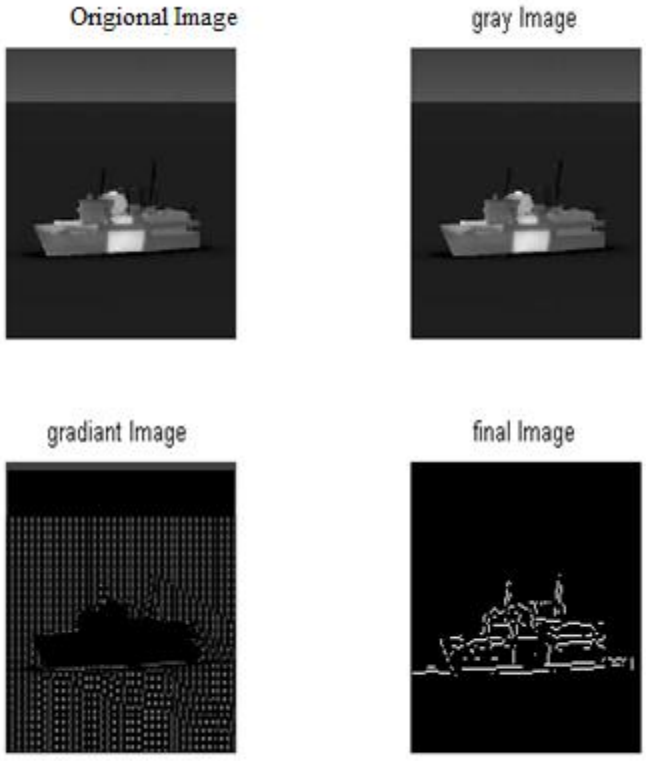

Figure 6.6 Outcomes of ACO Based Edge Detection of Small Ship

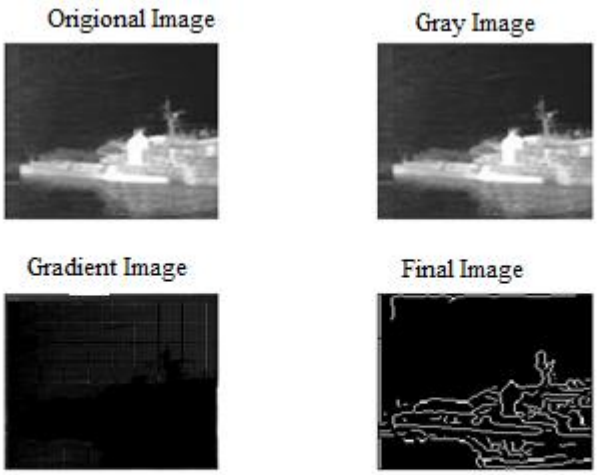

Figure 6.7 Outcomes of ACO Based Edge Detection of Partial Ship

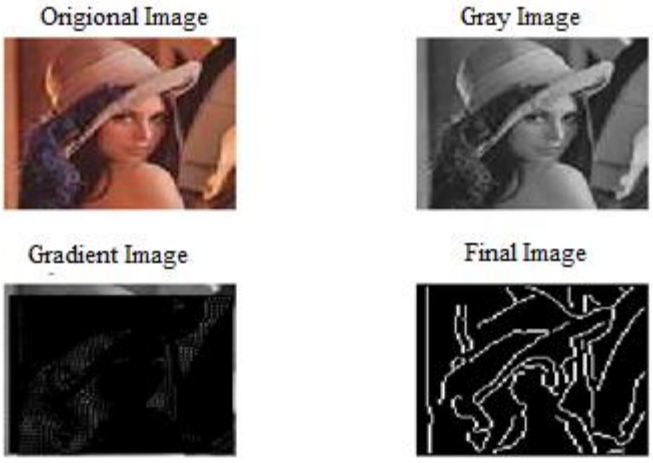

Figure 6.8 Outcomes of ACO Based Edge Detection of Girl‘s Image

Performance of proposed triangular fuzzy membership function based ACO is compared with well established Fuzzy C-Means ACO algorithm.The threshold value is taken

T=0.7. Following parameter are taken τ= 0.001, ρ=0.01, φ= 0.001 with 8- neighbourhood is considered to draw the edge's pixel, ant moves N=40 construction steps.

Table 6.1 Performance of Proposed Algorithm

Dimension of Image	**Number of Ants**	**Time required to find all the participating pixels to draw edge**	
		Fuzzy Membership Function based ACO	**Fuzzy C-Means ACO Algorithm**
256x256	4	13 second	14 second
256x256	8	6 second	7 second
256x256	16	2.57 second	3 second

After analyzing table 6.1, it is found that performance of proposed algorithm time complexity is better than well know Fuzzy C-Means ACO algorithm.

6.7. CONCLUSION AND FUTURE DIRECTIONS

This chapter introduced a new search methodology based on a triangular membership function based heuristic to detect edges of ship under sea water. Higher quantity of pheromone on a path gives clue, that, particular path was trailed by a large number of ants. Proposed Fuzzy membership function helps in producing better over other conventional methods of edge detection.

CHAPTER VII

ANALYSIS OF EDGE DETECTION ALGORITHMS AND NOISE FILTERS

7.1 INTRODUCTION

Edge detection is a key tool for image segmentation, which is used for object detection and analyzing the images. This triggers necessities of robust edge detector to produces the best results in all conditions. This objective can be achieved by analyzing performance of different methods of edge detection. In proposed work comparison of edge detection is carried out. This chapter evaluated and analyzed various edge detection algorithms. Moreover Classical Edge Detection Methods are combined with proposed OWA filter and median filter to remove impulse noise. These two filters are already discussed in chapter 4. Performance of these filter analyzed. There are many methods for edge detection, but most of them can be grouped into two categories,

(i) Measure of gradient magnitude (edge strength) based methods

(ii) Measure of Laplacian (zero-crossings of non-linear differential expression) based methods.

Therefore upcoming subsections focused on Gradient and Laplacian based edge detecting methods.

7.2 GRADIENT BASED EDGE DETECTORS

This method detects edges by first computing a measure of edge strength or gradient magnitude. Thereafter, searching for local directional maxima of the gradient magnitude by estimating local orientation of the edge or gradient direction [18].

Types of gradient based edge detectors:

- Prewitt edge detectors
- Sobel edge detectors

7.2.1 Prewitt Detectors

The Prewitt edge detector is a suitable means to assess the magnitude and orientation of an edge. Although to estimate the orientation from the magnitudes in both x and y directions, differential gradient edge detection requires lot of calculations which are time consuming. The Prewitt operator is restricted to eight possible orientations; while the accuracy of most direct orientations estimations is not so high. This gradient based edge detector is estimated in the 3x3 neighborhood for eight directions then all the eight convolution masks are calculated. One convolution mask is then selected, which is having the largest module. The convolution masks for horizontal and 45^0 aligned in positive direction of the Sobel edge detector is given below:

-1	+1	+1
-1	-2	+1
-1	+1	+1

0^0

+1	+1	+1
-1	-2	+1
-1	-1	+1

45^0

Figure 7.1 Convolution Masks of the Prewitt Edge Detector

7.2.2 Sobel Edge Detectors

The Sobel operator accomplishes a 2-D spatial gradient measurement on an image and it highlights the regions of high spatial frequency that relates to edges. Normally to find the approximate absolute gradient magnitude at each point in an input grayscale image, a Sobel operator is utilized. Due to the introduction of the average factor, it has some smoothing effect to the random noise of the image. Because it is the differential of two rows or two columns, so the elements of the edge on both sides has been enhanced, so that the edge seems thick and bright.The convolution masks of the Sobel edge detector is given below:

-1	0	+1
-2	0	+2
-1	0	+1

G_x

+1	+2	+1
0	0	0
-1	0	+1

G_y

Figure 7.2 Convolution Masks of the Sobel Edge Detector

7.3 LAPLACIAN BASED EDGE DETECTORS

The Laplacian is a second-ordered derivative, it can be directly apply to detect noise in it's original form. Because Laplacian yields double edge, which is an undesirable effect. On the other hand, Laplacian has some advantages too, e.g. it zero crossing property helpful in locating edges, whereas it also detect whether a pixel is on dark or light side of an edge. Therefore this second ordered derivative combined Gaussian and other operators. Some of them are discussed below.

Types of Laplacian based edge detectors

- Laplacian of Gaussian Edge Detector (LoG) Method
- Roberts Edge Detection Method
- Canny Edge Detector Method

7.3.1 Laplacian of Gaussian or (LoG) Edge Detection Method

Laplacian of Gaussian or LoG combines two mathematically similar approaches. Firstly, the image is convoluted with Gaussian smoothing filter and then it calculates results with Laplace. Secondly, image is the linear filtered which is the Laplacian of the Gaussian filter. This is also the case in the LoG. Gaussian filter is used for smoothing or filtering. By transforming edges into zero crossings, the enhancement is performed and for identification of its type, the detection is performed by detecting the zero crossings for the various samples of sharp images. Laplacian of Gaussian (LoG) tests wider area around the pixel and detects edges correctly, but malfunctions at corners and curves. LoG method is unable to find edge orientation because of Laplacian property.

0	-1	0
-1	4	-1
0	-1	0

Figure 7.3 Convolution Masks of the LoG Edge Detector with 4- Neighborhood

-1	-1	-1
-1	8	-1
-1	-1	-1

Figure 7.4 Convolution Masks of the LoG Edge Detector with 8- Neighborhood

7.3.2 Roberts Edge Detection Method

The Roberts edge detection method accomplishes a simple, quick to compute, 2-D spatial gradient measurement on an image. It shows regions of high spatial frequency which generally correspond to edges. Grayscale image is given as input to the operator, as is the output, in its general applications. A pixel value at every point in the output gives the estimated absolute magnitude of the spatial gradient of the input image at that point.

1	0
0	-1

0	+1
-1	0

Figure 7.5 Convolution Masks of the Robert Edge Detector

7.3.3 Canny Edge Detection Method

John Canny considered the device canny filter as a tool for developing a best smoothing filter which is used for localization and minimizing multiple responses to a single edge.

This is an optimal filter, which consists of four exponential terms and can be well approximated by first-order derivatives of Gaussians. Canny's edge detector is an optimal solution to problem of edge detection which gives better detection especially in presence of noise, but it is time consuming and require a lot of parameter setting. Canny filter based on opinion of non-maximum suppression, which means that given the pre smoothing filters, edge points are described as points where the gradient magnitude assumes a local maximum in the gradient direction.

-1	0	+1
-2	0	+2
-1	0	+1

Figure 7.6 Canny Convolution Masks for Vertical Edge Detection

+1	+2	+1
0	0	0
-1	-2	-1

Figure 7.7 Canny Convolution Masks for Horizontal Edge Detection

7.4 PERFORMANCE OF EDGED DETECTION METHODS

It is founded that Gradient based edge detectors like Prewitt and Sobel are relatively simple and easy to implement, but are very sensitive to noise. Figures 7.8 and 7.9 display edges of ship generated by Prewitt and Sobel Edge Detector respectively. These figures de-noised image with median filter and OWA based filter thereafter edges were detected.

Denoised image of Ship with median filter and prewitt edge detector

Denoised image of Ship with OWA most filter prewitt edge detector

Figure 7.8 Edges of Ship generated by Prewitt Edge Detector

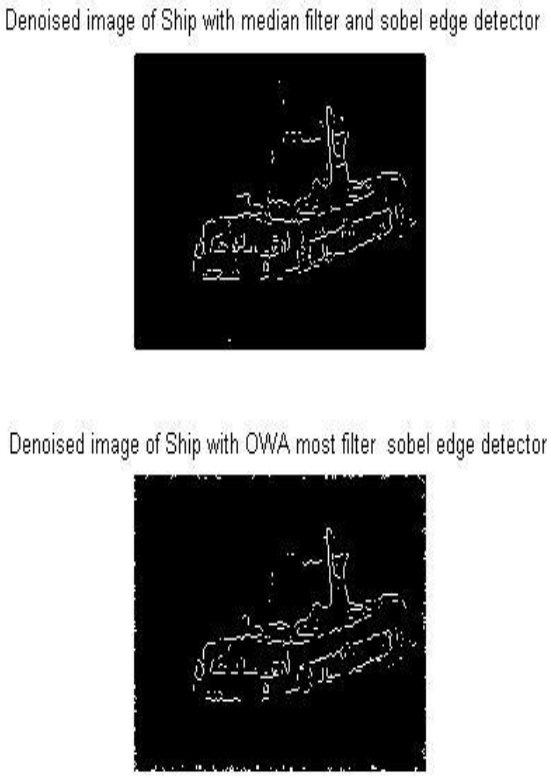

Figure 7.9 Edges of Ship generated by Sobel Edge Detector

On the seminal line in figures 7.10-7.12 performance of LoG, Robert, and Canny's operator are analyzed.

Denoised image of Ship with median filter and log edge detector

Denoised image of Ship with OWA most filter log edge detector

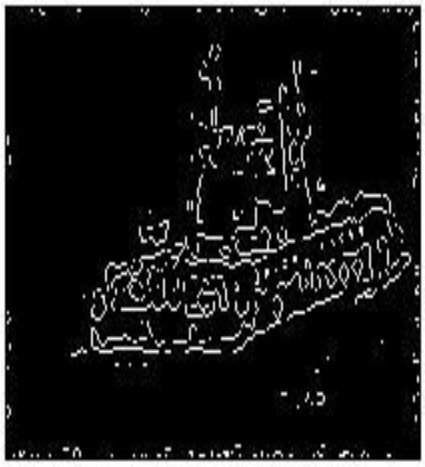

Figure 7.10 Edges of Ship generated by Laplacian of Gaussian Edge Detector

Denoised image of Ship with median filter and roberts edge detector

Denoised image of Ship with OWA most filter roberts edge detector

Figure 7.11 Edges of Ship Generated by Roberts Edge Detector

Denoised image of Ship with median filter and canny edge detector

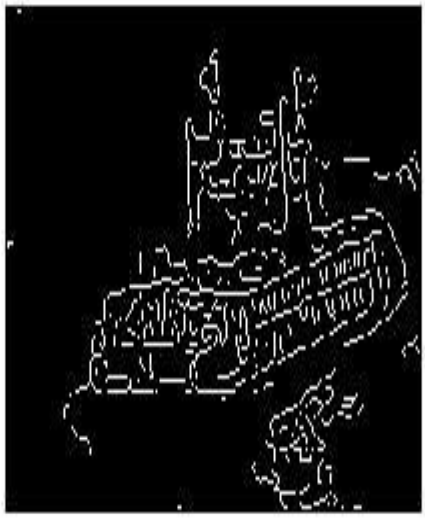

Denoised image of Ship with OWA most filter canny edge detector

Figure 7.12 Edges of Ship generated by Canny Edge Detector

7.5 ANALYSIS OF EDGE DETECTION TECHNIQUES

- Gradient based edge detectors like Prewitt and Sobel are relatively simple and easy to implement, but are very sensitive to noise.
- Laplacian of Gaussian tests wider area around the pixel and find the edges correctly, but malfunctions at corners and curves. It also does not find edge orientation because of using Laplacian filter.
- Canny algorithm is an optimal solution to problem of edge detection which gives better detection especially in presence of noise, but it is time consuming and requires a lot of parameter setting.
- Edge Generated by Roberts Operator in Median Filter are more prompt than most OWA operator.

7.6 CONCLUSION AND FUTURE DIRECTIONS

This chapter analyzed performance of Gradient based edge detectors as well as Laplacian filter. In future, more soft computing technique algorithm can be used to implement quick and adaptive edge detection methods.

CHAPTER VIII
CONCLUSIONS AND FUTURE DIRECTIONS

8.1 CONCLUSIONS

This chapter concludes the work of all the previous chapters. At a glance, it can be stated two category of image processing techniques viz. image enhancement and image segmentation are analyzed and compared.

In this research, continuity and discontinuity based segmentation is analyzed. Infrared image of ship is segmented from background, thereafter de-noised from impulse noise by using OWA filter. SCM algorithm is used to detect ship in sea water, while SAR image is used as input.

Infrared image is taken as input due to its high heat signature. There are two main techniques used to detect small objects using infrared image. Proposed Object Tracking algorithm is better if input images are infrared images; this technique is also capable to capture movement of enemy troops due to its heat sensing property, whereas SCM version of ship detection is useful when input image is taken from RADAR in highly agitated sea water.

Infrared image of ship in sea is de-noised from Impulse noise. Impulse noise may be introduced into thermal images either due to flood waves in sea water or during acquisition and transmission. A noise filter is introduced, that is based on ‘most fuzzy linguistic quantifier’. This naïve filter is compared with well-established median filter. A mask of 3X3 is generated by OWA operator and convoluted with every pixel of OWA images with 8-neighbors.Further to de-noised image from impulse noise a new OWA based method is compare with median filter. The proposed method produces better results in terms of Signal to noise ratio and visibility.

Moreover, this research extracted image on the basis of estimated global thresholding to identify the location of ship in sea water. Threshold value of heuristic approach based on visual inspection is 129. The value of global threshold produced by ‘most’ linguistic

quantifier is 115 whereas ‘at least half ’, and ‘as many as possible’ linguistic quantifier produces 131 and 125 respectively. Results produced by ‘at least half ’, and ‘as many as possible’ linguistic quantifier are much closer to visual inspection. On the other hand output of Sobel object detection is not very clear.

An improved version of the SCM algorithm for ship detection is analysed, which allows overlapping subaperture while mitigating aliasing. In earlier method infrared image is taken as input. It is observed we can observe peak point of CV i.e. strong contrast between the targeted ship and the surrounding water and flooding waves at $\beta=0$. Hence it is concluded, where the sub apertures are partially overlapped provides best contrast. Cases with highly agitated open sea states and the best choice of averaging filter window size should be investigated in the future. In proposed work Infrared and Sub-aperture Cross-Correlation Magnitude is used to detect stationary ship target in sea water. Experimental results are based on contrast enhancement and segmentation techniques. But proposed work is not used to detect moving target (ship in sea water). Only Averaging filter with 3X3 size is used to improve resulting image, use of more averaging filter should be done.

The proposed work introduces a new search methodology based on a triangular membership function based heuristic to detect edges of ship under sea water. The general idea underlying the Ant Colony System paradigm is that ants are directed by quantity of pheromone on the various path. Higher quantity of pheromone on any path from source to destination is indicated that, it was followed by a good number of ants and may leads to shortest path. Proposed work gives better results as compared to other conventional methods of edge detection.

What is more this work compare and analyzed some famous edge detection algorithms and evaluate them on the basis of their results to different images. Gradient based edge detectors like Prewitt and Sobel are relatively simple and easy to implement, but are very sensitive to noise. LoG tests wider area around the pixel and find the edges correctly, but malfunctions at corners and curves. It also does not find edge orientation because of using Laplacian filter. Canny’s algorithm is an optimal solution to problem of

edge detection which gives better detection specially in presence of noise, but it is time consuming and require a lot of parameter setting.

8.2 FUTURE DIRECTIONS

Current research work has potential to become basis to trigger more research on the basis of following key points.

- More, fuzzy quantifier like ‘as many as possible’ and ‘at least half’ can be used to de-noising the image.
- The filtered image can be used for tracking of ship or movement of military troops in the water territory by using different segmentation techniques.
- Proposed work is for static positions of ship, In future same methodology can be used for moving ship and it is accepted to produce good results.
- The output of Sobel object detection is not very clear. OWA operators can be used for segmenting ship in static images,
- If we used proposed methodology to detect moving ship and it is accepted to produce good results.
- In future more soft computing technics like neural network and genetic algorithm can be used to implement intelligent edge detection methods.
- The filtered image can be used for tracking of ship or movement of military troops in the water territory by using different segmentation techniques.

8.3 LIMITATIONS OF STUDY

- Proposed work is not used to detect moving target (ship in sea water).
- Averaging filter with 8-neihborhood is used to improve resulting image.
- In this work only fuzzy membership functions are used.
- Many intelligent system like machine learning, neural network and rough set based application yet to be explore.

REFERENCES

[1] R. R. Yager, "On OWA aggregation operators in multi-criteria decision making", *IEEE Transactions on Systems, Man, and Cybernetics*, vol. 18, pp.183–190, 1988.

[2] A. Emrouznejad and G. R. Amin, "Improving minimax disparity model to determine the OWA operator weights", *Information Science*, vol. 180, pp. 1477–1485, 2010.

[3] W. Zhang, S. Zeng, D. Wang, and X. Xue, "Weakly supervised semantic segmentation for social images", *Proceedings of IEEE Conference on Computer Vision Pattern Recognition, Boston, MA,USA*, pp. 2718–2726,2015.

[4] N. Pourian, S. Karthikeyan, and B. S. Manjunath, "Weakly supervised graph based semantic segmentation by learning communities of image parts", *Proceedings of IEEE International Conference Computer Vision, Santiago, Chile*, pp. 1359–1367,2015.

[5] D. Pei, Z. Li, R. Ji, and F. Sun, "Efficient semantic image segmentation with multi-class ranking prior", *Computer Vision Image Understand*, vol. 120, pp. 81–90, Mar. 2014.

[6] X. Yuan, J. Guo, X. Hao, and H. Chen, "Traffic sign detection via graph based ranking and segmentation algorithms", *IEEE Transaction Systems, Man and Cybernetics: System*, vol. 45, no. 12, pp. 1509–1521, Dec. 2015.

[7] J. Long, E. Shelhamer, and T. Darrell, "Fully convolution networks for semantic segmentation", *Proceedings of IEEE Conference on Computer Vision Pattern Recognition, Boston, MA, USA*, pp. 3431–3440, 2015.

[8] Y. Li, Y. Guo, J. Guo,M. Li,and X. Kong, "CRF with locality consistent dictionary learning for semantic segmentation", *Proceedings of 3rd IAPR Asian Conference on Pattern Recognition , Kuala Lumpur, Malaysi*a, pp. 509–513, 2015.

[9] J. Wang and A. L. Yuille, "Semantic part segmentation using compositional model combining shape and appearance", *Proceedings of IEEE Conference on Computer Vision Pattern Recognition, Boston, MA, USA*, pp. 1788–1797, 2015.

[10] S. Zheng et al., “Conditional random fields as recurrent neural networks”, *Proceedings of IEEE International Conference on Computer Vision, Santiago, Chile*, pp. 1529–1537, 2015.

[11] F. Wang, Q. Huang, M. Ovsjanikov, and L. J. Guibas, “Unsupervised multi-class joint image segmentation”, *Proceedings of IEEE Conference on Computer Vision Pattern Recognition, Columbus, OH, USA*, pp. 3142–3149,2014.

[12] L. Zhang et al., “A probabilistic associative model for segmenting weakly supervised images”, *IEEE Transaction Image Processing*, vol. 23, no. 9,pp. 4150–4159, Sep. 2014.

[13] P.O. Pinheiro and R. Collobert, “From image-level to pixel-level labeling with convolution networks”, *Proceedings of IEEE Conference on Computer Vision Pattern Recognition, Boston*, MA, USA, 2015, pp. 1713–1721.

[14] J. Dai, K. He, and J., “Sun,Box sup: Exploiting bounding boxes to supervise convolution networks for semantic segmentation”, *Proc. of IEEE International Conference on Computer Vision, Santiago, Chile*, pp. 1635-1643,2015

[15] Z. Li, J. Liu, J. Tang, and H. Lu, “Robust structured subspace learning for data representation”, *IEEE Transaction Pattern Analysis Machine Intelligent*, vol. 37, no. 10, pp. 2085–2098, Oct. 2015.

[16] L. Bazzani, A. Bergamo, D. Anguelov and L. Torresani, “Self-taught object localization with deep networks”, *Proceedings of IEEE Winter Conference Applications of Computer Vision(WACV),* Mar. 7–10, 2016. doi: 10.1109/WACV.2016.7477688.

[17] J.Tang, Z. Li, M. Wang, and R. Zhao, “Neighborhood discriminate hashing for large-scale image retrieval”, *IEEE Transaction Image Processing*, vol. 24, no. 9, pp. 2827–2840, Sep. 2015.

[18] Rafeal C. Gonzalez, Richard E. Wood, “Digital Image Processing”, Prentice Hall Publication, Second Edition.

[19] Linda G. Shapiro and George C. Stockman, “Computer Vision”, *New Jersey Prentice Hall*, ISB/n 0-1-030796, 2001.

[20] V. F. Vasiliev “Recognition of 2-D object on geometrical quasi-similarity of polygonal representations”, *in IEEE International Conference Systems, Man, and Cybernetics*, vol. 5, pp. 439W00, 1998.

[21] R. Stoica, J. Zerubia, M. Francos, “The two dimensional Word decomposition for segmentation and indexing in image libraries”, *in Proceedings of the 1998 IEEE International Conference on Acoustics, Speech, and Signal Processing*, vol. 5, pp. 2917 - 2980, 1998.

[22] P. A. Maragos, R. W. Schafer. and R. M. Mersereau, “Two dimensional linear prediction and its application to adaptive predictive coding of images”, *IEEE Transation Acoustics, Speech & Signal Process*, vol. ASSP-32, no.6. pp. 1213-1229, Dec. 1984

[23] Viola P, Jones M, “Rapid object detection using a boosted cascade of simple features”, *In: Proceedings of International Conference on Computer Vision and Pattern Recognition (CVPR)*, vol 1, pp. 511–518, b2001.

[24] Li H Sh, Lei Z Y, Wang Z M , “Principle and analysis of high altitude projectile location measurement using multi-screen target method”, *Journal of Chinese Journal of Scientific Instrument,* vol. 30, no. 3, pp.621-624, 2009.

[25] Jansen M, Malfait M, Bultheel A. “Generalization cross validation for wavelet thresholding”, *Journal of Signal Processing*,1997, vol. 56, no. 1, pp.463-479.

[26] Xu Yansun, “Wavelet transform domain filters:A spatially selective noise filtration technique”, *IEEE Transactions on Image Processing*, 1994, vol. 3, no. 6, pp.747-758.

[27] M.M.S. Beg, “User Feedback Based Enhancement in Web Search Quality”, *International Journal of Information Sciences, Elsevier*, vol. 170, no. 2-4, pp. 153-172, 2005.

[28] G. Beliakov, A. Pradera, T. Calvo, “Aggregation Functions: A Guide for Practitioners,” Springer, 2007.

[29] R. R. Yager, “Connectives and quantifiers in fuzzy sets”, *Fuzzy Sets and Systems*, vol. 40, pp. 39–75, 1991.

[30] H. B. Mitchell and D. D. Estrakh, “A modified OWA operator and its use in lossless DPCM image compression”, *International Journal of Uncertain Fuzziness, Knowledge Based Systems,* 5, pp 429–436,1997.

[31] G. Bordogna, M. Fedrizzi, G. Pasi, “A linguistic modeling of consensus in group decision making based on OWA operators”, *IEEE Transactions on Systems, Man and Cybernetics - Part A*, vol. 27, no.1, pp.126– 133, 1997.

[32] V. Torra, Y. Narukawa, “Modeling Decisions: Aggregation Operators and Information Fusion,” Springer, 2007.

[33.] R. R. Yager, L. S. Goldstein, and E. Mendels, “Fuzmar: an approach to aggregating market research data based on fuzzy reasoning”, *Fuzzy Sets and Systems,* vol. 68, no. 1, pp: 1–11, 199).

[34] R. Sadiq, S.Tesfamariam, “Developing environmental indices using fuzzy numbers ordered weighted averaging (FN-OWA) operators”, *Stochastic Environmental Research and Risk Assessment, Springer*, vol. 22, no.5, pp. 495-505, 2008.

[35] B.M. Imran, M.M.S. Beg, “Elements of Sketching with Words”, *in: Proc of IEEE International Conference on Granular Computing, (GrC2010), San Jose, California, USA,* pp. 241-246, August 14-16, 2010.

[36] K. Dabov, A. Foi, V. Katkovnik, and K. Egiazarian, “Image De-noising by Sparse 3D Transform-Domain Collaborative Filtering,” *IEEE Transaction Image Processing*, vol. 16, no. 8, pp. 2080-2095, Aug. 2007.

[37] M. Elad and M. Aharon,“Image de-noising via sparse and redundant representations over learned dictionaries,” *IEEE Transaction Image Processing*, vol. 15, no. 12, pp. 3736-3745, Dec. 2006.

[38] J. Mairal, F. Bach, J. Ponce, G. Sapiro, and A. Zisserman, “Non-local sparse models for image restoration,” *in Proceedings International Conference Computer Vision*, pp. 2272-2279, Sept. 29, 2009-Oct. 2, 2009.

[39] W. Dong, L. Zhang, and G. Shi, “Centralized sparse representation for image restoration,” *in Proceedings International Conference Computer Vision*, pp. 1259-1266, 6-13 Nov. 2011.

[40] W. Dong, L. Zhang, G. Shi, and X. Li, "Non-locally centralized sparse representation for image restoration," *IEEE Transaction Image Processing*, vol. 22, no. 4, pp. 1620-1630, Apr. 2013.

[41] W. Dong, L. Zhang, G. Shi, and X. Wu, "Image de-blurring and super resolution by adaptive sparse domain selection and adaptive regularization," *IEEE Transaction Image Processing*, vol. 20, no. 7, pp.1838-1857, Jul. 2011.

[42] J. Yang, J. Wright, T. Huang, and Y. Ma, "Image super-resolution via sparse representation," *IEEE Transaction Image Processing*, vol. 19, no.11, pp. 2861-2873, Nov. 2010.

[43] Z. He, S. Yi, Y. Cheung, X. You, and Y. Tang, "Robust Object Tracking via Key Patch Sparse Representation", *IEEE Transactions on Cybernetics*, no.99, pp.1-11, 2016.

[44] Francois G. Meyer and Xilin Shen, "Perturbation of the Eigenvectors of the Graph Laplacian: Application to Image De-noising", Applied and Computational Harmonic Analysis, vol. 36, no. 2, pp. 326-334, 2014.

[45] H. Talebi and P. Milanfar,"Global Image De-noising", *IEEE Transaction Image Processing*, vol. 23, no. 2, pp.755-768, Feb. 2014.

[46] W. Zuo, L. Zhang, C. Song, D. Zhang, and H. Gao, "Gradient Histogram Estimation and Preservation for Texture Enhanced Image De-noising," *IEEE Transaction Image Processing*, vol. 23, no. 6, pp. 2459-2472, Jun. 2014.

[47] R. Garnett, T. Huegerich, C. Chui and W. He, "A universal noise removal algorithm with an impulse detector," *IEEE Transaction Image Processing*, vol. 14, no. 11, pp. 1747-1754, Nov. 2005.

[48] S. Schulte, M. Nachtegael, V. De Witte, D. Van der Weken, and E. E.Kerre, "A fuzzy impulse noise detection and reduction method," *IEEE Transaction Image Processing*, vol. 15, no. 5, pp. 1153-1162, May. 2006.

[49] J. F. Cai, R. Chan, and M. Nikolova, "Two-phase methods for de- blurring images corrupted by impulse plus Gaussian noise," *Inverse Problem Imaging*, vol. 2, no. 2, pp. 187-204, 2008.

[50] J. Jiang, L. Zhang, and J. Yang, "Mixed Noise Removal by Weighted Encoding with Sparse Nonlocal Regularization," *IEEE Transaction Image Processing,* vol. 23, no. 6, pp. 2651-2662, Jun. 2014.

[51] J. Liu, X. C. Tai, H. Y. Huang, and Z. D. Huan, "A Weighted dictionary learning models for de-noising images corrupted by mixed noise," *IEEE Transaction Image Processing*, vol. 22, no. 3, pp. 1108-1120, Mar. 2013.

[52] Caselles V, Kimmel R, Sapiro G, "Minimal surfaces based object segmentation", *IEEE Transaction Pattern Anal Mach Intell*., vol. 19, no.4, pp. 394-397, 1997.

[53] Faghih F, Michael M., "Combining special and scale-space techniques for edge detection to provide a spatially adaptive wavelet-based noise filtering algorithm", *IEEE Transaction Image Processing*, vol.1, pp.1062–1071, 2002.

[54] Konishi S, Yulle AL, Coughlan JM, Zhu SC., "Statistical edge detection: learning and evaluating edge cues", *IEEE Transaction Pattern Anal Mach Intell*., vol. 25, no.1, pp.57–74, 2003.

[55] Suzuki K, Horiba I, Sugie N., "Neural edge enhancer for supervised edge enhancement from noisy image", *IEEE Transaction Pattern Anal Mach Intell*., vol. 25, no.12, pp.1582–1596, 2003.

[56] Martin DR, Fowlkes CC, Malik J. "Learning to detect natural image boundaries using local brightness, colour, and texture cues", *PAMI 26*, pp. 530-549, 2004.

[57] Lu S, Wang Z, Shen J., "Neuro-fuzzy synergism to the intelligent system for detection and enhancement", *Pattern Recognition,* vol. 36, no.10, pp. 2395-2409, 2003.

[58] Yu J, Wang Y, Shen Y. "Noise reduction and edge detection via kernel anisotropic diffusion", *Pattern Recognition Letter*, vol. 29, pp.1496-1503, 2008.

[59] Bezdek J, Chandrasekhar R, Attikouzel Y., "A geometric approach to edge detection", *IEEE Transaction Fuzzy System,* vol. 6, no.1, pp. 52-75, 1998.

[60] Tang H, Wu EX, Ma QY, Gallagher D, Perera GM, Zhuang T., "Brain image segmentation by multi-resolution edge detection and region", *Computer Medical Imaging Graph*, vol. 24, no. 6, pp. 349–357, 2000.

[61] Lopez-Molina C, Bustince H, Ferna´ndez J, Barrenechea E., "A t-norm based approach to edge detection", *In: IWANN 2009, part I, LNCS 5517*, pp. 302-309,2009.

[62] N. Dalal ; B. Triggs, "Histograms of oriented gradients for human detection", *Published in: 2005 IEEE Computer Society Conference on Computer Vision and Pattern Recognition (CVPR'05)*DOI: 10.1109/CVPR.2005.177, San Diego, CA, USA, USA 20-25 June 2005

[63] Sun G, Liu Q, Ji C, Li X., "A novel approach for edge detection based on the theory of universal gravity", *Pattern Recognition*, vol. 40, no.10, pp. 2766-2775, 2007.

[64] B.M. Imran, M.M.S. Beg, "Towards Computational forensics with f-geometry", *World Conference on Soft Computing' 2011, San Francisco State University, California, USA*, 2011.

[65] Abdul Rahman, M.M.S. Beg. "Estimation of f-validity of Geometrical Objects With OWA Operator Weights", *Fuzz-2013 IEEE International Conference on Fuzzy Systems* on July 7-10 , Hyedrabad India, 2013

[66**]** Liping et al., "Research and Analysis Small Infrared Object Detection Track Algorithm and Its Image Processing Technology", *Proceedings IEEE, 3rd International Conference on Computer Research and Development (ICCRD 2011) Shanghai, China*, vol.1, pp.30-33, 11 – 13, March 2011.

[67] Camilla Brekke, Yngvar Larsen, "Subband Extraction Strategies in Ship Detection With the Subaperture Cross-Correlation Magnitude", *IEEE Geoscience And Remote Sensing Letters*, vol. 10, No. 4, pp. 786-790, July 2013.

[68] R. Rajeshwari et al., "A Modified Ant Colony Optimization Based Approach for Image Edge Detection" *Proceedings of the IEEE International Conference on Image Information Processing (ICIIP 2011*), November 3 - 5, 2011.

[69] Xikui Sun et al., “A New Noise-resistant Algorithm for Edge Detection”, *Proceedings of the Second International Workshop on Education Technology and Computer Science*, pp. 47-50, 2010.

[70] L.S. Davis, “Edge Detection Technique”, *Computer Graphics and Image Processing*, vol. 4, pp. 248-270, 1995.

[71] V. B. Anna and O. Carlos, “Image Edge Detection using Ant Colony Optimization”, *International Journal of Circuits, Systems and Signal Processing*, vol. 4, no. 2, pp. 25-33, 2010.

[72] O. P. Verma, M. Hanmandlu, A. K. Sultania, Dhruv, “A Novel Fuzzy Ant System for Edge Detection”, *Proceedings of 2010 IEEE/ACIS 9th International Conference on Computer and Information Science, IEEE Computer Society Washington, DC, USA*, 2010.

[73] M. Dorigo and T. Stutzle, “Ant Colony Optimization”, *Cambridge: MIT Press*, 2004.

[74] H. B. Duan, “Ant Colony Algorithms: Theory and Applications”, *Beijing: Science Press*, 2005.

[75] M. Dorigo, V. Maniezzo and A. Colourni, “Ant System: Optimization by a Colony of Cooperating Agents”, *IEEE Transactions on Systems, Man and Cybernetics* ,Part B, vol. 26, pp. 29-41, February 1996.

[76] M. Dorigo and L. M. Gambardella, “Ant Colony System: A Cooperative Learning Approach to the Travelling Salesman Problem”, *IEEE Transactions on Evolutionary Computation*, vol. 1, pp. 53-66, 1997.

[77] Y. P. Wong, V. C. M. Soh, K. W. Ban, Y. T. Bau, “Improved Canny Edges using Ant Colony Optimization”, Proceedings of 5th International Conference on Computer Graphics, Imaging and Visualization, pp. 197-202, 2008.

[78] D. S. Lu, C. C. Chen, “Edge Detection Improvement by Ant Colony Optimization”, *Pattern Recognition Letters*, vol. 29, no. 4, pp. 416-425, 2008.

[79] A. Rezaee, ”Extracting Edges of Images with Ant Colony”, *Journal of Electrical Engineering*, vol. 59, no. 1, pp. 57-59, 2008.

[80] H. Nezamabadi-pour, S. Saryazdi and E. Rashedi, “Edge Detection using Ant Algorithms”, *Soft Computing* ,vol. 10, pp. 63-68, 2006.

[81] J. Tian, W. Yu and S. Xie, “An Ant Colony Optimization Algorithm for Image Edge Detection”, *IEEE Congress on Evolutionary Computation*, 2008.

[82] A.Colourni, M.Dorigo, V.Maniezzo, “Distributed Optimization by Ant Colonies”, *Proceedings of the First European Conference on Artificial Life, Paris, France, F.Varela and P.Bourgine (Eds.), Elsevier Publishing*, 134–142, 1991.

[83] M.Dorigo, “Optimization, Learning and Natural Algorithms”, *Ph.D. Thesis, Dip. Electronics Information , Politecnico di Milano, Italy*, 1992.

[84] A.Colourni, M.Dorigo, V.Maniezzo, “An Investigation of some Properties of an Ant Algorithm”, *Proceedings of the Parallel Problem Solving from Nature Conference (PPSN 92), Brussels, Belgium, R. Männer and B. Manderick (Eds.), Elsevier Publishing*, pp. 509-520, 1992.

[85] Jander Moreira and Luciano Da Fontoura Costa, “Neural-based colour image segmentation and classification using self - organizing maps”, *Anais do IX SIBGRAPI*, pp.47-54, 1996.

[86] L.A. Zadeh, “Some reflections on soft computing, granular Computing and their roles in the conception, design and utilization of information/intelligent systems”, *Soft Computing*, vol.2, pp. 23-25,1998.

[87] Xian Bin Wen, Hua Zhang and Ze Tao Jiang, “Multiscale Unsupervised Segmentation of SAR Imagery using the Genetic Algorithm”, *Sensors,* vol.8, pp.1704-1711, 2008.

[88] Mohamed N. Ahmed and Aly A. Farag, “Two-stage neural network for volume segmentation of medical images”, *Pattern Recognition Letters*, vol.18, pp.1143-1151,1997.

[89] Hichem Talbi, Mohamed Batouche and Amer Draa, "A Quantum Inspired Evolutionary Algorithm for Multi objective Image Segmentation", *International Journal of Mathematical, Physical and Engineering Sciences*, vol.1, no.2, pp.109-114, 2007.

[90] N. Senthilkumaran and R. Rajesh, "Edge Detection Techniques for Image Segmentation - A Survey", *Proceedings of the International Conference on Managing Next Generation Software Applications (MNGSA-08)*, pp. 749-760, 2008.

[91] Bouchet A, Pastore J and Ballarin V, "Segmentation of Medical Images using Fuzzy Mathematical Morphology", *JCS and T*, vol.7, no.3, pp.256-262, October 2007.

[92] Ian Middleton and Robert I. Damper, "Segmentation of magnetic resonance images using a combination of neural networks and active contour models", *Medical Engineering and Physics*, vol.26, pp.71-86, 2004.

[93] Wei Sun and Yaonan Wang, "Segmentation Method of MRI Using Fuzzy Gaussian Basis Neural Network Neural Information Processing", *Letters and Reviews*, vol.8, no.2, pp.19-24, August 2005.

[94] Mausumi Acharyya and Malay K. Kundu, "Image Segmentation Using Wavelet Packet Frames and Neuro fuzzy Tools", *International Journal of Computational Cognition*, vol.5, no.4, pp.27-43, December 2007.

[95] Dinesh K. Sharma, Loveleen Gaur and Daniel Okunbor, "Image Compression and Feature Extraction with Neural Network", *Proceedings of the Academy of Information and Management Sciences*, vol.11, no.1, pp. 33-38, 2007.

[96] Jander Moreira and Luciano Da Fontoura Costa, "Neural-based colour image segmentation and classification using self - organizing maps", *Anais doIX SIBGRAPI*, pp.47-54, 1996..

[97] J. Maeda, A. Kawano, S. Yamauchi, Y. Suzuki A. R. S. Marcal and T. Mendonc, "Perceptual Image Segmentation Using Fuzzy - Based Hierarchical Algorithm and Its Application to Dermoscopy Images", *IEEE Conference on Soft Computing in Industrial Applications (SMCia/08), Muroran, JAPAN*, pp.66-71, June 25-27, 2008.

[98] N. Senthil Kumaran and R. Rajesh, "A Study on Edge Detection Methods for Image Segmentation", *Proceedings of the International Conference on Mathematics and Computer Science (ICMCS-2009),* vol. I, pp.255-259, 2009.

[99] Kanchan Deshmukh and G. N. Shinde,"An adaptive Neuro-fuzzy system for colour image segmentation", *Journal of Indian Institution of Science,* vol. 86,pp.493-506, Sept.-Oct.2006.

[100] Lee. M.K. et al., "Edge Detection by genetic Algorithm", *Proceedings of the International Conference on Image Processing, 10-13, Sept. 2000.*

[101] Mantas Paulinas and Andrius Usinskas,"A Survey of Genetic Algorithms Applications for Image Enhancement and Segmentation", *Information Technology and Control*, vol.36, no.3, pp.278-284, 2007.

[102] Evelia Lizárraga Olivas, et al., "Ant Colony Optimization for Membership Function Design for a Water Tank Fuzzy Lozic Controller", *IEEE Workshop on Hybrid Intelligent Models and Applications,* 16-19 April 2013.

[103] Ibrahiem M. M., El Emary, "On the Application of Artificial Neural Networks in Analyzing and Classifying the Human Chromosomes", *Journal of Computer Science*, vol.2, no.1, pp.72-75, 2006.

[104] Lei Jiang and Wenhui Yang, "A Modified Fuzzy C-Means Algorithm for Segmentation of Magnetic Resonance Images", *Proceedings of VIIth Digital Image Computing: Techniques and Applications*, vol. 10-12,pp.225-231, 2003.

[105] Gonzalo A. Ruz, Pablo A. Estevez and Claudio A. Perez, "A neuro fuzzy colour image segmentation method for wood surface defect detection", *Forest Products Journal*, vol.55, no.4, pp.52-58, April 2005.

[106] S. Dhivya, Dr.R. Shanmugavadivu, "A Big Data Based Edge Detection Method for Image Pattern Recognition - A Survey", *International Journal of Engineering and Computer Science*, vol. 7, no.3,pp. 23755-23760, 2018.

[107] George Karkavitsas and Maria Rangoussi, "Object Localization in Medical Image using Genetic Algorithms", *International Journal of Signal Processing*, pp. 204-207, 2005.

[108] Y. Freund, R.E. Schapire, "A Short Introduction to Boosting", *Journal of Japanese Society for Artificial Intelligence*, vol.14, no. 5, pp. 771-780, 1999.

[109] Y. Freund, R.E. Schapire, "A decision-theoretic generalization on on-line learning and an application to boosting", *Journal of Computer and System Sciences*, vol. 55, no. 1, pp. 119-139, 1997.

[110] Sung K, Poggio T., "Example based learning for view-based human face detection", *IEEE Transaction on Pattern Anal Machine Intelligence*, Vol. 20, pp.39-51, 1998.

[111] Schapire R, Singer Y., "Improved boosting algorithms using confidence-rated predictions", *Machine Learning*, vol. 37, no. 3, pp. 297–336, 1999.

[112] Lienhart R, Maydt J., "An extended set of haar-like features for rapid object detection*", In: Proceedings of the IEEE International Conference Image Processing*, vol. 1, pp. 900–903, 2002.

[113] Viola P, Jones M., "Fast and robust classification using asymmetric AdaBoost and a detector cascade", *Neural Information Processing System*, vol. 14, 2002.

[114] Froba B, Stecher S, Kublbeck C., "Boosting a Haar-like feature set for face verification", *Lecture Notes in Computer Science*, pp. 617-624, 2003.

[115] Howe NR., "A closer look at boosted image retrieval", *In: Proceedings of the International Conference on Image and Video Retrieval*, pp.61-70, 2003.

[116] Jones M, Viola P., “Fast multi-view face detection”, *Mitsubishi Electric Research Laboratories, IEEE Conference on Computer Vision and Pattern Recognition (CVPR);* June 2003.

[117] McCane B, NovinsK.,“On training cascade face detectors”, *Image and Vision Computin*g, Palmerston North, New Zealand, pp. 239–244, 2003.

[118] Viola P, Jones M., “Robust real-time face detection”, *International Journal of Computer Vision*, vol. 57, no. 2, pp. 137-154, 2004.

[119] Treptow A, Masselli A, Zell A., “Real-time object tracking for soccer-robots without colour information”, *In: Proceedings of the European Conference on Mobile Robotics ECMR, 2003.*

[120] Kolsch M, Turk M., “Robust hand detection”, *In: Proceedings of the IEEE International Conference on Automatic Face and Gesture Recognition*, pp. 614-619, 2004.

[121] Le DD, Satoh S., “Feature selection by AdaBoost for SVM-based face detection”, *Information Technology Letters, The Third Forum on Information Technology (FIT2004),* 2004.

[122] Levi K, Weiss Y., “Learning object detection from a small number of examples: the importance of good features”, *In Proceedings of the International Conference on Computer Vision and Pattern Recognition (CVPR),* vol. 2, pp. 53-60, 2004..

[123] Li X,Wang L, Sung E., “Improving AdaBoost for classification on small training sample sets with active learning”, *In: Proceedings of the Sixth Asian Conference on Computer Vision (ACCV).,* Korea, 2004.

[124] Luo H, Yen J, Tretter D., “An efficient automatic redeye detection and correction algorithm”, *In: Proceedings of the 17th IEEE International Conference on Pattern Recognition, (ICPR’04),* Vol. 2, pp. 883–886, Aug 23–26 2004, Cambridge UK.

[125] Silapachote P, Karuppiah DR, Hanson AR., “Feature selection using AdaBoost for face expression recognition”, *In: Proceedings of the 4th IASTED International Conference on Visualization, Imaging, and Image Processing*, pp. 452–273, Marbella, Spain, September 2004.

[126] Le D, Satoh S., "Fusion of local and global features for efficient object detection", *IS& T/SPIE Symposium on Electronic Imaging,* 2005.

[127] Stojmenovic M., "Real time machine learning based car detection in images with fast training, *Machine Vision Application,* vol. 17, no. 3, pp. 163–172, 2006.

[128] Felzenszwalb, Pedro F., "Object Detection with Discriminatively Trained Part-Based Models", *IEEE Transactions on Pattern Analysis and Machine Intelligence,* vol. 32, No. 9, pp. 1627– 1645, 2010.

[129] Jayanta Kumar Basu, Debnath Bhattacharyya, Tai-hoon Kim, "Use of Artificial Neural Network in Pattern Recognition", *International Journal of Software Engineering and Its Applications,* vol. 4, no. 2, April 2010.

[130] Gualdi, Giovanni Prati, Andrea, Cucchiara, Rita, "Multistage Particle Windows for Fast and Accurate Object Detection", *IEEE Transactions on Pattern Analysis and Machine Intelligence,* vol. 34, no.8, pp**.** 1589 – 1604, 2012.

[131] Beaugendre, A.,Chenyuan Zhang; Jiu Xu; Goto, S, "Enhanced moving object detection using tracking system for video surveillance purposes", *IEEE Transactions on Visual Communications and Image Processing (VCIP),* pp. 1- 6, 27-30 Nov. 2012.

[132] Lan, J., Li, J. Xiang, Y., Huang, T., Yin, Y. ; Yang, J., "A fast Automatic Target Detection System Based on Visible Image Sensor and Ripple Algorithm", *IEEE Sensors Journal, ,*vol. 35, pp. 1-12, 2013.

[133] Oreifej, Omar ; Li, Xin ; Shah, Mubarak , "Simultaneous Video Stabilization and Moving Object Detection in Turbulence", *IEEE Transactions on Pattern Analysis and Machine Intelligence,* vol. 35 , No. 2, pp. 450-462, 2013.

[134] Han, J. He, S. Qian, X., Wang, D. Guo, L. Liu, T., "An object-oriented visual saliency detection framework based on sparse coding representations", *IEEE Transactions on Circuits and Systems for Video Technology,* vol.35, no. 99, pp. 1, 2013.

[135] Bleszynski, Elizabeth H., Bleszynski, Marek K., Jaroszewicz, Thomas ; Albanese, R. , "Imaging Through Obscuring, Discrete-Scatterer Media With Chirped Trains

of Wide-Band Pulses", *IEEE Transactions on Antennas and Propagation*, vol. 61, no. 1, pp. 310-319, 2013.

[136] Wan-Lei Zhao, Chong-WahNgo,"Flip-Invariant SIFT for Copy and Object Detection", *IEEE Transactions on Image Processing*, vol. 22, no. 3, pp. 980-991, 2013.

[137] Tsung Han Tsai ; Chung-Yuan Lin ; Sz-Yan Li, "Algorithm and Architecture Design of Human–Machine Interaction in Foreground Object Detection With Dynamic Scene", *IEEE Transactions on Circuits and Systems for Video Technology*, vol. 23, no.1, pp.15-29, 2013.

[138] A. Arnaud, "Ship detection by SAR interferometry," *in Proceedings: IEEE International Geoscience Remote Sensing Symposium, Hamburg, Germany*, vol. 5, pp. 2616–2618, Jun. 28–Jul. 2 1999.

[139] Souyris, C. Henry, and F. Adragna, "On the use of complex SAR image spectral analysis for target detection: Assessment of polarimetry," IEEE *Geoscience Remote Sensing*, vol. 41, no. 12, pp. 2725–2734, Dec. 2003.

[140] K.Ouchiand, H.Wang,"Interlook cross-correlation function of speckle in SAR images of sea surface processed with partially overlapped subapertures," IEEE *Geoscience Remote Sensing*, vol. 43, no. 4, pp. 695–701, Apr. 2005.

[141] K.Tomiyasu,"Phase and doppler errors in a space borne synthetic aperture radar imaging the ocean surface," *IEEE Journal Ocean Engineering*, vol. OE-1, no. 2, pp. 68–71, Nov. 1976.

[142] B. Slade, "RADARSAT-2 product description," MDA Ltd., Richmond, BC, Canada, Tech. Rep. RN-SP-S2- 1238, Nov. 2009

LIST OF PUBLICATIONS OUT OF THESIS

List of Published Paper in International Journal

S. No	Title of the Paper	Name of the Journal	Volume & Issue	Year	Page No.
1	Role of linguistic quantifier and digitally approximated Laplace operator in infrared based ship detection",	International Journal of System Assurance Engineering and Management, (Springer)	Vol. 8 (Suppl. 2):	2017	S1336–S1342
2	Estimation of Global Threshold of Infrared Image By Using Fuzzy Granule.	ICIC Express Letters Part B: Applications 2017 An International Journal of Research and Surveys	Vol. 8, No. 10	2017	1401-1407
3	De-noising Infrared Image Using OWA Based Filter,	International Journal of Computer and Information Engg. (WASET)	Vol:11, No:4,	2017	487-492
4	Application of 'Most' Fuzzy Linguistic Quantifier to Filter Impulse Noise,	International Journal of Information Technology (Springer)	https://doi.org/10.1007/s41870-018-0145-9	2018	1-8
5	Tracking of Ship by using Ordered Weighted Averaging Method,	International Journal of Electronics Engineering.	Vol.9 • No.1	2017	150-154

List of Papers Accepted to International Journal

S. No	Title of the Paper	Name of the Journal	Impact Factor	Vol. & Issue	Year & Page No	Publisher/ Indexing
1	Bio Inspired Edge Detection Technique Based On Fuzzy Triangular Membership Function	International Journal of System Assurance Engineering and Management	0.331	Not Mentioned	Not Mentioned	Springer; Scopus Indexed

List of Papers Published in International Conference

S.No	Title of the Paper	Conference Name	Publisher Name and Date
1.	Threshold Based Ship Tracking with Fuzzy Linguistic Quantifier, pp. 6105-6108, ISSN 0973-7529; ISBN 978-93-80544-24-3	Proceedings of the 11th INDIACom; INDIACom-2017; **IEEE Conference ID: 40353** 2017 4th International Conference on "Computing for Sustainable Global Development	BharatiVidyapeeth's Institute of Computer Applications and Management (BVICAM), New Delhi (INDIA), 01st - 03rd March, 2017

BRIEF PROFILE OF THE RESEARCH SCHOLAR

RUCHIIKA RANI is working as an Associate Professor in the Electrical and Electronics Engineering Department at the KIET Group of Institutions, Ghaziabad, UP India. She has passed her Bachelor of Engineering in Electronics Engineering from Nagpur University, Nagpur in 2002, Master of Engineering in Electronics and Communication Engineering from NITTTR Chandigarh in 2007 and pursuing Ph.D. from J.C. Bose University of Science and Technology, YMCA Faridabad, India. She is having 15 years' experience including Teaching and Research. She is currently doing research on Image Processing. Her areas of interest are in the field of Image Processing, Microproceesor, and Microcontroller. She has published over 10 research papers in various international journals and conferences. Some of reputed publishers including, Springer, WASET etc. and attended National and International conferences.